5-2022

Using Safety Performance Models, Autonomous Vehicle Data, and Machine Learning to Develop Contextual Complexity Criteria to Establish a Standardized Process for On-Road Evaluation of Medically At-Risk Drivers Considering Static and Dynamic Factors of the Roadway Environment

Vijay Bendigeri
vbendig@g.clemson.edu

USING SAFETY PERFORMANCE MODELS, AUTONOMOUS VEHICLE DATA, AND MACHINE LEARNING TO DEVELOP CONTEXTUAL COMPLEXITY CRITERIA TO ESTABLISH A STANDARDIZED PROCESS FOR ON-ROAD EVALUATION OF MEDICALLY AT-RISK DRIVERS CONSIDERING STATIC AND DYNAMIC FACTORS OF THE ROADWAY ENVIRONMENT

A Dissertation
Presented to
the Graduate School of
Clemson University

In Partial Fulfillment
of the Requirements for the Degree
Doctor of Philosophy,
Civil Engineering

---

by
Vijay Gangadhar Bendigeri
[May 2022]

Accepted by:
Dr. Jennifer H. Ogle, Committee Chair
Dr. Johnell O. Brooks (Co-chair)
Dr. Wayne A. Sarasua
Dr. Mashrur R. Choudhury

ABSTRACT

The field of transportation engineering has an opportunity to positively impact the medical community, specifically the clinicians who evaluate, train, and rehabilitate at-risk drivers. Driving Rehabilitation Specialists (DRSs) have an essential role in making roads safer for medically-at-risk drivers, their passengers, and other road users. DRSs conduct on-road driving evaluations, which are considered the gold standard to make fitness-to-drive decisions due to their high face validity. Most DRSs use a fixed route, meaning the exact same route is used to evaluate each client. When a DRS develops a fixed route, that clinician identifies characteristics of the roadway they think are most important (e.g., signalized intersections, unprotected left-turns, protected left-turns). While transportation engineers are trained to know that the combination of static (e.g., roadway type, median, presence of lighting) and dynamic (e.g., traffic density, traffic speed, weather) conditions together define the complexity of a driving environment, transportation engineers have not previously developed materials specifically for DRSs. On the other hand, clinicians do not receive specialized training on these engineering topics and, as a result, do not have the skill set or tools to quantify and measure critical aspects of the roadway context in which the on-road evaluation is conducted.

This dissertation sought to create a methodology to measure the contextual complexity of the driving environment considering the roadway's static and dynamic characteristics with the long-term goal of providing DRSs the tools to design and evaluate routes using tools similar to those available to transportation engineers. This study utilized comprehensive open-source data collected by Waymo autonomous vehicles that allow for

the development of models to estimate the roadway environment's complexity considering both static and dynamic traffic characteristics. An unsupervised machine learning technique using clustering algorithms was used to measure and classify the driving environment's dynamic characteristics (e.g., vehicle, pedestrians, bicycles) into appropriate risk categories to develop a dynamic complexity model. A static complexity model was developed utilizing safety performance models and critical variables identified in the American Association of State Highway and Transportation Officials (AASHTO) Highway Safety Manual (HSM). The dynamic and static complexity models were then combined to build an absolute complexity model that provides a comprehensive and quantitative evaluation of the roadways. The knowledge and insights gained from the models developed to quantify static, dynamic, and absolute complexity is foundational work that would enable development of the tools for DRSs to evaluate their routes to ensure the most critical roadway components from the transportation engineering perspective are considered in evaluation of driving context. This process is anticipated to revolutionize the process in which on-road driving assessments are designed and evaluated by the clinicians who assess medically at-risk drivers.

DEDICATION

I dedicate this dissertation to my family. My Mom, Dad, Nammu, Ishank, and Veenu. You have been my bedrock and my greatest motivation.

ACKNOWLEDGMENTS

This was not the kind of journey I anticipated embarking on when I started. It has been a long journey with setbacks and triumphs. The people I met and my experiences have contributed tremendously to my success and helped shape me into becoming a better version of myself.

First and foremost, I would like to express my earnest gratitude to my adviser Dr. Jennifer Ogle. I couldn't have asked for a better mentor and a guide for this journey. Your support, faith, and belief kept me going during the most challenging times. Your dedicated involvement at every step of the process and the ability to guide and clear the confusion with ease and finesse are incredible. I am very proud of and grateful for the privilege I have had working with you.

I would also like to extend my deepest gratitude to my co-advisor Dr. Johnell O. Brooks. It all started with you when you introduced me to the community of Driving Rehabilitation Specialists. Never would I have imagined as a Civil Engineer to be able to make contributions to the medical community. Your feedbacks were blunt, humorous, and insightful, which expanded my thinking beyond the engineering realm.

I am also grateful to my committee, including Dr. Wayne Sarasua, and Dr. Mashrur "Ronnie" Chowdhury, for their teachings and mentorship. I would also like to thank certified driving rehabilitation specialist (CDRS) Leah Belle for her time going through my work and giving me feedback from a clinician viewpoint. I would also like to thank the community of Driving Rehabilitation Specialists (DRSs), whose work motivated me to take up this research and contribute.

I very much appreciate my research colleague Fengjiao Zou, with whom I had several hours of brainstorming and problem-solving sessions during this research which was very valuable. I gratefully acknowledge the assistance of Kushal Kusram, who taught me to work with sensor fusion data obtained from autonomous vehicles. I would also like to thank Waymo for releasing autonomous vehicle data for public research. I am also thankful to all my research colleagues, professors, and staff for their constant support and cooperation. I would also like to thank Bentley Systems for supporting me with their professional development program.

I would not have made this achievement without the extraordinary support of my family (my parents, wife, in-laws, and family-like friends). It was their dream as much as it was mine. Thank you for making my dream a reality with your sacrifices and unconditional love. Lastly, special thanks to my most vital support, my wife, Namratha Yajaman, who endured this long process and was my soundboard and encouraging support.

TABLE OF CONTENTS

LIST OF TABLES

LIST OF TABLES (continued)

Table Page

LIST OF TABLES (continued)

Table Page

LIST OF FIGURES

List of Figures (Continued)

Figure Page

CHAPTER ONE

INTRODUCTION

This research study develops and assesses a methodology to assist Driving Rehabilitation Specialists (DRSs) to understand and estimate the complexity of routes used for on-road driving evaluations for medically-at-risk[1] drivers considering both static[2] (e.g., lane-width, functional class, parking, etc.) and dynamic[3] (e.g., vehicle density, proximity, traffic speed, etc.) variables. A DRS is a professional who plans, develops, coordinates, and implements driving services for medically-at-risk individuals. These professionals are typically allied health personnel, driving instructors, and others who have specialized in this area and have received continuing education in this field. These professionals play an essential role in making roads safer for medically-at-risk drivers, their passengers, and other road users. A referral to a DRS for a driver with a medical risk can be made by physicians, eye doctors, occupational therapists, family members, the DMV, etc. Driver training for a medically-at-risk client is a service provided by a DRS and is often custom-designed after a thorough driving evaluation. A driving assessment consists of clinical and behind-the-wheel assessments or on-road assessments. The on-road assessment evaluates safe driving capabilities by assigning various driving-related tasks at pre-specified

[1] A medically-at-risk driver is a person with a medical condition that may deter completion of daily tasks using traditional methods. Risk types include physical impairments, such as an amputation, cerebral palsy, Parkinson's disease, a spinal cord injury, or a stroke; sensory impairments, such as poor vision or hearing loss/deafness; cognitive impairments, such as dementia, Autism Spectrum Disorder, or a traumatic brain injury; and psychiatric conditions, such as schizophrenia and or severe anxiety disorders.

[2] Static variables are conditions that remain constant. For example, lane width, speed limit, shoulder width, parking type, etc. are examples of static variables.

[3] Dynamic variables that are conditions that fluctuate. For example, traffic density, the proximity of vehicles, platoon speed, etc., are examples of dynamic variables.

locations on a driving route. DRS investigate their client's driving capabilities by monitoring performance on each driving-related task (i.e., maintaining safe following distance, negotiating lane changes, making left turns at unsignalized and signalized intersections, and managing speed) to determine if an individual is fit to drive.

From an engineering perspective, the ability to demonstrate safe driving capabilities to a sufficient degree on a given driving task depends upon the complexity of the driving context. However, no single tool, material, or resource exists that will aid DRSs in determining the roadway context in which the driving task is assessed. Measuring the driving context's complexity may help DRSs from different geographic locations design comparable standardized routes for on-road evaluation. Using the methodology presented in this research, DRSs will be able to empirically determine the driving complexity of a road based upon the following factors that define the roadway environment:

- Static characteristics of the roadway are based on roadway geometry (i.e., lane width, shoulder width, and the number of lanes) as well as contextual factors (i.e., roadside hazards, level of business development, type of area (rural or urban), etc.)

- Dynamic characteristics of the roadway reflect the mix of traffic (i.e., pedestrians, bicycles, and vehicles) and the traffic density, proximity, and speed.

The static contextual complexity metrics were derived from the contents of the American Association of State Highway and Transportation Officials (AASHTO) *Highway Safety Manual* (National Research Council et al., 2010), which transportation

engineers predominantly use to assess the safety of the roadway environment. Contributory effects of each roadway element to the overall safety were evaluated using their respective crash modification factors (CMFs). This material was condensed and tailored to the needs of DRSs. The dynamic contextual complexity was estimated using unsupervised machine learning techniques to categorize driving scenes by varying levels of complexity. The proposed Contextual Risk Factor (CCF) model combines the driving environment's static and dynamic variables and classifies the complexity into a graduated risk scale that ranges from high-risk to low-risk. Using the CCF model, DRSs will be able to assign a numerical rating to a road segment or intersection and categorize it appropriately depending upon the relevant conditions of the road that define it. Such a capability will help establish common standards for DRSs to design fixed routes of comparable complexity across various locations in the United States. While transferability of the model beyond the U.S. is possible, the Highway Safety Manual is specific to U.S. conditions and may not capture the variety and safety of roadway design elements in other countries.

Background

In the United States, the screenings of medically at-risk drivers are conducted by Driving Rehabilitation Specialists (DRSs). DRSs are often occupational therapists with a background in health care or driver education who have completed additional training and education in driver rehabilitation. DRSs assess a broad spectrum of clients, ranging from young, novice drivers to older, experienced drivers suffering from functional limitations that may affect their ability to drive safely. Typically, evaluations of medically at-risk

clients include both an in-clinic assessment (also referred to as pre-road or off-road evaluation) and an on-road assessment (Di Stefano & Macdonald, 2010). The in-clinic evaluation includes a clinical assessment of an individual's visual, perceptual, cognitive, and physical skills necessary for driving.

The DRSs conduct on-road assessment on either a standard, fixed route or a non-standard, variable route. A standard, fixed-route is a pre-planned route with pre-specified instructions to the driver and is designed by DRSs to assess a driver's capabilities at pre-specified locations on the route. The route planning and design process is currently carried out to incorporate various roadway features. Non-standard, variable routes are local routes used by DRSs who travel to the client's location or can be used for clients who drive in a limited capacity or environment. Following the on-road evaluation, if the DRS determines that the person cannot drive safely, further training to develop skill and competency is offered, or the person is reported to the state Department of Motor Vehicles (DMV) for revocation of the driving license (Janke & Eberhard, 1998).

Motivation

The on-road assessment is considered the gold standard due to its high face validity and widespread use by practicing DRSs (Shechtman, O et al., 2010). DRSs assess their clients' specific driving skills (i.e., visual scanning, gap acceptance, driver planning of the travel route to a destination, etc.) by assigning various driving tasks and activities at critical locations on a fixed or variable route designed by the DRS.

In a study conducted by Di Stefano & Macdonald (2010), 55 clinicians practicing driving rehabilitation were interviewed. Among clinicians interviewed, there was a high level of agreement (84%) on the need to improve the reliability and validity of the on-road procedures. Most participants indicated that the on-road evaluation should include a standard set of driving-related tasks. However, the difficulty of these driving-related tasks is influenced by the roadway environment's characteristics[4]. According to the authors, the extent to which standardization can be achieved is limited by the varying roadway conditions where assessments are conducted (Di Stefano & Macdonald, 2010). Dickerson (2013) surveyed 227 North American DRSs to determine the various assessment tools used for in-clinic and on-road assessments. The study found that at least 40 different in-clinic assessments were listed as the top five choices for making fitness-to-drive decisions, thus illustrating the diversity of assessment techniques across different clinics. The on-road assessment was considered by far to be the primary component in decision-making (Dickerson, 2013). Another study by Di Stefano & Macdonald, (2012), involving interviews with 22 DRSs, revealed that the outcome of the on-road test is influenced by the different traffic levels and associated road and environmental conditions. The ability of a driver to display adequate driving skills for an on-road evaluation depends upon the complexity of the driving environment (Pellerito, 2006; Schultheis et al., 2001). This, in turn, has an impact on the validity of any on-road assessment process, whether for novice or medically at-risk drivers. The need for all road tests to be sufficiently consistent and

[4] Roadway environment is the current condition of the road which includes the physical conditions (i.e., single lane/multi-lane road, lane width, shoulder width, speed limit, intersection type) and variable conditions of traffic (i.e., low density/high density traffic, pedestrian traffic).

challenging was determined by DRSs as a primary concern and is widely acknowledged in the literature (Di Stefano & Macdonald, 2012; Kay et al., 2008).

The roadway environment in which the driving assessment is conducted influences an individual's driving behavior. Specifically, the roadway environment impacts both the driver's perceptual and cognitive resources as well as their ability to coordinate motor responses under realistic time pressures. This is important because these aspects of driver competency are critical to road safety (Di Stefano & Macdonald, 2012).

Research studies have also revealed inconsistencies in the inclusion of desirable roadway test features in DRSs' routes (Stefano & Macdonald, 2006). The Victorian Occupational Therapy Professional Group and the Licensing Authority in Australia have established guidelines related to on and off-road driving assessments. The guidelines list compulsory and desirable features that need to be included while planning a fixed route. Australian researchers (Di Stefano & Macdonald, 2012) surveyed occupational therapy driver assessors (similar to DRS in the USA) to determine the list of compulsory route features that DRSs should use when designing a fixed route. Table 1.1 shows the list of mandatory route features and the number of DRSs practicing in urban and rural areas who mentioned each feature.

Table 1.1. Frequency of DRSs Using Compulsory Route Features (Source: Di Stefano & Macdonald, 2012).

The route features specified in guidelines as compulsory	**Percent of urban DRSs (n=15)**	**Percent of regional/rural DRSs (n=7)**
Drive along following the road with the following features:		
Single lane road with centerline	100	100
Multi-laned road	100	100
Crossing (pedestrian/children/railway)	93.33	100
Strip shopping center	93.33	85.71
Single lane road with no center line	86.67	71.43
Negotiate intersection (straight through or turn) in the following context:		
Intersection with parked cars occluding the view	100	100
Intersection controlled with a yield sign	100	100
Intersection controlled with a stop sign	100	100
T-intersection	100	100
Roundabout	100	100
Intersection controlled by traffic lights	100	85.71
Perform other driving tasks or maneuvers:		
Quiet drive through low-density area/familiarization opportunity	100	100
Lane change to the left	100	100
Lane change to the right	100	100
Parking: 90 deg/angle, or reverse	100	100
Vary required vehicle speed	100	100
Lane change when instructed, and as required, e.g., to go around parked cars	93.33	85.71
Locate a street sign	33.33	28.57
Types of environmental conditions:		
Low-density traffic	100	100

High-density traffic	100	100
Road with visual distractions, e.g. traffic, pedestrians, scenery	100	100
Distraction, e.g. intentional general discussion/answering questions in the vehicle to create a distraction	73.33	100

The authors found high compliance with compulsory route features by DRSs practicing in rural and urban areas yet saw very low compliance with desirable features in their routes. About 48% of the desirable features were absent from the standard routes used. Table 1.2 shows the frequency of DRSs using desirable features when designing fixed routes, for rural and urban DRSs.

Table 1.2. Frequency of DRSs Using Desirable Route Features (Source: Di Stefano & Macdonald, 2012)

The route features specified in guidelines as 'desirable'	**Percent of urban DRSs (n=15)**	**Percent of regional/rural DRSs (n=7)**
Speed zone changes	100	100
Merging/slip lane	86.67	100
Road marking information, e.g. exit arrows	73.33	85.71
Speed humps	86.67	57.14
Curved/highly cambered road	80	57.14
One way street	53.33	85.71
Freeway/highway (70+km/hour speed limit)	46.67	42.86
100 km/hour speed limit	46.67	42.86
Trams	46.67	14.29
No entry street	13.33	57.14

Road dips (blind vertical curves)	20	42.86
Narrow bridges (one car at a time)	6.67	14.29
Unsealed roads/Gravel (specified for rural areas)	0	0
Negotiate intersection (straight through or turn) in the following contexts:		
Traffic lights with a turning arrow	100	85.71
Non-uniform intersection	86.67	57.14
Multi-laned roundabout	66.67	42.86
Perform other driving tasks or maneuvers:		
Locate and negotiate a car park	86.67	57.14
Turning onto a high-speed road	80	57.14
The navigational task, return to entry point form within a shopping center car park	60	57.14
U turn	46.67	42.86
Simulated emergency braking	13.33	28.57
Overtaking	13.33	28.57
Types of environmental conditions:		
Underground car park	20	14.29

Some of the route features mentioned in Table 1.2 are encountered routinely by drivers during normal driving. For example, it is typical for a driver to confront a road with a 60 mph (100 kmph) speed limit in ordinary driving activity. Yet, only 45% of DRSs reported incorporating roads with higher speeds in their route. This is important because failing to include these features in fixed routes may decrease the utility of the assessment, weakening the authenticity of the evaluation.

Designing a fixed route using a checklist provides a mechanism for DRSs to assess specific driving skills in the presence of crucial roadway features. However, the difficulty of operating through a given road stretch is not governed by individual roadway features; instead, a myriad of road factors, traffic, and surroundings, collectively influence the complexity of the driving environment. For example, consider two roadway scenarios: scenario A (see Figure 1.1) and scenario B (see Figure 1.2).

Figure 1.1. Scenario A, a road with low traffic, a median divider, and no driveways.

Figure 1.2. Scenario B, a road with a high traffic volume, left-turn traffic, and driveways.

The amount of information that needs to be processed for a driver to navigate safely on both of these roads is very different. In scenario A the driver does not need to worry about turning vehicles or vehicles coming out of a driveway. There is a median divider separating the traffic in opposite directions. The level of traffic is low, so the cars are distributed far from each other on the road, and there are no vulnerable road users (i.e., no pedestrians or bicyclists) present. However, in scenario B, the driver needs to keep track of other vehicles in the left turn lanes that are waiting to make turns. In addition, the driver needs to observe if there are any vehicles in the driveways waiting to make turns. The driver must keep track of the cars, and judge the course of action from surrounding information. The traffic level is high, meaning the vehicles are closely spaced. In addition, the area is busy with many commercial establishments. The driver must discern crucial information amidst all the clutter to make driving-related decisions.

There is a significant difference in the cognitive load on the driver in both scenarios. The first scenario requires a lower cognitive load on the driver when compared to the second roadway scenario. Thus, the amount and type of information that needs to be processed are partially determined by the characteristics of the roadway environment. As such, DRSs must understand the roadway context in which the on-road assessment is conducted. Diverse elements of the roadway context collectively influence the range of skills, knowledge, and functional abilities that need to be used. However, guidance on considering the interdependencies of roadway features and their influence on driving behavior have not been identified in extensive literature searches.

1.2 Problem Statement

Driving Rehabilitation Specialists in the United States use fixed and/or variable routes to evaluate the driving competencies of medically at-risk drivers; however, DRSs may be unaware of the circumstances that form the roadway environment for a driving evaluation. As mentioned previously, the complexity of the driving environment is governed by the roadway geometry, traffic volumes, and the roadside environment.

While Transportation Engineers know that the combination of roadway geometry, operations, and associated environmental conditions together define the complexity of a driving environment, DRSs are not trained on these engineering topics and as a result, do not have the skill set or tools to quantify and measure critical aspects of the roadway context in which the on-road evaluation is conducted. Several researchers have emphasized the importance of establishing guidelines and standards in designing fixed routes to enhance the consistency and validity of on-road driving evaluation procedures (Di Stefano &

Macdonald, 2010; Di Stefano & Macdonald, 2012; Korner-Bitensky, Bitensky, Sofer, Man-Son-Hing, & Gelinas, 2006); however, there are no materials or guidelines currently available to help DRSs design routes of comparable complexities across different locations in the United States.

When one's driver's license status is impacted by the outcomes of the in-clinic and on-road assessments, ensuring the on-road evaluation is reliable and valid is essential for medically at-risk drivers. Thus, it is vital to provide DRSs with the knowledge, skills, and ability to design on-road routes to be consistent in driving complexity (i.e., geometric, operational, and environmental features).

1.3 Goals and Objectives

This research aims to establish guidelines for developing common standards to design fixed routes for on-road evaluations for at-risk drivers. The guidance is based on a thorough understanding of the driving context -- the circumstances that form the setting for a driving evaluation (i.e., operational, geometric, and environmental) and in quantitative terms that can be fully understood and assessed by a non-technical DRSs.

The research objectives to support this goal are as follows:

1. To develop a dynamic complexity model to measure dynamic complexity and categorize each scene appropriately from high to low risk.
2. To develop a static risk model to measure static risk and categorize each scene appropriately from high to low risk.

3. To build an absolute contextual complexity model combining results from dynamic complexity and static risk models to measure and categorize total complexity of the scene from high to low risk.
4. Develop metrics to measure and classify dynamic complexity, static risk, and absolute complexity of the drivng environment.

1.3 Expected Research Contributions

The outcome of this research is expected to make the following contributions:

1. Develop a methodology to measure the dynamic and static risk of the driving environment.
2. Develop static risk and dynamic complexity metrics along with a rating system for DRSs to measure and score the total contextual complexity of the entire route.

CHAPTER TWO

LITERATURE REVIEW

Approximately 60 million people in the United States have a medical condition that affects their ability to drive safely (Warren & Smalley, 2014). With 10,000 baby boomers turning 65 years of age every day (Center for Disease Control and Prevention, 2020), there is an ever-increasing need for healthcare professionals, primarily occupational therapists, to screen and comprehensively evaluate individuals who are potentially at-risk drivers (Di Stefano & Macdonald, 2003; McGwin et al., 2000). Due to this surge in the need to assess, evaluate and rehabilitate medically at-risk drivers, there is an increased onus on the specialists who address driving to have research-based best practices to enhance the validity and reliability of on-road driving evaluations.

Aside from occupational therapy, DRSs may also have backgrounds in kinesiotherapy, driver education, or other related fields. A DRS plans, develops, coordinates, and implements driving services for individuals with disabilities (Association for Driver Rehabilitation Specialists, 2022). Additionally, a DRS evaluates their client's driving skills, recommends rehabilitation as needed, and suggests vehicle and route modifications (e.g., avoiding driving at night) to enable a person to resume or continue driving or in some instances, recommends the individual no longer drives. Many DRSs gain experience, complete additional training and take a national certification exam offered by the Association for Driving Rehabilitation Specialists (ADED) to become Certified Driving

Rehabilitation Specialists (CDRS) (Association for Driver Rehabilitation Specialists, 2022).

The two most common reasons why DRSs evaluate driving performance are to determine whether the client meets acceptable competency requirements (e.g., whether he or she would be likely to pass a standard license test at the state Department of Motor Vehicles) and to identify impairment-related deficiencies in driving performance to develop a remediation program (Stefano & Macdonald, 2006). A DRS's driving assessment objectives are somewhat different from those of entry-level license testing, although both have a paramount concern with road safety. The majority of DRSs' clients are not novice drivers. Most DRSs' clients are experienced drivers with visual, physical, and/or cognitive impairments that may negatively impact their ability to drive safely, such as dementia, stroke, arthritis, low vision, limb amputations, neuromuscular disorders, spinal cord injuries, cardiovascular diseases, and other causes of functional deficits (Association for Driver Rehabilitation Specialists, 2019). One of the primary aims of DRSs is to identify and assess how an individual's health, disability, or age-related impairments impact their ability to drive safely (Ashman et al., 1994). In addition to these impairment-related assessment topics, there are also safety-related requirements to determine whether the driver demonstrates sufficient competence in executing various driving maneuvers in a wide range of road traffic conditions. This outcome justifies a driver's ability to obtain a full or a restricted driver's license (Di Stefano & Macdonald, 2012; Shechtman, et al., 2010; Stutts & Wilkins, 2003).

The ability to drive safely changes by the driving environment's contextual complexity. The driving context consists of static components (i.e., roadway type, speed limit, road width, presence of median, etc.) and fast-changing dynamic components such as moving objects (i.e., vehicles, pedestrians, bicyclists, etc.). Weather and other externalities also influence the contextual risk of the driving environment. Researchers define all the visual cues and information that a driver must process to operate a vehicle as visual demand. Visual demand encompasses both the static and dynamic content (Dewar & Olson, 2002). Human factors experts generally believe that crashes increase when the visual demand rises (Dewar & Olson, 2002). Research studies documented more crashes on roads with heavy traffic or complicated roadway geometric configurations, both of which pertain to dynamic and static constituents of the driving ecosystem (Shinar et al., 1977). DRSs have inexplicably considered the complexity of the driving environment in the design of their on-road evaluation route based upon their experience and knowledge of the geographic region.

The literature review summarizes what is known about planning practices and challenges facing the design of fixed routes for on-road evaluations. Further discussion is divided into seven sections. Sections 2.1 and 2.2 discuss the two main components of the assessment procedure used by DRSs (i.e., the in-clinic and on-road evaluation) to determine a client's ability to drive safely. Section 2.3 discusses current route planning and design practices used in the field of driving rehabilitation. Section 2.4 presents the issues related to the reliability and validity of the current route design practices and discusses the importance of considering the roadway context. Section 2.5 describes attributes of the

roadway environment and its influence on the driving context and driver behavior. Section 2.6 discusses the visual demand and cognitive load research as well as its impact on driving complexity. Section 2.7 summarizes the literature about route planning and design practices of DRSs' routes and highlights the importance of DRSs having the ability to empirically determine the complexity of roadway environment features in which on-road driving tasks are assessed.

2.1 In-Clinic Evaluation

The in-clinic evaluation assesses a client's fundamental performance areas that are considered crucial to driving a vehicle. The word "clinical" refers to the frequent practice of administering tests or assessments in a clinical setting. The clinical evaluation serves a variety of purposes, including helping DRSs to

- determine the client's ability to meet state-mandated criteria (e.g., visual acuity) by the driver licensing agency for maintaining and securing a driver's license;
- identify a client's strengths and weaknesses related to driving activities (e.g., transferring into the vehicle and stowing a mobility aid) and motor skills;
- identify the need for initiating referrals to other specialists (e.g., neuropsychologists, low-vision specialists, mobility and seating specialists) ;
- determine the client's need for adaptive driving equipment; and
- identify compensatory strategies for driving or alternatives to driving that enable community mobility (Radloff, 2014).

The predictive value of the in-clinic evaluation is still an ongoing effort to develop evaluation protocols that are both reliable and valid. There is no single consensus among DRSs as to which clinical test can most effectively predict driver readiness; however, there are numerous assessments used by DRSs .

Dickerson (2013) surveyed 184 DRSs in the United States to determine which tools they valued. Participants were asked to list their top five assessment tools. The study results indicated that 40 different assessments comprised the top five for making fitness-to-drive decisions, illustrating the discord in tools clinicians use. When the author compared the results with a survey done in 2006, the data suggested that the tools used in driver rehabilitation practice in 2013 had not changed significantly.

Another study by Korner-Bitensky et al. (2006) found inconsistency in the duration of the in-clinic assessment. Out of 114 DRSs, 37% indicated the average in-clinic evaluation length between 30 to 60 minutes, and 61% reported greater than 60 minutes. When asked about typical in-clinic assessments, 85% of DRSs said performing a visual evaluation, 86% assessed visual perception, 84% assessed motor functioning, and 84% assessed cognition (Korner-Bitensky et al., 2006).

Although there are inconsistencies in the selection of tests, the data collected during the in-clinic evaluations allow DRSs to determine if a client possesses sufficient skill for the on-road assessment. This research will focus only on the on-road assessment.

2.2 On-Road Assessment

Typically, on-road evaluations are conducted after the in-clinic evaluation. Although the number and types of clinical assessments vary, they can be limited in their capacity to predict an individual's complex multidimensional on-road driving abilities (Janke & Eberhard, 1998). Relatively simple driving-related tasks, such as starting the car and entering a traffic stream in a quiet traffic environment, require coordination of perceptual, cognitive, and motor skills. Multiple skills are needed to adequately perform tasks such as problem-solving, reasoning, judgment, planning, perceptual-cognitive, and motor operations (Cushman, 1996). Due to its comprehensive nature, the on-road evaluation is seen as the "gold standard" evaluation of driving ability (Di Stefano & Lovell, 2006; Di Stefano & Macdonald, 2010, 2012; Justiss et al., 2006; Kay et al., 2008; Siegrist, 1999).

An on-road driving evaluation is conducted using a specialized vehicle that includes a passenger brake and extra mirrors, as well as other necessary adaptations that may be needed for a given client's physical accommodations (i.e., hand controls, left foot gas pedal, pedal extensions, turn signal extensions, key extensions, steering column extensions, etc.) An on-road evaluation includes assessing the client's ingress/egress; mobility aid management (e.g., ability to transport and store a walker); vehicle control; adherence to traffic rules and regulations; environmental awareness and interpretation; and consistent use of compensatory strategies for any visual, cognitive, physical and/or behavioral impairments (Stefano & Macdonald, 2006). Clients are typically instructed to drive on a pre-determined standardized route and asked to perform different driving-related tasks

(e.g., left and right turns at the intersections, lane changes, etc.) to a certain level of performance to demonstrate competency.

Research has confirmed that the on-road assessment has high face validity in determining safe driving capabilities (Shechtman, O et al., 2010). Many practicing DRSs in the United States routinely use established routes to evaluate their client's driving performance. Rather than a variable course, a fixed route allows DRSs to make comparisons across clients since the same route is used for all clients.

2.3 Route Planning and Design Practice

The premise of the on-road evaluation for medically at-risk drivers is similar to the concept of the license test for novice drivers (Stav, 2004). However, the test for medically at-risk drivers is different in its nature and approach than the entry-level license test due to the differences in evaluation goals and driver characteristics. Siegrist (1999) explains that entry-level tests are used with driving candidates for three main reasons:

- maintain safety standards by ensuring that the driver can demonstrate specific competencies consistently;
- apply a procedure to all applicants that are fair and efficient, and
- influence the nature of the practice and formal training undertaken by the applicant.

Consistent with the aims described above regarding the initial license testing, only a "minimum set of competencies is required. The novice car driver may not be required to perform at the same level as an experienced driver" (Siegrist, 1999). Therefore, the

modified structure of the basic skills assessed with medically at-risk drivers is essential and substantiated by researchers (Dobbs et al., 1998; Janke & Eberhard, 1998).

One basic framework for an on-road test is the Washington University Road Test (WURT) (Hunt et al., 1997). The WURT is a performance-based assessment route developed from a study to assess older drivers with dementia, specifically Alzheimer's. The on-road test was designed to distribute performance difficulty evenly across the assessment. It consisted of a six-mile (9.6 km) course with urban two-, four- and six-lane streets that provided various road and traffic conditions. These conditions were selected to enable the detection of driving behaviors associated with crashes in the elderly (Hunt et al., 1997). A commercial driving instructor and a researcher accompanied each participant during the on-road evaluation.

The introductory element of the WURT includes DRS (seated in the front passenger seat), leading the participant to a large empty area such as a parking lot for familiarization with the test vehicle (a standard model automatic transmission with a dual brake pedal for the driving instructor). The open space provides a non-demanding environment for the client and a chance for the evaluator to assess the client's basic vehicle operation and positioning skills before progressing to a more risky, open context. This initial familiarization period in a parking lot is a crucial component of WURT since the client is completing the evaluation in a different vehicle from their own and who are often highly anxious.

Then, the WURT proceeds from a parking lot to a quiet street with little traffic (e.g., a residential area with a low-speed limit). The test progressively gets more challenging for

the driver with an increase in the difficulty of the route's environment, including higher speeds, more traffic and other types of road users, and more complex maneuvers. At the end of the test, one of the three global safety ratings is assigned:

- safe behavior, unlikely to result in a crash;
- marginal/small to moderate risk of a crash; or
- unsafe/substantial risk of a collision (Hunt et al., 1997).

Using the graduated difficulty framework of WURT allows the DRS to do the following:

- perform preliminary checks and prerequisite tasks, such as adjusting seating, mirrors, and any adaptive devices;
- determine the adequacy of basic vehicle handling skills in a safe environment;
- assess whether the driver can follow instructions; and
- develop some rapport with the driver (Messinger-Rapport, 2002).

Using the framework of the WURT, the next step in the route planning and design process incorporated frequencies of some roadway features and driving tasks/activities. The Center for Biomedical Engineering Rehabilitation Science at Louisiana Tech University provides one such checklist, as shown in Table 2.1 (Center for Biomedical Engineer Rehabilitation Science, 2016).

Table 2.1. Route Planning Checklist (Center for Biomedical Engineer Rehabilitation Science, 2016)

ACTIVITY	CONDITIONS	FREQUENCY	
Turns: Left & right	2-lane - 2-lane (uncontrolled low traffic)	Two each	
	2-lane - 2-lane (uncontrolled high traffic)	Two each	
	2-lane - 4-lane (Stop sign low traffic)	Two each	
	4-lane - 4-lane (Stop sign high traffic)	Two each	
	Traffic light (low traffic)	Two each	
	Traffic light w/ turn on red (low traffic)	One each	
	Traffic light w/turn on red (high traffic)	One each	
	Traffic light w/turn on red (restricted view)	One	
	T-intersection (uncontrolled)	One	
	T-intersection (stop-controlled)	One	
Right turns	Yield sign (with turn lane)	One	
	Yield sign (without turn lane)	One	
Lane changes			
Left and right turn lanes	Multiple lane streets	Two each	
	Left	Two each	
	Right	One each	
	Center	Two each	
Parking	Uphill-along curb	One	
	Downhill-along curb	One	
	Parallel (between vehicles)	One	
	Parking log-angle or perpendicular	One	

Entering or merging	Limited access roadway	One	
Exiting or diverging	Limited access roadway	One	
Speed control	School zone	One	
	Railroad crossing (controlled)	One	
	Railroad crossing (uncontrolled)	One	
	Bridge	One	
	Increase 10 mph	One	
	Increase 20 mph	One	
	Decrease 10 mph	One	
	Decrease 20 mph	One	
	Deceleration-exiting limited access	One	
Backing	Straight line	One	
	Right turn	One	
Vehicle position	Passing parked vehicles – right	Two	
	Passing parked vehicles – left	Two	
	Left lane ends	One	
	Right lane ends	One	
Vehicle control	Stop sign	Two	

Table 2.1 includes driving-related activities (i.e., making a left or right turn) that need to be included in a particular roadway condition (i.e., at a traffic light with no right turn on red). The items provided in the checklist are included in the fixed route to assess specific driving skills such as visual scanning, gap acceptance, driver planning of the travel route, etc., within each given driving context. A traffic light with no right turn on red is a static contextual variable that affects the driving complexity. Furthermore, different traffic

levels considered by DRSs in route planning to make left or right turns address recognizing dynamic contextual elements.

Another catalog is provided by the Association for Driver Rehabilitation Specialists (ADED), a non-profit organization that provides education and support for professionals working in driving rehabilitation (Pellerito, 2006). The ADED education committee offers coursework that provides guidelines and instruction on designing a standard fixed route. According to the course materials, the DRSs should consider all types of roads in their surrounding region to include vast possibilities of different traffic scenarios while developing their standard fixed route. In addition, the ADED guidelines recommend the extent of the course should not exceed approximately 25 square miles. However, there can be an exception for a DRS practicing in a rural area. The course material also provides the following checklist of traffic densities and essential components while designing the fixed route (Table 2.2 and Table 2.3).

Table 2.2. Description of Different Traffic Density Descriptions Provided in ADED Route Planning Course Material (Pellerito, 2006).

TRAFFIC DENSITY	CONDITION DESCRIPTION
Low	Fewer than three vehicles per minute; one lane of travel in both directions, usually residential area
Medium	Three to ten cars per minute; streets with signalized intersections and one or two travel lanes in both directions
High	eleven or more vehicles traveling in the direction of travel; a minimum of two travel lanes in both directions

Table 2.3. Route Planning Checklist Provided in ADED Course Material (Pellerito, 2006).

ACTIVITY	CONDITIONS
Turns: left and right	Single lane approach to single lane approach (controlled and uncontrolled)
	Two-lane approach to two-lane approach
	Two-lane approach to four-lane approach
	Four-lane approach to two-lane approach
	Four-lane approach to four-lane approach
Lane changes: left and right	Two-lanes to four (single direction) lanes with 45-55 mph speed limit
Stops and starts	Stop controlled intersection
	Signalized intersection
	Intersection with poor visibility
	High-density intersection
Speed reduction or modulation	Uneven road, bridge, railroad crossing, etc.
	School zones
	Speed bumps
	Gravel to pavement transition (or paved roads that may have loose gravel or sand)
Merge and yield	Interstate or expressway
Backing	Backing straight and right turn
Passing	Passing parked vehicles
Mid-block crossing	Entering controlled and uncontrolled mid-block crossing
	Leaving controlled and uncontrolled mid-block crossing
Negotiate intersections	T-intersection
	Four-way intersection
	Intersection with straight through
	Blind intersection (intersections with visual blockages usually found in residential areas)
Driving through congested areas	Chaotic parking lots (Walmart, or a shopping mall, etc.)

The checklist provided by ADED includes components from the entry-level driving test (i.e., changing lanes, negotiating intersections, backing straight, making a three-point turn, and driving in school zones). It is interesting to note that the checklist includes both static and dynamic components of the roadway environment that influence the contextual complexity. For example, the list in Table 2.2 recognizes traffic density as an essential component for DRSs to consider in their route design. Nonetheless, the framework provided to gauge traffic density (i.e., low density if there are fewer than three vehicles observed per minute, medium density if there are three to ten vehicles per minute, and high density if there are more than eleven vehicles observed per minute) is ambiguous and difficult to quantify with certainty. For example, the range used to count cars to classify appropriate density categories is unclear.

Research studies have shown that traffic demand varies with the time of the day, functional classification of the road, and the area type (Roess et al., 2004). However, the ADED course materials for route design do not provide any information to accommodate these factors. In the absence of such information, categorization of a particular road stretch as low, medium, or high traffic density very much depends upon the time the specific DRS collected the data, therefore introducing additional variability.

Another component included in the checklist that correlates to the contextual complexity of the driving environment is the intersection density. While the ADED course material encourages DRSs to incorporate a stop and start at a poor visibility and a high-density intersection in the route, it does not include any information on what characteristics of an intersection would constitute a high density or poor visibility intersection. Few

components included in the checklist (i.e., left and right turns at controlled and uncontrolled intersections) indicate that DRSs might consider the complexity of the driving environment in their route planning. The current knowledge base in driving rehabilitation lacks the needed resources that would allow DRSs to considering many of the important roadway components and their inter-dependencies in estimating the complexity of the driving context. This research study aims to fill this gap by developing metrics to quantify static and dynamic scene complexity from a driver's perspective.

2.4 Reliability and Validity of an On-Road Assessment

Reliability and validity are crucial for any test. A valid and reliable test produces consistent outcomes and does not vary significantly between different testing conditions. In an article discussing the evaluation of medically impaired drivers, "On-road evaluations have been regarded as a direct measure of driving abilities. Unfortunately, these evaluations often lack reliability and objectivity" (Galski et al., 1990). Improving the standards of professional practice have been a topic of discussion and research amongst DRSs. While efforts have been made to improve the reliability and validity of on-road evaluations through the development of a standard rating procedure, considering the features of the roadway environment to determine the complexity of the driving context is needed. Considering the driving context is essential due to the nature of the road traffic environment and required driving maneuvers for a particular route the types of errors likely to occur are important to consider (Schultheis et al., 2001). For example, a route having intersections with a dedicated left-turn lane with a protected left turn signal will reduce the opportunities for right-of-way errors. If there are no multi-lane sections of the road, there

will be fewer possibilities for drivers to perform poorly when lane-keeping or passing (Pellerito, 2006).

The route's driving context is the primary determinant of overall task difficulty. For example, suppose a particular course presents elementary conditions (e.g., low traffic and simple maneuvers); in that case, drivers whose functional abilities differ substantially from each other may all perform equally well (Pellerito, 2006). Similarly, if a route is challenging, a group of drivers with generally poor, but differing abilities may all perform poorly. In such cases, inappropriate route selection results in an evaluation lacking sensitivity. The route designed and planned for a medically at-risk driver must consist of a range of segments and intersections with appropriate complexity for typical drivers. When the central purpose of an evaluation is to identify the effect of an impairment, a lack of sensitivity can be a significant disadvantage because it will make it more challenging to quantify a driver's progress during their rehabilitation process (Korner-Bitensky et al., 2006).

To improve the reliability of the on-road assessment, many DRSs are using standard fixed routes with specific driving-related tasks designed for their clients at predetermined locations. Korner-Bitensky et al. (2006) surveyed 114 DRSs from the United States and Canada who had on-road driving evaluation experience. Results showed that 78% of the DRSs used a standard driving route to evaluate their clients. Yet, there was variation in the elements of the on-road assessments amongst the DRSs. The variations were

predominantly related to the roadway context (i.e., traffic level, highway functional class[5], area type). For example, many respondents (55%) reported not using the freeway element at all in their on-road assessment (Korner-Bitensky et al., 2006). This variability in the inclusion or exclusion of roadway elements is likely due to the lack of widely accepted standards related to route requirements by the DRSs.

Many research studies related to improving the reliability and validity of on-road driving assessments have stressed the need to define core requirements of roadway elements and the need for standardization (Di Stefano & Macdonald, 2012; Hunt, et al., 1997; Kay, et al., 2008; Korner-Bitensky, et al., 2006; Stav, 2004; Unsworth, 2007). In a study conducted by Di Stefano and Macdonald (2012), DRSs were asked to develop a list of desirable numbers of specific route features in a standard route. Table 1.2 shows the frequencies of 'desirable' route features in standard courses, separately for DRSs from urban and rural areas. The authors found differences in the opinions of desirable route features between urban and rural settings. In addition, there was variability within the groups of urban and rural DRSs regarding their views of desirable route features. This is of some concern because a few of the driving maneuvers and roadway features listed in Table 1.2 are quite demanding and are routinely encountered by many drivers, such as 100 km/hr (60 mph) speed zones and overtaking maneuvers. Routes without these features may be insufficiently complex to test a client's ability to drive safely in common driving conditions.

[5] The U.S. DOT's Federal Highway Administration (FHWA) classifies our Nation's urban and rural roadways by road function. Each function class is based on the type of service the road provides to the motoring public, and the designation is used for data and planning purposes.

One argument that can be made is that the geographical conditions restrain the inclusion of certain roadway contextual features. This is especially true with the DRSs practicing in rural areas. It may be difficult to locate specific roadway features such as heavy traffic conditions or areas with significant driving distractions (i.e., driveways, advertising signage, closely spaced intersections). Furthermore, some DRSs may find certain roadway features, such as the number of driveways on a stretch of road, unnecessary to include, or they may have a skewed perception of safety related to specific roadway features. Because DRSs and Transportation Engineering are two very different professions, it may be argued that DRSs may not necessarily know why they should consider particular attributes of roadways while planning the fixed routes. However, there are no studies to support this hypothesis.

The outcome of this research project aids in improving the quality and consistency of on-road evaluations. Quantifying dynamic and static complexity to measure total scene complexity will benefit driver evaluation, training, and rehabilitation efforts. This will allow DRSs to evaluate driving tasks in an empirically quantifiable driving context.

2.6. Cognitive Load to Measure Contextual Complexity

Everyday routine trips expose drivers to massive amounts of input that is either static (i.e., roadway configuration and traffic control devices) or dynamic (i.e., movement of surrounding vehicles and other vulnerable road users) (Olson, 1996). An important concept related to driver information processing is one's useful field of view (UFOV). The UFOV is defined as "the total visual field from which target characteristics can be acquired

when the head and eye movements are excluded"; and the extent of the UFOV differs between drivers, depending on how well they select and process relevant information from the environment (Dewar & Olson, 2002). While drivers may scan the whole driving environment, the focus is typically the view in front of them, the UFOV. Researchers define all the information that a driver must process to operate a vehicle as the visual demand, including traffic on the road, roadway environment, information in the vehicle, etc. (Dewar & Olson, 2002). Human factors experts generally believe that when the visual demand increases, the risk of traffic crashes increases (Dewar & Olson, 2002). Prior research determined that more crashes occur on roads with heavy traffic or complicated geometric configurations (Shinar et al., 1977). Abdel-Aty and Radwan (2000) modeled crash occurrence and involvement to find that heavy traffic increases the likelihood of crashes. One reason for crashes increasing with traffic complexity or object-density is that the driver's cognitive load increases. It is believed that one's cognitive load plays a vital role in performing complex tasks (Paas et al., 2003), such as driving. In addition, variability in dynamic inputs, such as speed, adds another level of complexity that the driver must process. Researchers (Schultheis et al., 2001) have determined that crash rates increase as the speed variations between the driver and other traffic increase, especially at higher traffic volumes. Yet, methods to incorporate complexity into risk assessments are not currently available.

Complicating matters, UFOV decreases for numerous reasons including vehicle speed, traffic congestion, rain, increasing age, and additional high-demand tasks (Dewar & Olson, 2002; Rogé et al., 2004). Researchers estimated that when drivers are traveling at

30 mph, they can see targets in a visual field of 150 degrees; however, when speed is doubled (60 mph), drivers can only see targets in half of the visual field (approximately 75 degrees) (Dewar & Olson, 2002). As speeds increase, the distance required to perceive hazards and react appropriately increases because drivers need to look further down the road for objects in one's potential collision zone, this is referred to as the stopping sight distance or SSD (AASHTO, 2018). As the UFOV narrows with speed, it expands in length due to increased SSD. Research also reveals that the UFOV decreases when the quantity of information to be processed in the driver's peripheral field increases (Monty & Senders, 1976), meaning that when the level of object density is high and the road scene is complex. As prior research suggests, specific combinations of static and dynamic parameters increase the likelihood of crash occurrence due to increased complexity. This dissertation adopts the UFOV recommendation from Dewar and Olson's (2002) and uses it to build and measure dynamic contextual complexity within driver's control/view and compare it to the complexity of the entire driving scene.

2.6 Summary

Driver rehabilitation is an industry that needs to grow due to an increase in the older driver population which increases the number of medically at-risk drivers. DRSs play a vital role in evaluating clients' physical and functional deficiencies and then rehabilitating those individuals to become safe drivers as appropriate. At the same time, the field of driving rehabilitation is developing and there is a need for DRSs to exhibit best practices. The tests conducted in the in-clinic evaluation typically supplement the on-road

assessment. The on-road assessment is considered the “gold standard” in driving rehabilitation and is widely used to make fitness-to-drive decisions.

The Washington University Road Test (WURT) enables DRSs to incorporate a driving test route with a steadily increasing task difficulty approach (Hunt et al., 1997). Starting from a low risk, uncomplicated driving environment (i.e., empty parking lot) and gradually progressing into higher activity driving environments that increase the utilization of the driver's perceptual and cognitive resources. Using this approach, the driver can first get accustomed to the evaluator’s vehicle and others in the vehicle prior to completing more complex driving tasks. Using WURT’s framework, DRSs can design their fixed driving route by incorporating frequencies of roadway features and driving maneuvers provided by route planning checklists, such as those offered by the Center for Biomedical Engineering Rehabilitation Science and the ADED coursework (Hunt et al., 1997; Center for Biomedical Engineer Rehabilitation Science, 2016). Although the items in such lists include features of the road environment that influence its complexity, the specialists in the field of driver rehabilitation currently lack the resources to incorporate the driving context into these routes.

Previous research studies have stressed the importance of improving the reliability and validity of the on-road assessment. Considering the driving context within which the skills are assessed can enhance both the validity and reliability, as this context can directly influence the client’s driving behavior and skills demonstrated during fixed on-road routes. In the field of Traffic Engineering, the driving context is the primary determinant of overall

task difficulty. Previous studies in Australia noted the importance of quantifying the roadway context of the fixed route (Di Stefano et al., 2010, 2012; Korner-Bitensky et al., 2006).

This dissertation developed metrics to measure static and dynamic scene complexity from a driver's perspective using speed, density, and proximity of the objects around the vehicle to account for dynamic complexity and the roadway geometric characteristics listed in AASHTO's Highway Safety Manual for static complexity. A statistical model was developed to estimate absolute contextual complexity to classify its contextual risk appropriately. The output is a matrix that classifies the driving environment's complexity into graduated risk categories from low to high.

This study used open-source LiDAR and video data collected by Waymo autonomous vehicles to estimate static and dynamic complexity frame by frame. The LiDAR data provided rich real-world activity information around the car, including stationary and non-stationary objects such as vehicles, pedestrians, and signs. The video data provided the knowledge of the static variables included in the AASHTO's Highway Safety manual. This study considered the speed, density, and proximity of the objects in the entire driving environment and within the driver's cone of vision to develop a measure of the driving environment's complexity.

CHAPTER THREE

METHODS

3.1. Introduction

This dissertation sought to create a methodology to measure the contextual complexity of the driving environment considering the roadway's static and dynamic characteristics. This model will assist DRSs in evaluating and potentially rehabilitating medically-at-risk drivers who use on-road assessments as a primary tool to assess safe driving capabilities. The study utilized comprehensive open-source data collected by Waymo autonomous vehicles to build models to estimate the road environment's complexity considering static and dynamic traffic conditions. This chapter details the methods designed to achieve the goals and objects of this dissertation.

The method section of this document is divided into three parts to achieve the dissertation's goals and objectives. Figure 3.1 shows a framework with the principal components in this chapter.

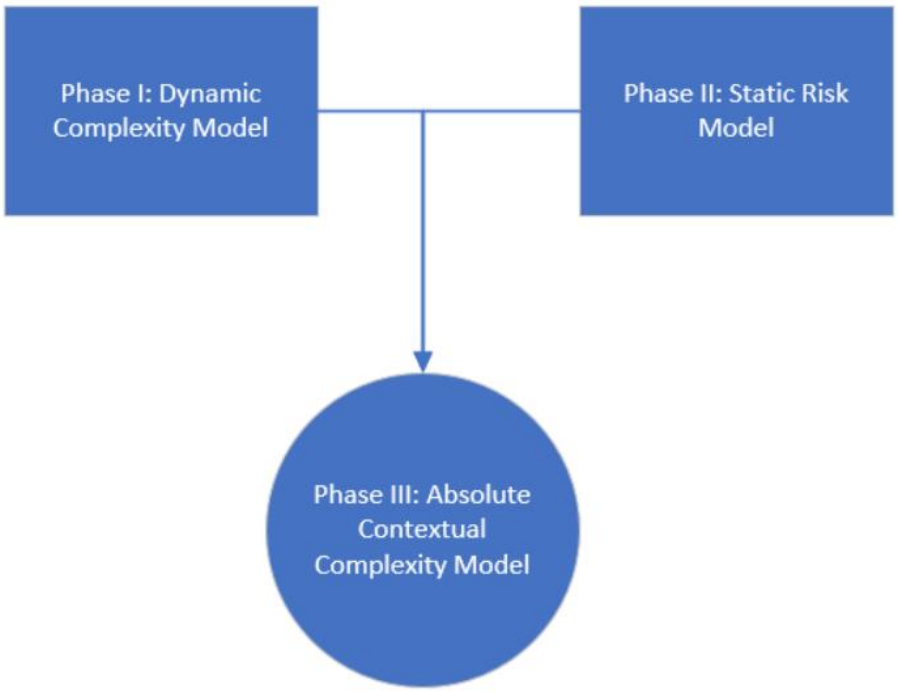

Figure 3.1. Methodology Flow Chart.

The phases and their objectives are listed below:

- Phase I - Dynamic complexity model: The tasks outlined in this phase focused on developing a dynamic complexity model that measures and classifies the driving environment into appropriate clusters considering non-stationary (i.e., vehicles, pedestrians, bicycles) objects. This phase dive deep into the rich elements of the Waymo AV open data source and how it was utilized to understand the dynamic complexity.
- Phase II - Static Risk Model: The tasks in this phase were targeted towards developing a model to measure the static risk of the driving environment using the critical variables identified in the AASHTO's Highway Safety Manual. A

sensitivity analysis was completed to determine each variable's importance prior to categorizing them into different risk zones.

- Phase III - Absolute contextual complexity Model: This step combined the models developed in phases one and two (i.e., the dynamic and static models) to build a model that assessed the absolute complexity of the driving environment. Additionally, a few select trips by the Waymo AV were used as case studies to demonstrate the estimation of absolute contextual complexity. The Waymo trips were divided into individual segments and intersections, and the total contextual complexity (i.e., static and dynamic) was estimated.

Detailed descriptions of each phase and the associated relevant task descriptions are provided in sections 3.2, 3.3, and 3.4.

3.2. Phase I - Dynamic Complexity Model,

The advent of autonomous vehicle open datasets has created new opportunities to measure dynamic complexity to incorporate dynamic interaction metrics into complexity estimates and safety assessments. Several AV datasets have been published in recent years; however, the open dataset published by Waymo in 2019 is by far the largest, richest, and most diverse self-driving dataset released for research. Phase I of the methodology capitalizes on this open-source autonomous vehicle dataset obtained from the Waymo AV program to build the dynamic complexity model.

3.2.1. Data Source:

The raw dataset consists of high-quality LiDAR and video data obtained from multiple sensors mounted on Waymo autonomous vehicles. Figure 3.2 shows a picture of the Waymo AV with its sensor layout and the relative coordinate systems. The system used five Lidar sensors and five high-resolution pinhole cameras (Sun et al., 2020).

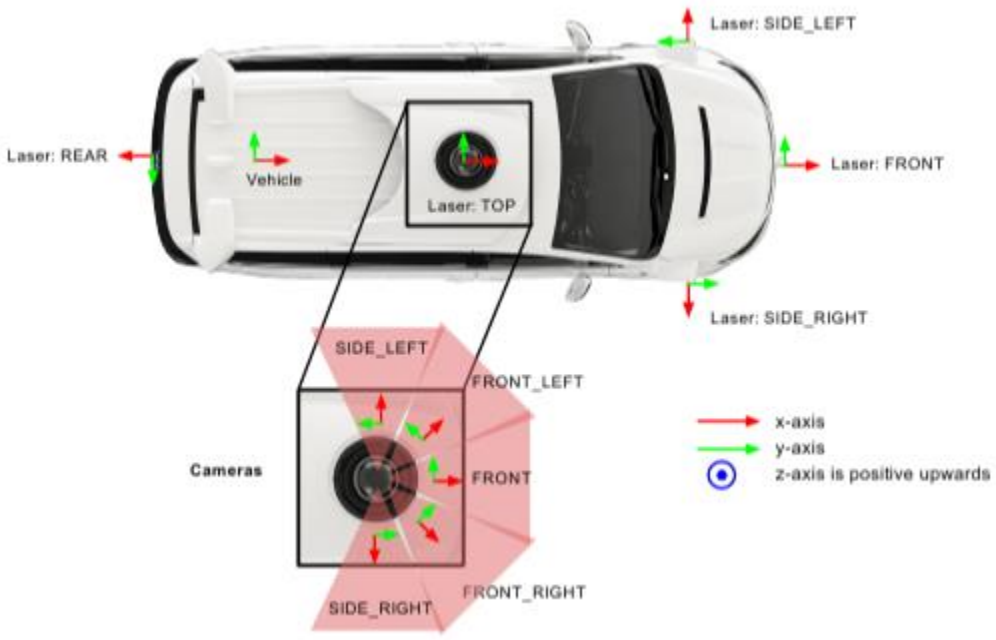

Figure 3.2. Sensor layout and coordinate system of Waymo autonomous vehicle (Sun et al., 2020).

The coordinate system moves with the vehicle. The LiDAR dataset included 3D bounding boxes with object type annotations manually checked for accuracy by trained labelers, see Figure 3.3 (Sun et al., 2020). The tracked object types include vehicles, pedestrians, bicyclists, and traffic signs. Additionally, vehicle speed vectors in 3-dimensional space for

each frame were provided. The data were collected in San Francisco, Phoenix, and Mountain View, see Figure 3.4 (Sun et al., 2020).

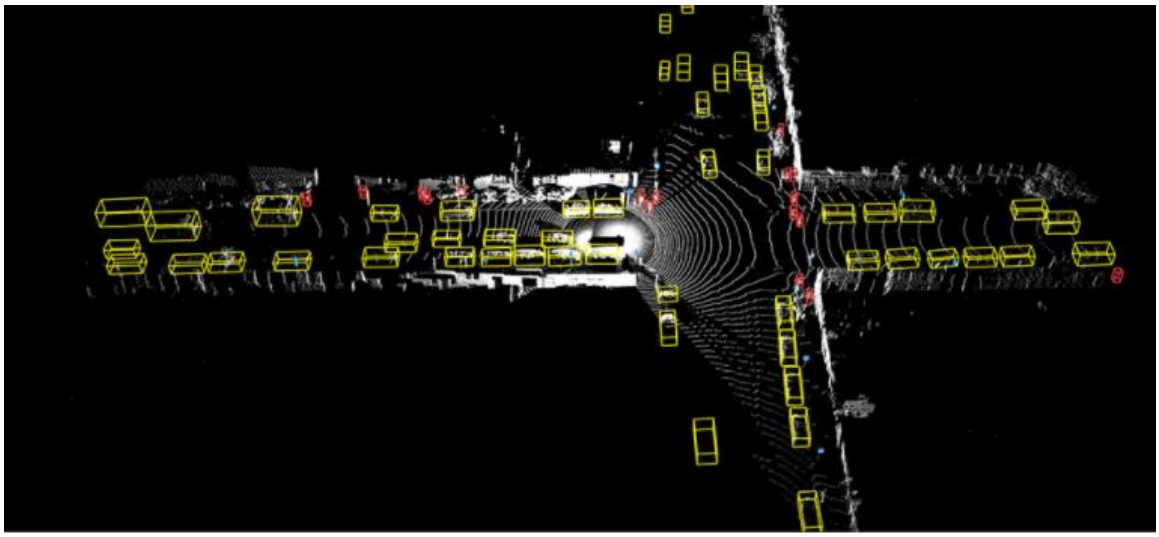

Figure 3.3. LiDAR 3D bounding box example, Yellow = vehicle, Red=Pedestrian, Blue=sign, Pink = cyclist (Waymo Open Dataset Available for Autonomous Vehicle Researchers, 2019)

San Francisco Mountain View Phoenix

Figure 3.4, Waymo self-driving car data collection areas (Sun et al., 2020).

Figure 3.5 shows the workflow with the main tasks and their associated sub-tasks carried out in this phase. Work associated with each task is discussed.

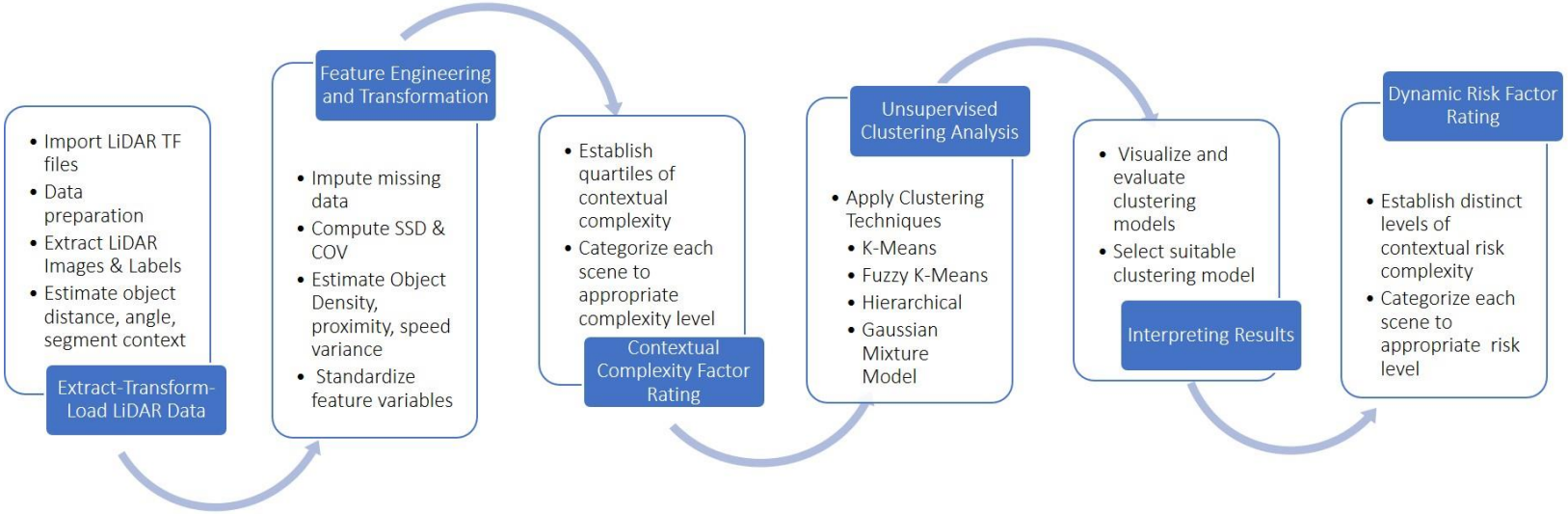

Figure 3.5. Method Flowchart - Dynamic Contextual Complexity

3.2.2. Extract Transform Load LiDAR Data

A total of 798 scenes of perception data, each spanning 20 seconds at 10 Hz/second (i.e., ~200 LiDAR frames), were analyzed during this phase. All scenes were stored in a Google cloud bucket in a TensorFlow file format. The files were downloaded, and the raw LiDAR data were extracted. The raw data contains a segment context, LiDAR images, and LiDAR labels. The LiDAR point-cloud data reference each object with x, y, and z coordinates in a three-dimensional space with respect to the autonomous vehicle as to the origin. The distance of the objects and their angle from the autonomous vehicle is estimated from x, y, and z coordinates. Vehicle speed for each frame was obtained from the segment context metadata. The driving context assessment was limited to lower speeds (<40 mph) due to the limited range of LiDAR technology, which has a published maximum range of 250 feet, though extended distances were contained in the datasets (Waymo Open Dataset Available for Autonomous Vehicle Researchers, 2019).

3.2.3. Feature Engineering and Transformation:

The total number of objects in each LiDAR frame and its proximity to the driver was estimated as a measure of scene complexity. From the literature review an important concept related to the driver information processing is the useful field of view (UFOV) (Dewar & Olson, 2002). As speeds increase, the distance required to perceive hazards and react appropriately increases because drivers need to look further down the road for objects in the potential collision zone or the the stopping sight distance (SSD) (AASHTO, 2018). The vehicle's speed was used to derive SSD and select an appropriate UFOV. The SSD and

UFOV were then used to construct a 3-dimensional filter cone, the cone of vision (COV), to identify any objects that fall within that cone.

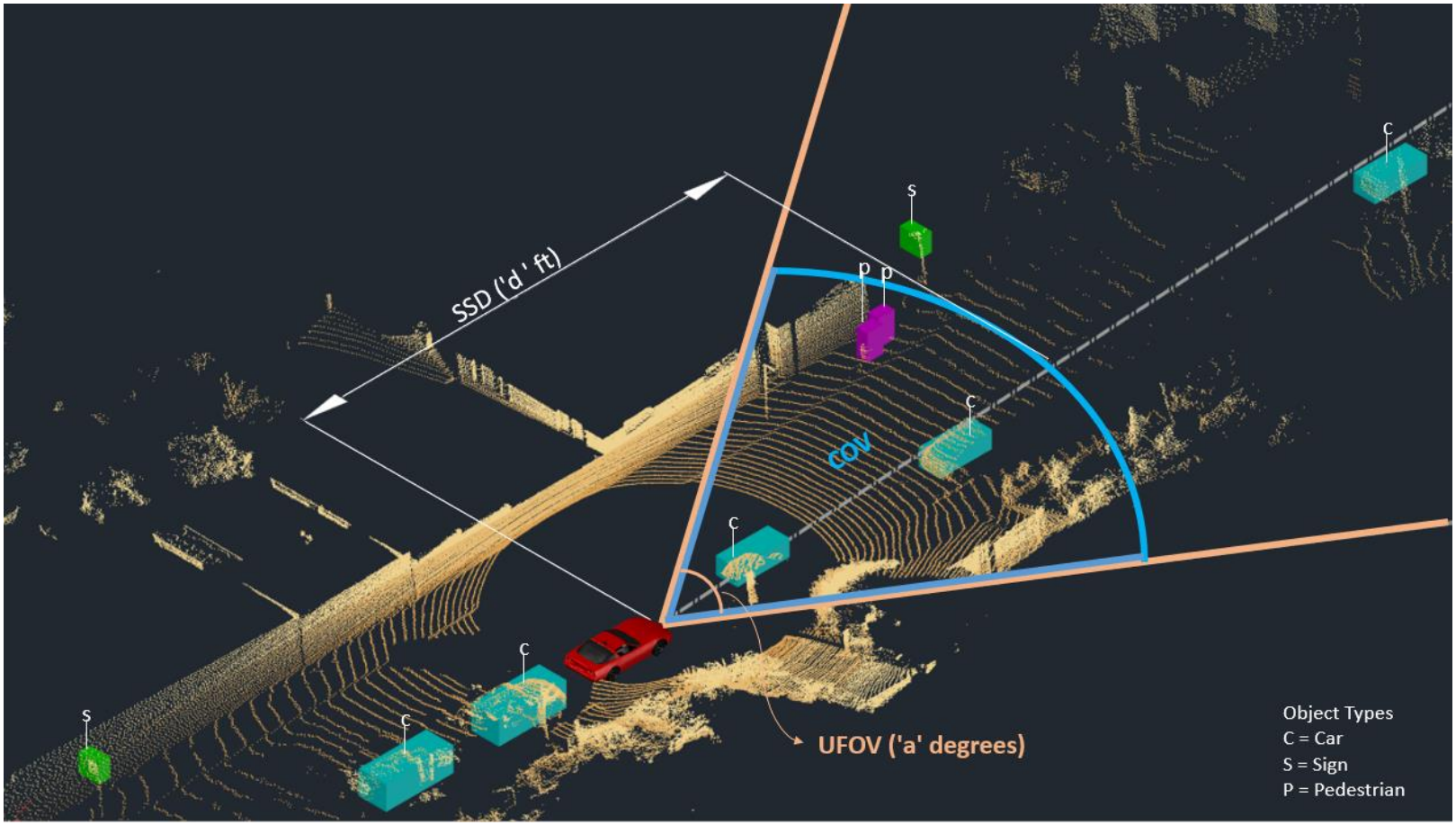

Figure 3.6. LiDAR point-cloud, SSD, UFOV, and COV representation with object types.

Figure 3.6 provides a pictorial representation of the SSD, UFOV, and COV in the LiDAR point cloud. The orange dots represent the LiDAR points. The red car in the center is a representation of the autonomous vehicle. The blue bounding boxes with the label "c" are the locations of detected cars. The pink bounding boxes with the label "p" represent the location of the pedestrians. The green bounding boxes with label "s" represent the location of the traffic signs. The white dotted line in the center represents the direction of travel of the autonomous vehicle. The UFOV is the angle "a" between the orange lines that extends from the red car. The SSD is a distance that extends from the red car to a distance "d." COV is the 3-dimensional volume of space constructed from SSD & UFOV represented by the blue boundary. Objects that fall within this COV were identified for each frame, along with the total objects in the scene. In Figure 3.6, there are a total of 9 objects in the entire scene (five cars, two pedestrians, and two signs) and only four objects within COV (two cars and two pedestrians).

COV is a function of SSD and UFOV. Thus, to determine the COV for each frame, the SSD and UFOV were first computed. The SSD of the vehicle for each frame was calculated using the relationship in Equation 1. A standard driver's reaction time of 2.5 (Roess et.al., 2004) seconds and a flat grade (i.e., grade = 0%) were assumed in all SSD estimations. UFOV shares an exponential relationship with speed. Following Dewar and Olson (2002), the UFOV is 160 degrees at zero speed, which reduces to 150 degrees at 30 mph speed and further scales down to 75 degrees at 60 mph speed. UFOV was computed using linear interpolation for all fractional speeds that fall in-between the speed ranges mentioned above (i.e., 0 mph, 30 mph, and 60 mph) within each scene. The COV boundary

was calculated within the LiDAR point cloud using SSD & COV values. Objects that fall within the COV boundary were summarized along with the total objects in the scene.

$$SSD = 1.47st + \frac{s2}{30*\frac{a}{g}} \qquad \text{Equation 3.1}$$

Where,

SSD = Total stopping sight distance for the vehicles (feet)

s = speed of the vehicle (mph)

t = standard reaction time of the driver (2.5 seconds)

a = standard deceleration rate (11.2 ft/s^2)

g = acceleration due to gravity (32.2 ft/s^2)

3.2.4. Contextual Complexity Factor Model

From the literature review, the key variables that measure visual-clutter and cognitive load are the density of the objects and their proximity to the vehicle. As the number of objects in the driving environment increases, the amount of information that needs to be processed by the driver also increases, increasing the driver's cognitive load. Near objects present a greater risk to the driver compared to distant objects. A Contextual Complexity Factor (CCF) was estimated for each frame to measure these two important parameters using Equation 3.2.

$$CRF = \sum \left(\frac{1}{obj_{distance}}\right) \text{ - Equation 3.2}$$

Where,

$obj_{distance}$ = distance of the object from the autonomous vehicle (feet)

Inverse distance assignments were weighted in descending order, with near objects getting higher weights and farther objects getting lower weights. The summation of these inverse distances accounted for the total number of objects in the scene, i.e., object density. The scene CCF was estimated for each frame considering all the objects. Additionally, the CCF was estimated from the COV filter in each frame. Statistical quartiles for the total sample size were calculated for the whole scene CCF and CCF within the COV. An individual frame was categorized as high if the CCF > 75th percentile, medium if CCF was within the inter-quartile range (between 25th percentile and 75th percentile), and low if CCF was less than the 25th percentile, respectively. All the frames were assigned a high, medium, or low category based on the scene CCF's respective quartile range.

3.2.5. Unsupervised clustering analysis

The complexity of multiple variable analysis required a more sophisticated approach for analysis. Thus, unsupervised clustering analysis was carried out to identify natural clusters and identify acceptable boundaries that are impossible with dividing the entire sample size into quartiles. Thus, to overcome this design deficiency and to obtain accurate boundaries, clustering analysis was performed on the processed AV data to overcome this design deficiency to get precise boundaries. Specifically, k-means clustering and hierarchical clustering were used to analyze the data. These clustering methodologies have been used for various pattern recognition modeling such as traffic condition

recognition, driver classification, and air pollution hotspot recognition, among others (Montazeri-Gh & Fotouhi, 2011); (Govender & Sivakumar, 2020). Table 3.1 provides a brief description of these algorithms.

Table 3.1. K-Means and Hierarchical Clustering techniques.

Clustering	Method Description	Cluster Representation
K-means clustering (Kanungo et al., 2002)	A simple and effective method in classifying the data into a certain number of clusters. The number of clusters is determined by the value "k." Each point is assigned to the nearest cluster. Different cluster numbers (K) can be applied to classify the scene complexity accurately and choose an optimal number of groups. K-means clustering is used to rank high crime areas and identify spam emails.	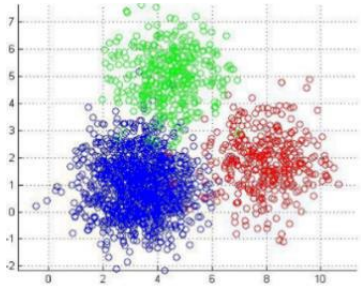 (Chen, 2022)
Hierarchical clustering (Murtagh & Contreras, 2017)	Build a clustering tree by grouping data points closest to each other and further grouping those clusters creating a hierarchy. Hierarchical clustering does not need the specification of several clusters. The number of clusters that best fit the data can be chosen by visualizing the tree.	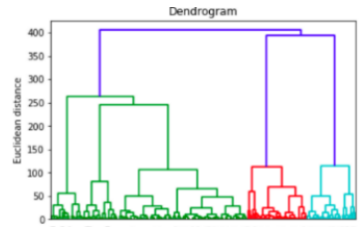 (Chauhan, 2019)

3.2.6. Results Interpretation

The k-means and hierarchical clustering techniques were analyzed and compared. This task involved reviewing these results and comparisons and selecting the best fit model. The task consisted of generating visuals of clustering results, recognizing the clustering patterns, and concluding on a choice model. A multi-dimensional clusters visualization tool was created to better visualize and understand the clusters' boundary division.

3.2.7. Dynamic Complexity Factor Rating

This step involved identifying the optimal number of cluster classes and classifying each LiDAR scene into the appropriate category. Additionally, a list of the most influential variables affecting dynamic complexity and their cluster ranges was identified. The results from the multi-dimensional cluster visuals were converted into a two-dimensional table with ranges defined for each cluster variable to classify a dynamic environment into appropriate complexity categories for use by the DRSs.

3.3 Phase II: Static Risk Model

The second phase of the project, consisted of tasks to meet the second objective, which was to develop a rating procedure to categorize a road segment into appropriate levels, depending upon the relative safety of the driving environment (predominantly related to characteristics of the infrastructure design such as lane widths, presence of lighting, etc.). Figure 3.7 shows the workflow with main tasks and their associated sub-tasks performed in this phase.

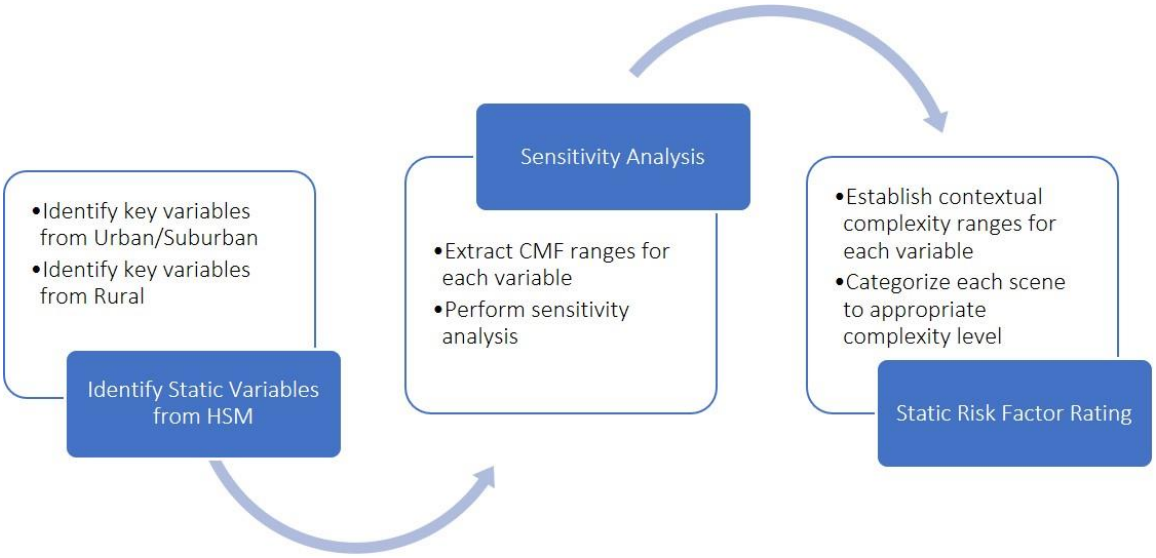

Figure 3.7. Method Flowchart - Static Contextual Risk

3.3.1. Identify static variables

In this step, all the safety performance model variables listed in the highway safety manual for urban and suburban arterials were identified for sensitivity analysis. Table 3.2 lists all these variables.

Table 3.2. Variables considered for sesitivity analysis (National Research Council et al., 2010)

Sl. No.	Segment	Intersection
1	Roadway Type	Intersection Type
2	Length of Segment	Lighting
3	Type of on-street parking	Number of approaches with left-turn lanes
4	The proportion of curb length with on-street parking	Number of approaches with right-turn lanes
5	Median width	Number of approaches with left-turn signal phasing
6	Lighting	Type of left-turn signal phasing for approach 1
7	Auto speed enforcement	Type of left-turn signal phasing for approach 2
8	Major commercial driveways	Type of left-turn signal phasing for approach 3
9	Minor commercial driveways	Type of left-turn signal phasing for approach 4
10	Major industrial / institutional driveways	Number of approaches with Right Turn On Red (RTOR) prohibited
11	Major residential driveways	Intersection red light cameras
12	Minor residential driveways	Sum of all pedestrian crossing volumes for signalized intersection
13	Other driveways	Maximum number of lanes crossed by pedestrian
14	Speed category	Number of bus stops within 1000 ft of intersection

15	Roadside fixed object density	Schools within 1000 ft of the intersection
16	Offset to roadside fixed objects	Number of alcohol sale establishments within 1000 ft of the intersection

3.3.2. Sensitivity Analysis

Sensitivity analysis is a technique used to determine how different values of an independent variable will impact a particular dependent variable under a given set of assumptions (Frey & Patil, 2002). A sensitivity analysis is carried out to understand the importance of attributes for each data category. The analysis outcome can help determine the most influential features, which also helps estimate weights.

Several methods exist for sensitivity analysis (i.e., mathematical, statistical, and graphical methods). Mathematical models demonstrate output sensitivity to the range of variation in input. Nominal Range Sensitivity Analysis (NRSA) and Differential Sensitivity Analysis (DSA) are examples of such sensitivity analysis methods (Frey & Patil, 2002). The graphical method demonstrates the sensitivity analysis through graphs, charts, etc. The graphical format is the most common, and shows how variations of inputs affect the outputs. Examples of this method include scatter plots and Conditional Sensitivity Analysis (Frey & Patil, 2002). A statistical method can be used for stochastic models which involve running the simulation based on the chosen input which comes from a probability distribution. Examples of statistical analysis methods include Sample and Rank Correlation Coefficients, Regression Analysis, Rank Regression, Analysis of Variance, Classification, and Regression. A disadvantage of the statistical approach is that

it requires large amounts of data to run the model to achieve satisfactory results. Unfortunately, the location-anonymity of the Waymo dataset does not allow for the collection of the static data with an adequate sample size. As such, a statistical method did not serve as an appropriate method for the intended purposes of this task.

Mathematical models can predict the essential variables with reasonable accuracy. The NRSA method was selected for use. The NRSA assesses the effect of varying the value of only one model input through its possible range while fixing all other inputs at their base-case value of nominal values (Frey & Patil, 2002). Thus, the model's sensitivity can be defined by different output values due to the change of inputs for that particular parameter. This method is beneficial whenever the inputs of the deterministic model consist of plausible values. The formula for this method is provided in Equation 3.3.

$$Sensitivity = \frac{Output_{Max\ input} - Output_{Min\ input}}{Output_{Nominal\ input}} \quad \text{Equation 3.3}$$

Where

$Output_{Max\ input}$ = output of maximum value for input

$Output_{Min\ input}$= output for minimum value for input

$Output_{Nominal\ input}$= output of nominal or base-case of the input

The result of this analysis supported the definition of appropriate ranges of CMFs for each risk level (i.e., high, medium, and low-risk levels) and aided in building an accurate risk assessment matrix.

3.3.3. Static Risk Factor Rating

The context in which a driver needs to perform a driving-related task can vary (i.e., *high risk, medium risk,* or *low risk*), depending upon the characteristics of the environment. After applying the proper weighting factor from the sensitivity analysis, individual roadway characteristics were categorized into risk groups. The corresponding class defined the context of the risk category in which the highest numbers of roadway components were classified (i.e., high, medium, or low).

3.4. Phase III: Absolute Contextual Complexity

The project's third phase assembled the results obtained from the dynamic contextual complexity from phase one along with the static contextual complexity from phase two to construct an absolute contextual complexity. Since no data sources existed which provided both the static and dynamic features, this research used clues from the Waymo data to georeference a small test population of the dynamic data to develop an absolute contextual complexity metric to be classified and then compared. Figure 3.8 shows the workflow including the main tasks and their associated sub-tasks performed during this phase.

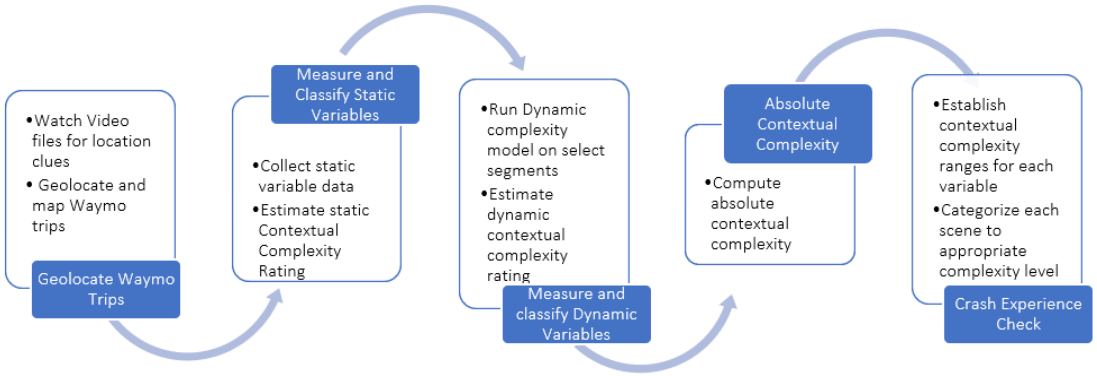

Figure 3.8. Method Flow-Chart - Absolute Contextual Complexity Model Building Process

3.4.1. Geolocate Waymo Trips

Waymo's open-source data did not include the location of the autonomous vehicle. Due to privacy concerns, location data was excluded from the dataset. However, location data is essential to obtain static characteristics of the driving scene to estimate Static Contextual Complexity. Furthermore, it is critical to retrieve crash data for validation tests which are linked to specific locations ("Crash Experience Check," see Figure 3.8). An indirect method was used to identify the location of the Waymo trip using wayfinding and landmarks. The subsequent steps used to obtain location data are listed below:

- Step 1: Identify points of interest (POI): The video of the Waymo trip segments were scanned for any POI information. Examples of the POI included street names, hospitals, restaurants, etc., that could be searched and located on a Google map.

Figure 3.9 shows an example of POI information from video footage of an actual Waymo trip. The POI is the street name sign, “Grant O Farrel”, in San Francisco.

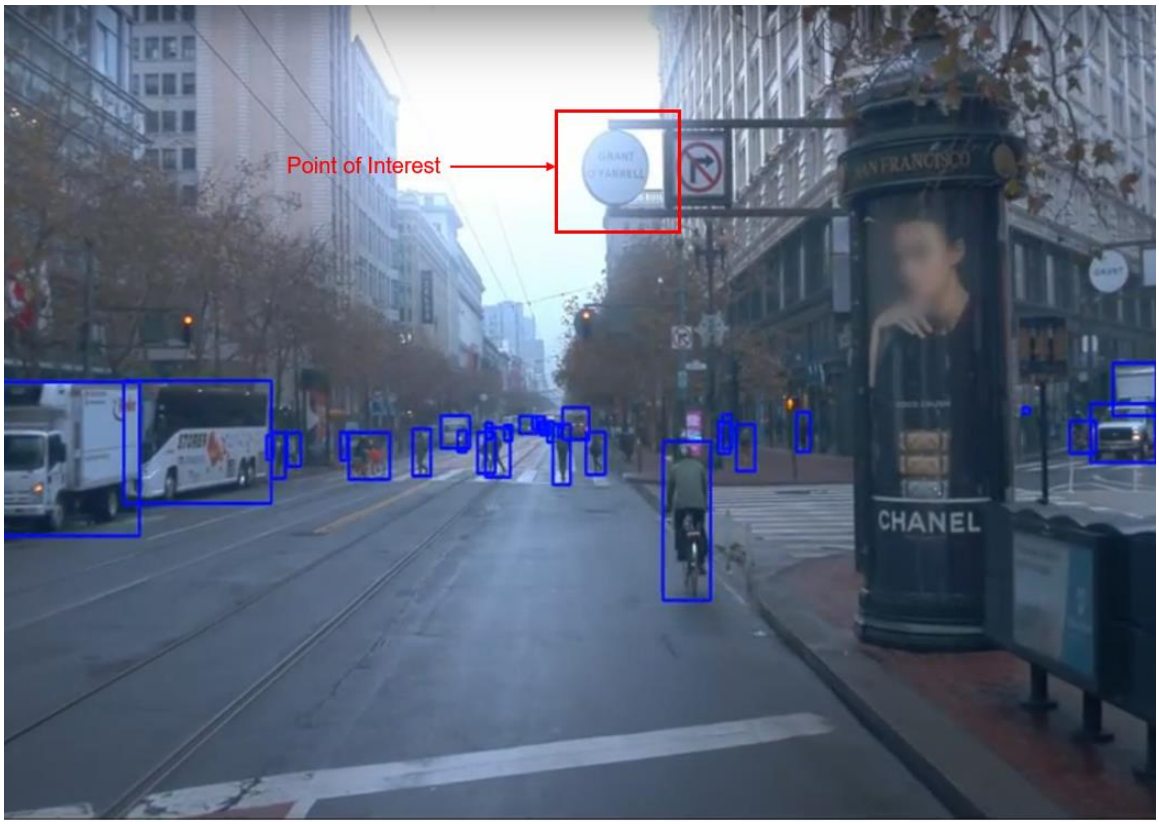

Figure 3.9. POI information from video footage.

- Step 2: Geolocate POI on Google Maps: The location of the POI was found on Google maps and recorded. Figure 3.10 shows the location of “Grant O Farrel Street” on Google maps.

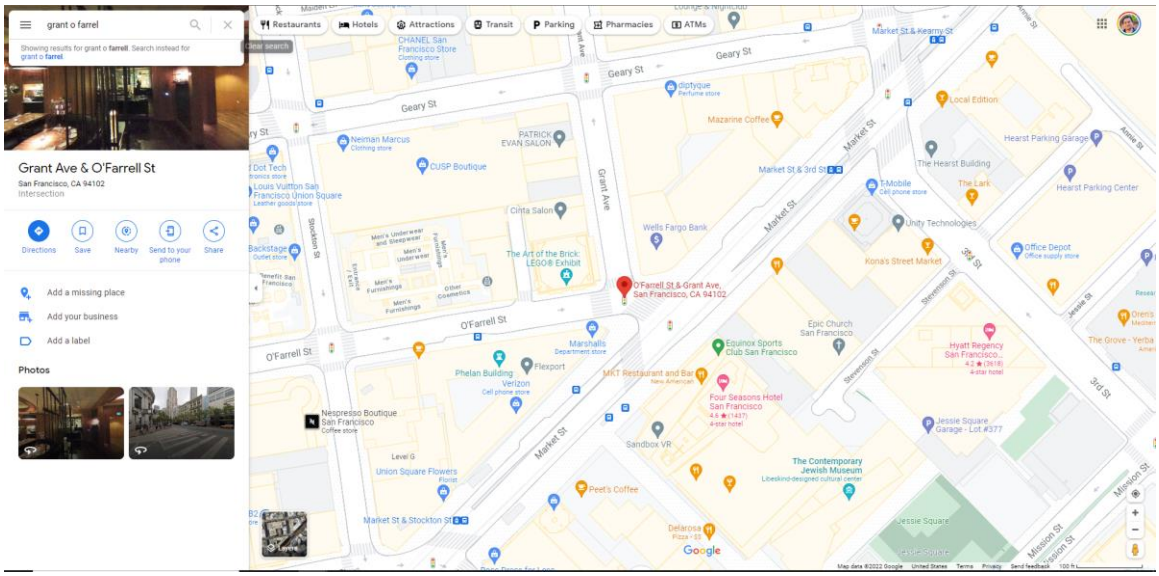

Figure 3.10. Location of "Grant O Farrel" on Google maps.

- Step 3: Verify location using Google street view: After locating the POI, Google Street View was used to match the scene with the Waymo video footage. Figure 3.11 shows a side-by-side verification of "Grant O Farrell Street" which was identified in the video footage and linked to the Google street view.

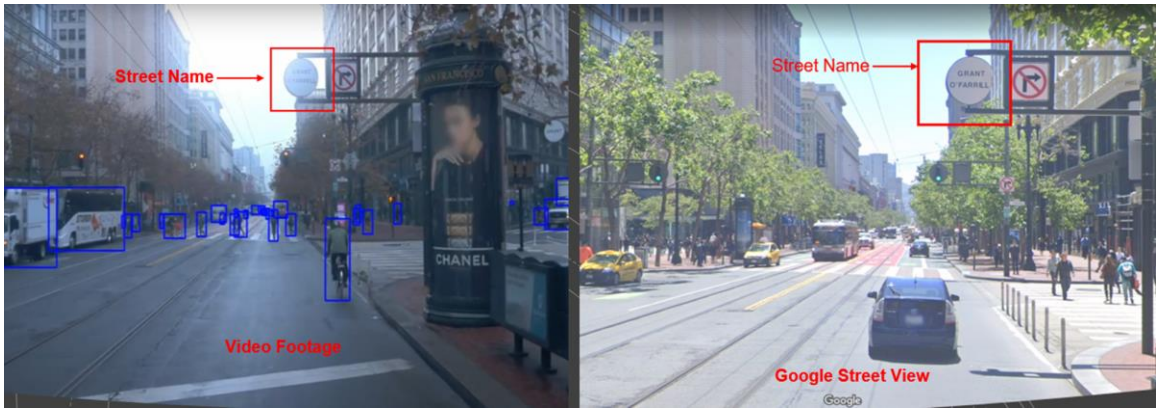

Figure 3.11. Google Street View and Waymo video footage verification.

- Step 4: Geo-locate and trace the path: When the Waymo video and Google Street View footage were identical, the course of the trip was geo-mapped using Geographical Information Systems (GIS) software (e.g., QGIS). Figure 3.12 below shows an example of a Waymo path geo-coded in QGIS software.

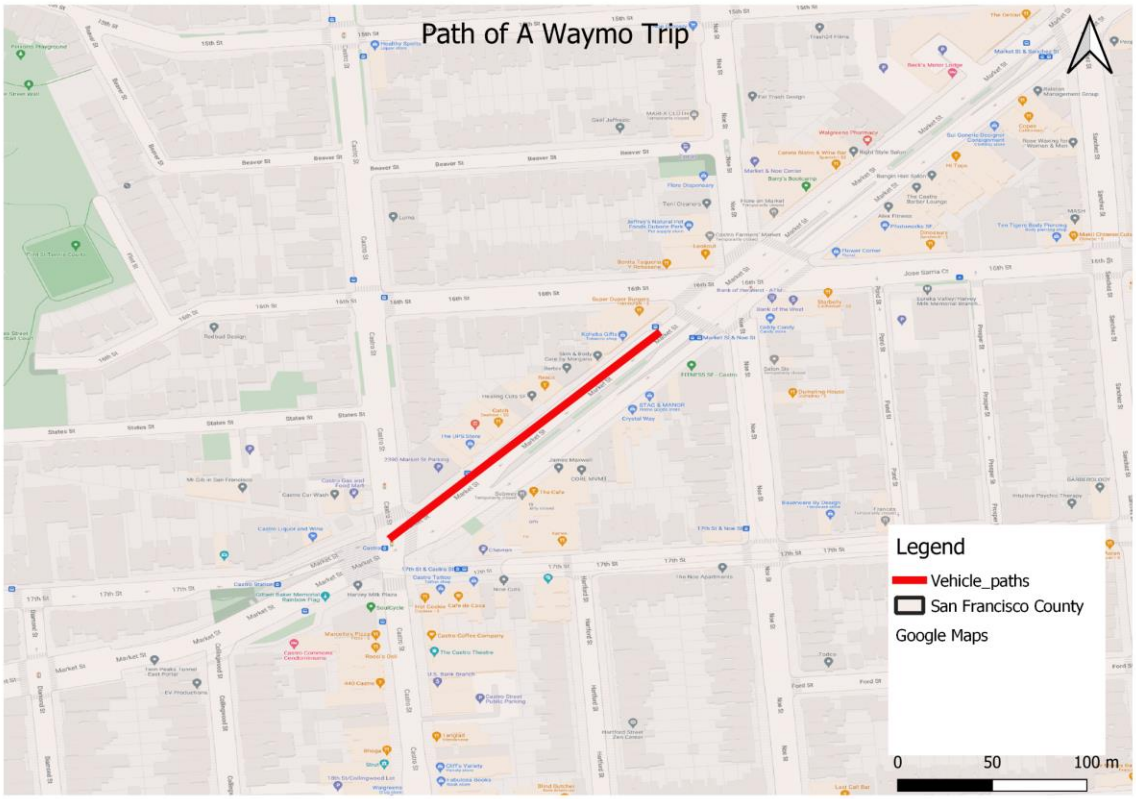

Figure 3.12, Path of a Waymo Trip

The open-source dataset consisted of AV data in three locations, namely, San Francisco, Mountain View, and Phoenix. San Francisco was the only city with publicly available historical crash data out of these three cities. As a result, data analysis efforts focused on San Francisco. A total of nine trip locations were identified and traced using the steps outlined above. Figure 3.13 shows the locations of the vehicle paths within the boundary of San Francisco County.

Figure 3.13, Locations of Waymo Trips in San Francisco City.

3.4.2. Measure and Classification of Static Variables

After a trip's location and its path were identified, the path was fragmented into individual intersections and segments. These intersections and segments were analyzed independently by measuring the critical variables (listed in Table 3.2) and classifying them into the appropriate risk categories. This procedure was carried out for all nine trips mapped in Figure 3.13. Table 3.3a, 3.3b, and 3.3c are associated with trips on Market Street (between 3rd Street and Grant O'Farrel street) (Figure 3.12). The trip encompasses two intersections and one segment, respectively. Table 3.3a lists the variables, measurements/values, and their risk category for the segment component of the trip.

Table 3.3a, Static variables and their risk on the Market Street segment (between 3rd street and Grant O'Farrell Street).

SEGMENTID	**segment-4641822195449131669_380_000_400_000_with_camera_labels**	
Market Street		**Risk**
Roadway Type	4U	Medium
Length (miles)	0.078	NA
Parking Type	Parallel Commercial	High
Parking Length	0.078	High
Median Width (ft)	10	High
Lighting Present	Present	Low
Auto Speed Enforcement	Not Present	High
SEGMENT RISK		**HIGH**

The risk category with the highest frequency of variables will ultimately be the category for the entire segment/intersection. For the segment presented in Table 3.3a, 4 out of 6 variables were classified as high-risk. Therefore, the segment was categorized into “high-risk.” Similarly, the intersection at Market Street and 3rd Street (Table 3.3b) and Market Street and Grant O’Farrel Street were classified as “high-risk” intersections since the majority of the variables were classified as “high”.

Table 3.3b, Static variables and their risk at the intersection of Market Street and 3rd Street.

Intersection: Market St and 3rd St		**Risk**
Lighting	Present	Low
# Approaches with a left-turn lane	0	High
# Approaches with a right-turn lane	0	High
# Approaches with a left-turn phasing	0	High
Type of Signal Phasing	Permissive	High
Approaches RTOR Prohibited	0	High
Bus-stops Near Intersection	2	Medium/High
Schools Near Intersection	None	Low
# Alcohol Establishments	12	High
INTERSECTION RISK		**HIGH**

Table 3.3c, Static variables and their risk for at the intersection of Market Street and O'Farrel Street.

Intersection: Market St @ O'Farrel Street		**risk**
Lighting	Present	Low
# approaches with a left-turn lane	1	Medium
# approaches with a right-turn lane	0	High
# approaches with a left-turn phasing	0	High
Type of Signal Phasing	Permissive	High
Approaches RTOR Prohibited	0	High
Bus-stops near intersection	2	Medium
Schools Near Intersection	None	Low
# Alcohol establishments	12	High
INTERSECTION RISK		**HIGH**

The absolute static risk of the trip was determined by categories with a maximum frequency of segments and intersections. Both intersections and segments were classified as high-risk for Market Street between 3rd Street and Grant O'Farrel. Therefore, the absolute static risk of the trip is high, indicating the static environment is risky (Table 3.3d).

Table 3.3d, Absolute static risk of the trip.

Trip ID	**segment-4641822195449131669_380_000_400_000_with_camera_labels**
Market Street	High
Market St and 3rd St	High
Market St and Grant O Farrel St	High
Absolute Static Risk	**High**

3.4.3. Measure and Classify Dynamic Variables

To measure and classify a segment's dynamic complexity, the model developed in phase-1 of this methodology was applied to the trip under consideration. The result of the model determined the dynamic complexity of the segment. For the example trip under consideration in Figure 3.12, which is on Market Street (3rd Street and Grant O'Farrel Street) in downtown San Francisco, the model results are shown in Figure 3.14 below.

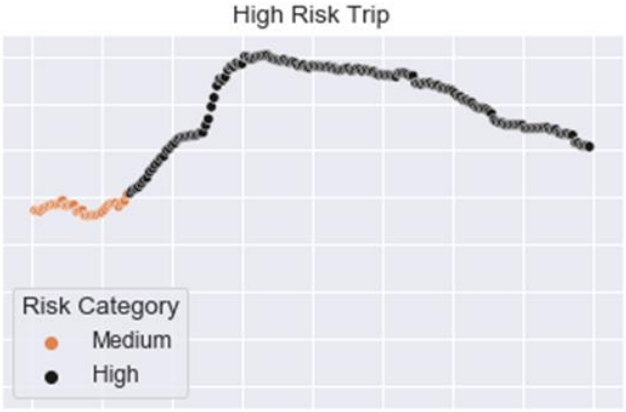

Figure 3.14, Dynamic complexity of trip on Market Street (between 3rd street and Grand O'Farrel Street).

The figure shows 200 point clusters (one point for each LiDAR data frame) categorized into High and Medium complexity. The trip started as a medium complexity trip and transitioned into a high-complexity trip and remained there. The greatest number of points were classified as high-complexity; therefore, the dynamic complexity of this trip was high.

3.4.4. Absolute Contextual Complexity

Absolute contextual complexity is the combination of static and dynamic contextual complexity. The results of the total static risk and dynamic complexity from the previous steps were used to determine the total complexity of the trip. For example, the trip on Market Street (between 3rd Street and Grant O'Farrell Street) in San Francisco, the static and dynamic complexity was ‘high’; therefore, the method classified the absolute complexity of the entire trip as ‘high.’

Table 3.4, Absolute contextual complexity

Trip Location	**Static Risk**	**Dynamic Complexity**	**Absolute Complexity**
Market Street (Between 3rd & Grant O’Farrel Street)	High	High	High

3.4.5. Crash Experience Check

In this step, the historical crash data was extracted, and it was correlated with the absolute contextual complexity for validation of the method. A public repository of San Francisco county crash data was downloaded. Figure 3.15 shows a map of all the crash data locations for the county of San Francisco.

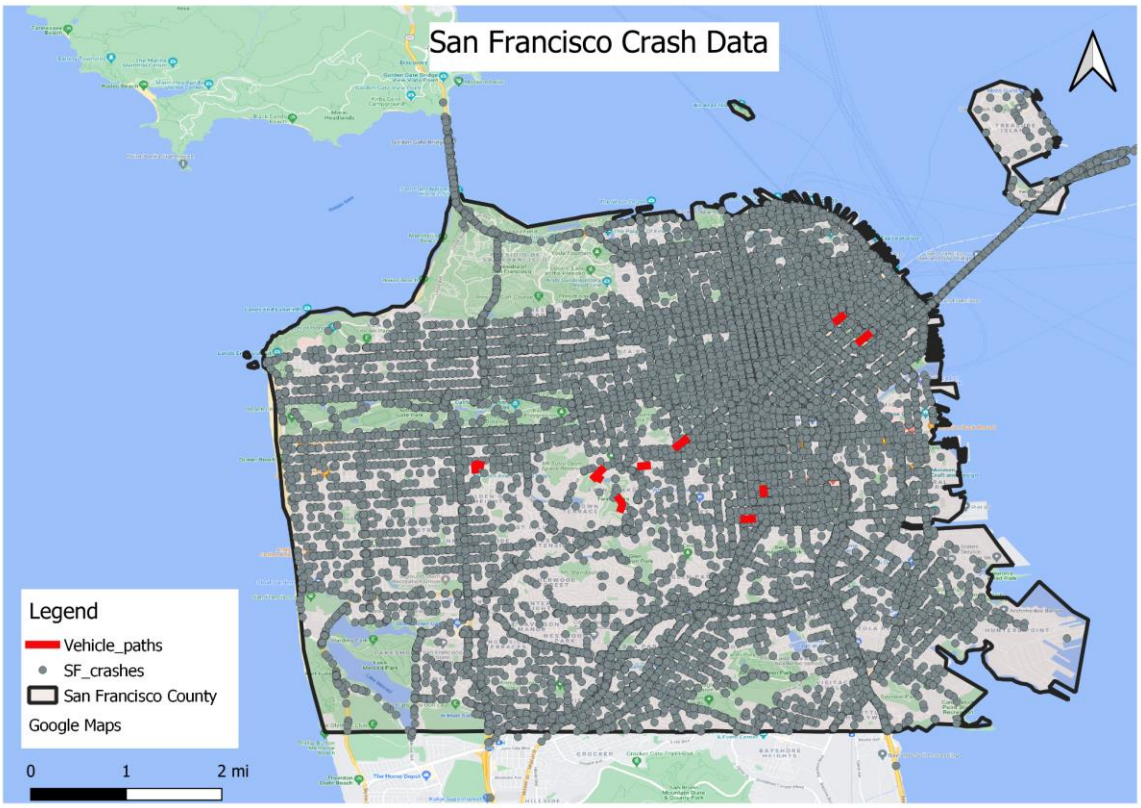

Figure 3.15. Crash data for San Francisco County

CHAPTER FOUR

ANALYSIS AND RESULTS

This research study focused on developing a methodology to assist DRSs in understanding and estimating the complexity of the routes used for on-road driving evaluations for medically-at-risk drivers considering both static and dynamic characteristics of the roadway environment. The study utilized the autonomous vehicle dataset released by Waymo to build the driving environment's static and dynamic complexity models. This chapter discusses the analysis process and the results while using a similar structure as the preceding methodology chapter.

This chapter has been divided into four phases to achieve the study's goals and objectives. Figure 4.1 shows the framework highlighting the four stages.

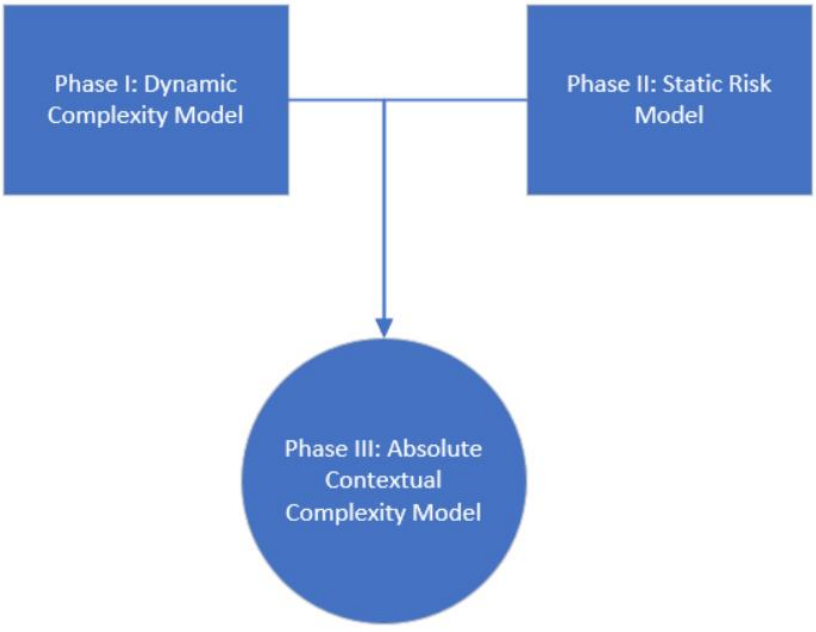

Figure 4.1. Analysis chapter flow-chart

The phases and their objectives are reiterated below:

1. Phase I – The Dynamic Complexity Model: focuses on the analysis of the results which allows for the dynamic model to estimate contextual complexity.
2. Phase II – The Static Risk Model: This phase describes the sensitivity analysis of the variables outlined in AASHTO's Highway Safety Manual (National Research Council et al., 2010) to determine the most critical variables. This phase discusses the risk ranges for each variable which lead to tables for the guidance manual.
3. Phase III - Absolute Contextual Complexity Model: This step is the culmination of the work from the previous two phases. This section discusses results from the model implementation on a sample of segments from the AV trip repository to determine the total contextual complexity.

4.1. Dynamic Complexity Model:

The discussion in this section is divided into two parts:

1. The first part presents the analysis and results of the model development using a statistical approach (i.e., Section 3.2.4 Contextual Complexity Factor Model from Chapter 3).
2. The second part explains the analysis and results of the model development using an unsupervised clustering approach (i.e., Section 3.2.7 Dynamic Complexity Factor Rating from Chapter 3).

4.1.1. Statistical Modeling Approach

A total of 798 trips of perception data, comprised a total of 158,090 LiDAR point cloud frames, were analyzed to develop the contextual complexity factor (CCF) model to measure dynamic complexity. Table 4.1 provides a list of all the variables available after processing the raw AV data. The first column of Table 4.1 includes the variable's name, the second column describes the variable, and the third column provides information on the variables derived from one or more combinations of raw variables.

Table 4.1. Variables extracted after processing the AV data

Variable Name	Description	Derived
file_name	This is the waymo trip segment ID	N
frame	Lidar frame number	N
velocity	Waymo vehicle velocity (mph)	N
ssd_2.5	Stopping sight distance of the Waymo vehicle with given velocity and reaction time of 2.5 seconds (feet)	Y
cov	Cone of vision expressed in degrees	Y
tot_objs_video	Total objects identified in the Waymo's 6 camera frames	N
tot_objs	Total objects identified in the Waymo's LIDAR point cloud	N
mean_obj_dist	Average distance of all the objects from Waymo AV (feet)	N
min_dist	Distance of the nearest object from Waymo AV (feet)	N
max_dist	Distance of the farthest object from Waymo AV (feet)	N
dist_sdev	Standard deviation of the object distances from Waymo AV	N
inv_dist_sum	Sum of inverse distance sum of all the objects in the LIDAR frame	Y
objs_within_180	Total objects with in 180 degrees cone of vision of the Waymo AV (1st and 4th quaderant with vehicle driving north)	Y
inv_dist_sum_within_180	Sum of inverse distance of the objects within 180 degree cone of vision	Y
objs_within_ssdcov	Total objects within the cone of vision (COV) and stopping sight distance	Y
inv_dist_sum_within_ssdcov	Sum of inverse distance of objects within COV and SSD	Y
weather_rain	Presence of rain (binary)	N
weather_sunny	Sunny day (binary)	N
location_location_other	Other location (binary)	N
location_location_phx	Phoenix location (binary)	N
location_location_sf	San francisco location (binary)	N
time_Dawn/Dusk	Dawn/Dusk (binary)	N
time_Day	Day (binary)	N
time_Night	Night (binary)	N

Figure 4.2 provides statistical distributions of the sample size for all the critical variables used to develop the CCF model. The maximum accurate range of the long-range LiDAR

mounted on the vehicle was 250 feet, corresponding with a maximum safe operating speed of 35 mph based on human SSD requirements. Objects beyond that range were less likely to be detected or classified. Thus, frames with vehicle speeds exceeding 35 mph were excluded from the analysis (approximately 13% of the total frames). Additionally, there were a substantial number of frames where the vehicle was not moving (zero speed) due to the urban and ultra-urban settings along with stop-and-go traffic operations. The SSD and the COV were also zero, which skewed the sample towards zero. Thus, frames with speeds less than 0.1 mph were excluded from the analysis. After clipping the frames with speeds greater than 35 mph and less than 0.1 mph, the sample size was reduced to 108,369 frames (68.54% of the total possible frames). Figure 4.3 shows the distribution of the critical attributes for 68.54% of the data after the trimming process was used in the CCF model building.

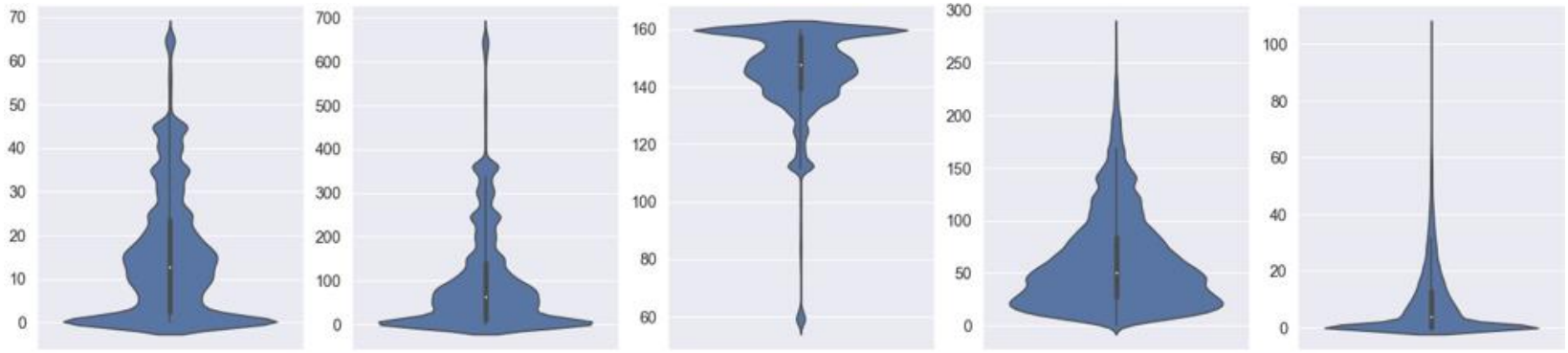

Figure 4.2. Statistical distributions of critical variables before the clipping.

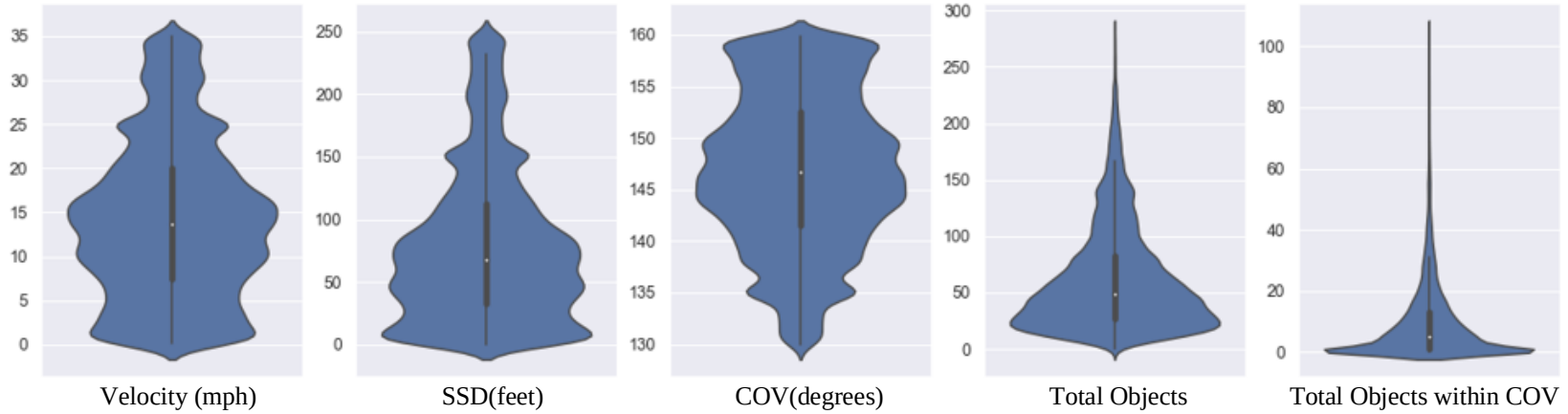

Figure 4.3. Statistical distributions of critical variables after the clipping the frames with speeds greater than 35 mph and less than 0.1 mph.

From the literature review, the key variables when measuring visual-clutter and cognitive load are the density of the objects and their proximity to the vehicle. As the number of objects in the driving environment increases, the amount of information that needs to be processed by the driver also increases, thus increasing the driver's cognitive load. Further, near objects present a greater risk to the driver than more distant objects. To measure these two important parameters, a CCF was estimated for each frame using Equation 4.1.

$$CCF = \Sigma(1/obj_{distance}) \quad \text{- Equation 4.1}$$

Where $obj_{distance}$ = distance of the object from the autonomous vehicle (feet)

The inverse distance assignments allowed scene elements to be weighted in descending order, with near objects receiving higher weights and more distant objects having lower weights. This accounted for the limited reaction time associated with objects that are nearer to the driver's vehicle. The summation of these inverse distance assignments for objects in the driving environment accounted for the total number of objects in the scene, i.e., object density. The scene CCF was estimated for each frame considering all the objects. Additionally, CCF was estimated for the COV filter in each frame. This provided an estimate of complexity within the driver's COV. Statistical quartiles for the total sample were estimated for the entire scene CCF and for CCF within the COV. A frame was categorized as high if the CCF > 75th percentile, medium if CCF was in inter-quartile-range between 25th percentile & 75th percentile, and low if CCF was less than 25th

percentile, respectively. All the frames were assigned a high, medium, or low category based on the scene CCF's respective quartile range.

The analysis provided a frame-by-frame comparison of contextual complexity based upon the density of objects and their proximity to the autonomous vehicle as represented by the CCF. All trips were categorized as high, medium, or low-complexity trips based upon the statistical mode of the trip's CRF category.

Figure 4.4 provides an example of three such trips categorized as low, medium, and high-contextual complexity trips. The figure consists of a 2x3 matrix of complexity plots. Each column contains two graphs of an individual trip. The left column is for a low-complexity trip, the middle column is for a medium- complexity trip, and the right column is for a high-risk trip. The x-axis represents time in seconds. The y-axis describes the CRFs. The top row illustrates CCF for the entire scene, and the bottom row displays CCF within the COV. The corresponding video of each of these trips is provided in the respective hyperlinks (High link.link; Medium link.link; Low link.link).

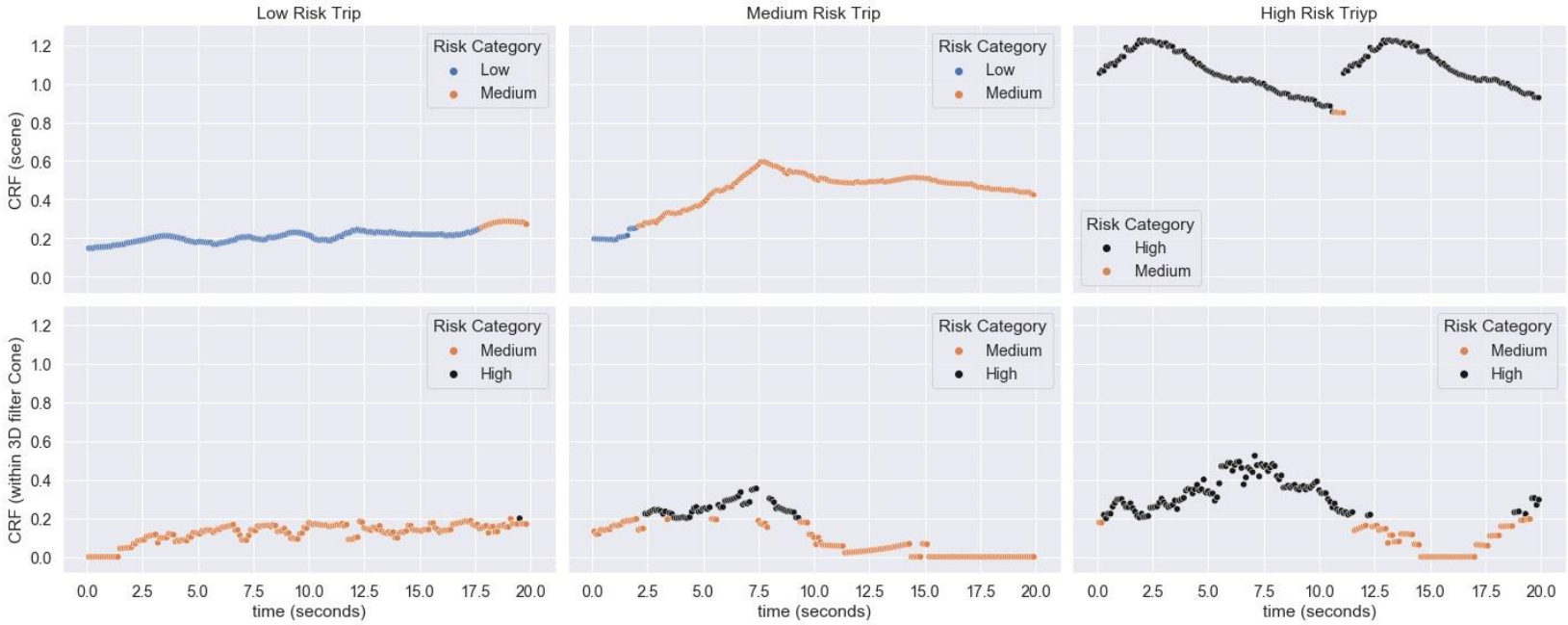

Figure 4.4. CCF plots for high, medium, and low-complexity trips (velocity >0.1 mph and <= 35mph)

The upper right plot in Figure 4.4 shows a high-complexity trip on a 2-lane urban road in an ultra-urban area. The trip predominantly consisted of a high density of objects close to the vehicle. The trip started with a medium-complexity context for 3 seconds and transitioned into a high-complexity context for the remainder of the trip. After 3 seconds, the vehicle entered an intersection with many vehicles, pedestrians, and bicyclists, thus elevating the CCF. After traversing the intersection, the vehicle entered another 2-lane urban road with curbside parking, moving vehicles and pedestrians nearby, maintaining an elevated CCF. The bottom right plot shows the resulting CCF within the driver's COV. The CCF within the driver's COV (bottom right plot in Figure 4.4 and the overall CCF of the scene (top right plot in Figure 4.4) vary greatly. This is because many objects fall within the driver's COV at the start of the trip as the vehicle traversed the intersection, making it high complexity for the driver. The contextual complexity in the driver's COV later diminished to a medium and then a low complexity as the vehicle decelerated and came to a standstill (between 15-17 seconds).

The medium-complexity trip (middle top and bottom plots in Figure 4.4 consisted of an urban multi-lane highway with a center two-way-left-turn lane. At the start of the trip, there were a few objects in the scene, making it a low-complexity environment. At the 2-second mark, pedestrians and bicyclists prepared to cross the road and were detected, which elevated the complexity gradually to medium as the vehicle advanced. This trend is noticeable in the top middle plot. The corresponding CCF within the driver’s COV also intensified to a high-complexity, which is represented in the bottom middle plot.

The low-complexity trip was comprised of vehicles driving on a local neighborhood road with no moving vehicles, pedestrians, or bicyclists. The entire scene complexity remained low for a significant part of the trip. On the contrary, the CCF within the COV remained at medium complexity throughout the trip except at the beginning when the vehicle accelerated from standing still.

Based on the visual inspection of the trips, the three examples (high, medium, and low) accurately characterized the contextual complexity of the driving environment. Table 4.2 below provides the ranges for all critical variables to classify into appropriate complexity categories.

Table 4.2., Critical variables and their complexity class ranges.

Dynamic Variables	**High**	**Medium**	**Low**
Velocity (mph)	0-40	0-66	0-67
Object Density	44-282	8-64	0-53
Object Distance (feet)	89-196	38-143	0-337

The statistical modeling approach satisfactorily represents the contextual complexity of the driving environment. However, one impediment of the methodology is that the quartiles do not paint the picture with sufficient granularity. It can be seen from Table 4.2 that the variables overlap between different complexity classes. To overcome this, a machine learning approach using an unsupervised clustering method was tested, which is discussed in the next section.

4.1.2. Machine Learning Approach

This section explains the approach using an unsupervised clustering analysis to build a model to classify complexity accurately. Specifically, k-means were used for clustering and hierarchical clustering algorithms to building the model.

Figure 4.5 and 4.6 show the statistical distribution of the critical variables chosen for modeling. Figure 4.5 provides the histograms of the variables, while Figure 4.6 demonstrates the density of the data points.

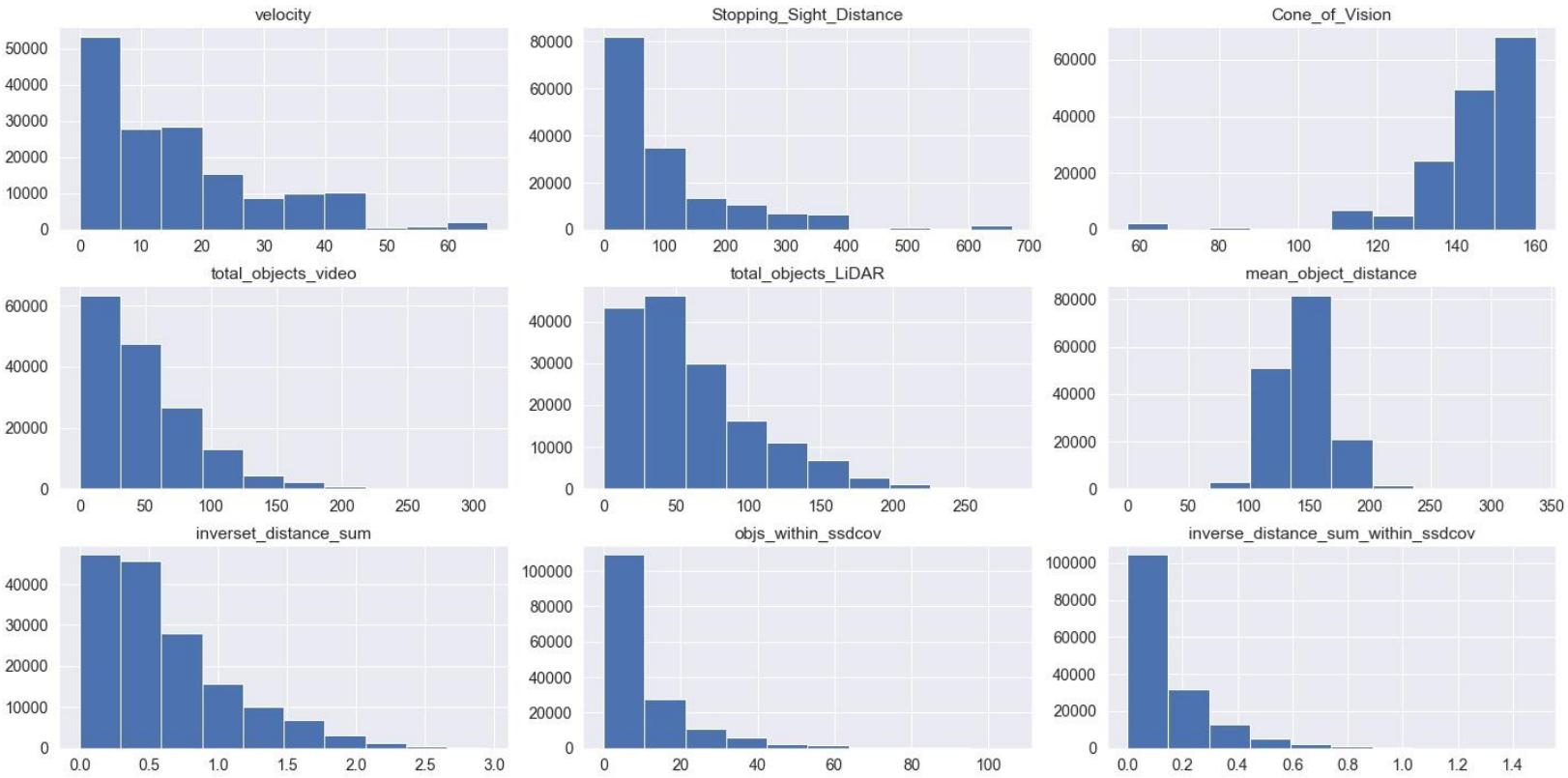

Figure 4.5, Histogram of different attributes from Waymo Autonomous Vehicle Data

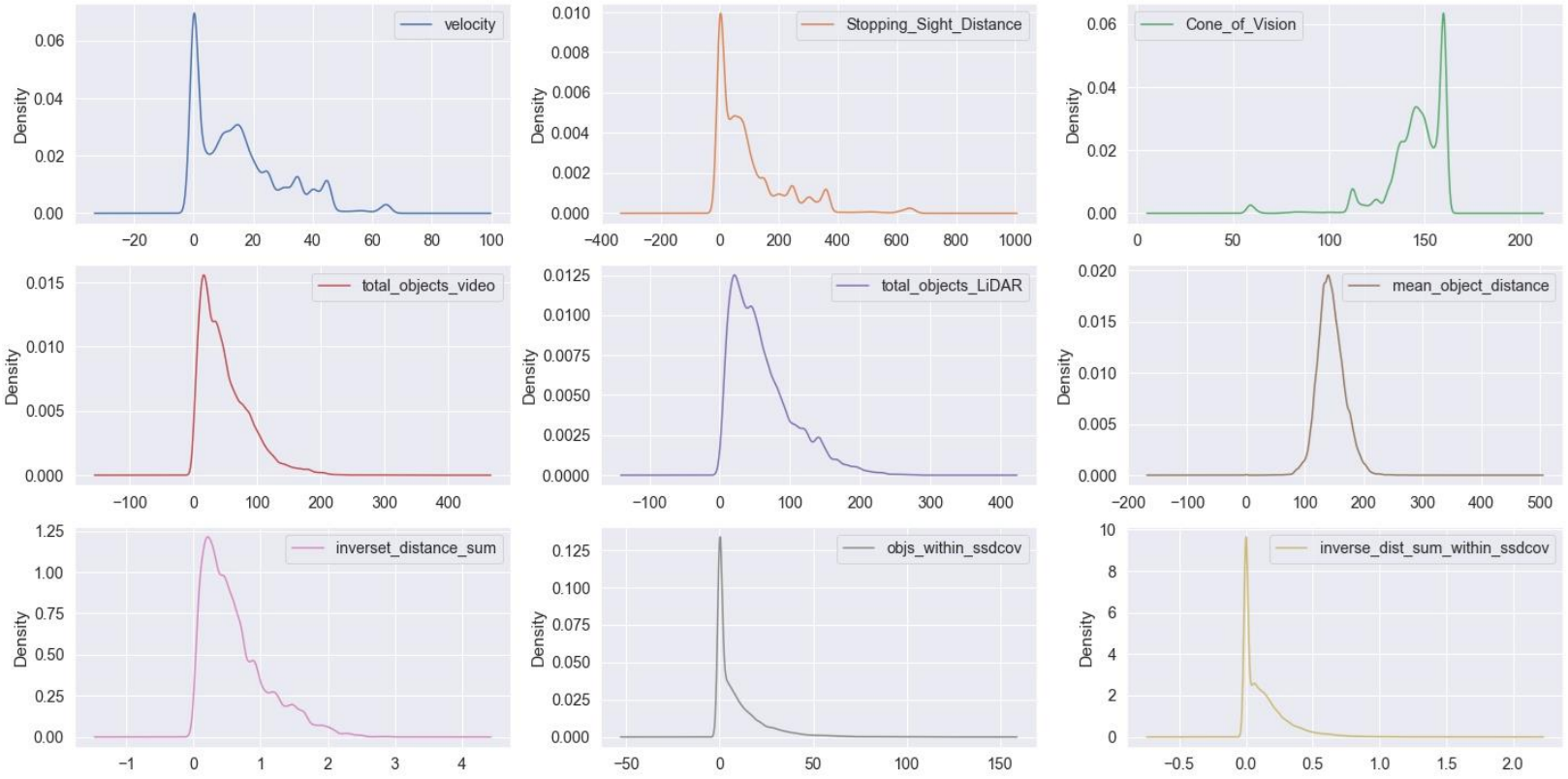

Figure 4.6, Density plots of different attributes from the AV data

It is evident from the density plots in Figure 4.6 that the data for different variables are not uniformly represented. For example, velocity, stopping sight distance, and object density are skewed towards the left (i.e., more samples are available). This is because a substantial number of frames included vehicles at a standstill when the data were collected in urban and ultra-urban settings with stop-and-go traffic. The SSD and COV were also zero at zero speed, which resulted in oversampling. In the statistical approach, this data was clipped to eliminate the bias. However, in the machinel learning approach a consolidation technique was applied which is explained further.

Most machine learning algorithms developed for classification were designed to assume an equal number of samples for each class. Using highly skewed or imbalanced data results in poor classification performance models (Krawczyk, 2016). This is true for k-means and hierarchical clustering algorithms used for clustering model. The skew can be mitigated in two ways:

1. Undersampling of the over-represented class
2. Oversampling of the under-represented class

An undersampling approach was considered for these analyses. The LiDAR frames are represented as a factor of time, i.e., the point cloud was collected at a frequency of 10 Hz/Second. Thus, every trip of 20 seconds has 200 frames of LiDAR point cloud data. Since substantial LiDAR frames were collected at a very low or zero speed, a logical

solution was to aggregate the data by distance. An aggregation distance of 10, 20, and 30 feet were considered for normalizing the data.

Figure 4.7 shows the normality plots for the variable velocity at different aggregation distances. The red line that extends diagonally on the chart is a theoretical normal curve plot. The thick blue dots below the theoretical normal curve (see the red-line) represents the normal curve of the Waymo data. The top left plot exhibits the normality plot for unaggregated data (i.e., 0 feet aggregation). The top right plot represents 10 feet aggregation, the bottom left displays 20 feet aggregation, and the bottom right shows 30 feet aggregation. It is evident from the graphs that the raw data has a lot of frames clustered at a velocity of zero. At 10 feet aggregation, this improves, and more points move towards the theoretical normal curve. Further, this condition improves at both 20- and 30- feet aggregation, and the sample more closely resembles a normal curve. Subsequent consolidations did not improve the normality of the dataset. Thus, a consolidation distance of 30 feet was selected for use for the model development.

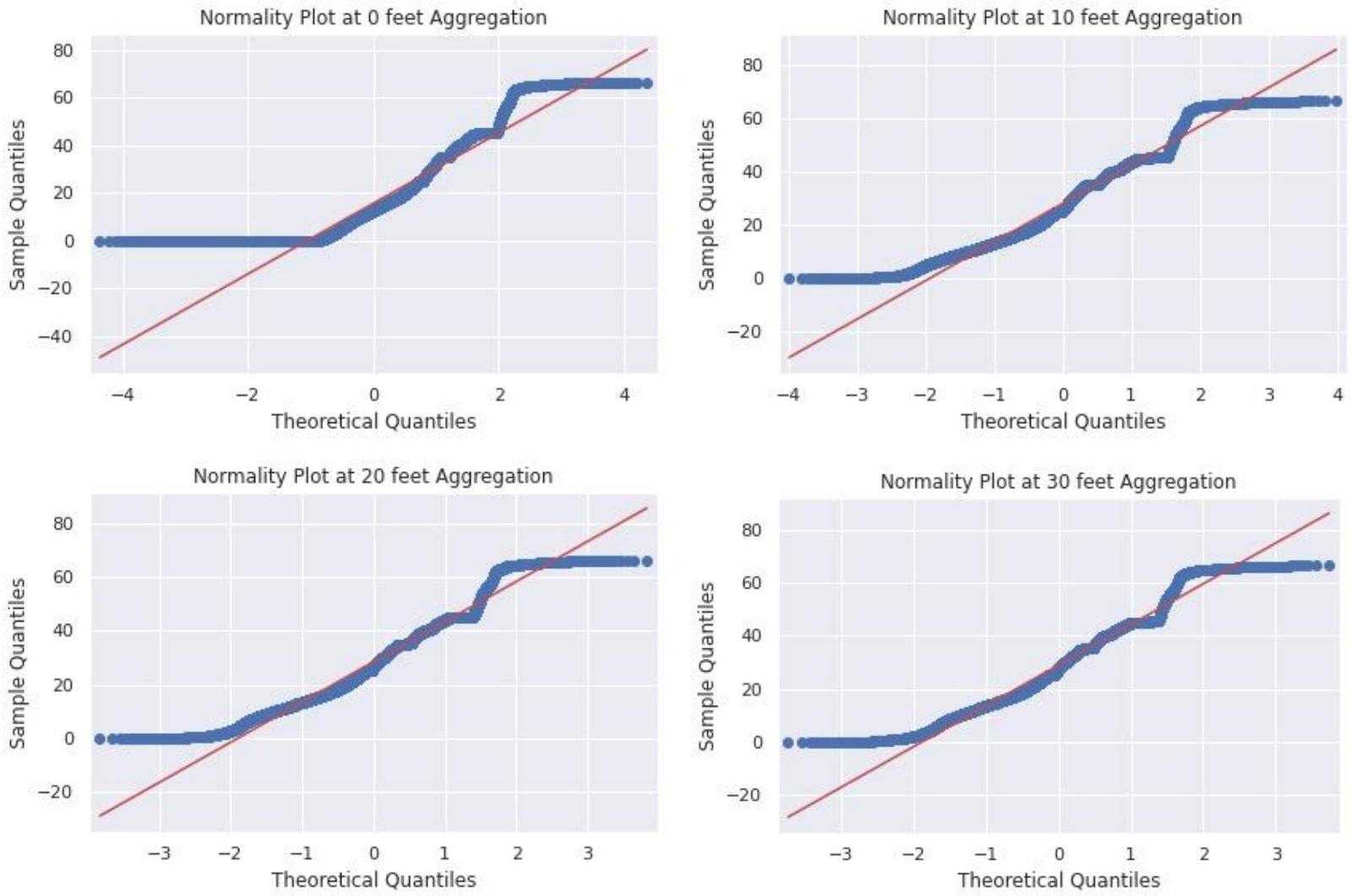

Figure 4.7. Normality plots for different aggregate distances

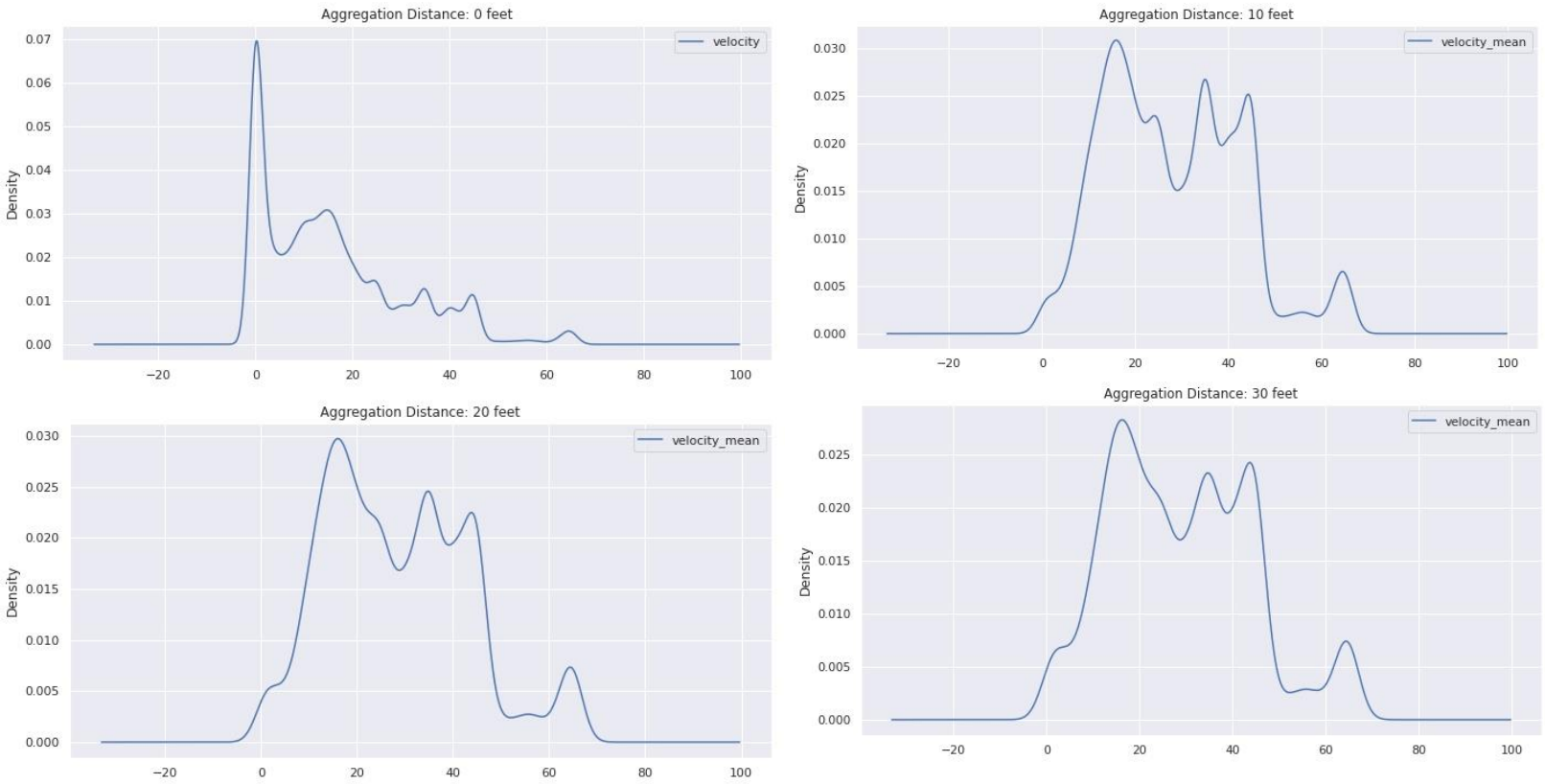

Figure 4.8. Density plots for different aggregation distances

Figure 4.8 demonstrates density curves at different levels of data consolidation. The aggregation reduced the number of zero velocity frames from the analysis while simultaneously increasing the number of high-velocity frames. There is a noticeable change in the data distribution between the unaltered dataset (i.e., 0 feet consolidation) and 30 feet consolidation. Although the density distribution of the dataset looks less than the ideal curve characteristic of a normal curve, the data is closer to representing data between all the classes.

Identifying optimal aggregation distance is crucial for model development. Excess consolidation reduces the sample size significantly, rendering it insignificant for model development. On the other hand, insufficient consolidation retains the bias in the data, resulting in poor model performance. Figure 4.9 shows the plot of the sample size at different consolidation distances. Table 4.3 represents the same in tabular format. It can be observed that as the consolidation distance increases, the sample size reduces. At 30 feet aggregation, the sample size is 11003 frames. Further consolidation did not yield any improvement in the distribution of the samples. Thus, consolidation of 30 feet and sample size of 11003 was considered for building the unsupervised clustering model.

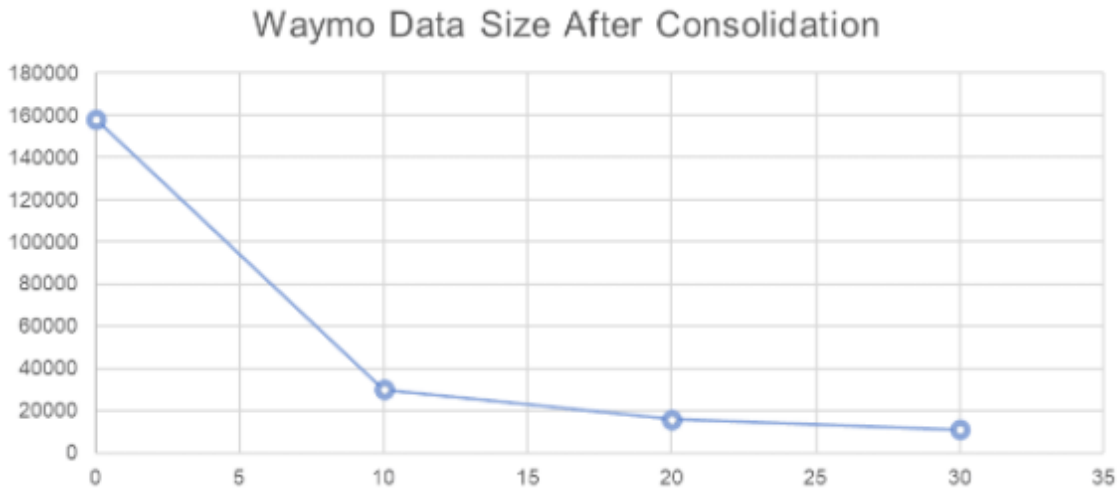

Figure 4.9. Data size at different aggregation distances

Table 4.3. Data size at different aggregation distances

Aggregation Distance	**Sample Size**
0	158090
10	29964
20	15851
30	11003

4.1.2.1. Feature selection

The variables that we use to train the machine learning models greatly influence the performance of the models. Irrelevant or partially relevant features can negatively impact model performance. The author performed principal component analysis (PCA) to identify the most important variables. Figure 4.10 and Table 4.4. below present the variables and their explained variance.

Table 4.4. PCA analysis results

Attributes	Explained variance
velocity	0.8818025176
obj_density_video	0.0047732978
obj_density_lidar	0.0034133763
mean_proximity	0.0011882991
inv_dist_sum	0.0002242688
objs_within_ssdcov	0.0000621344
inv_dist_sum_within_ssdcov	0.0000029339
dist_trav	0.0000023591
cum_dist	0.0000017586
weather_rain	0.0000009873
weather_sunny	0.0000001214
location_other	0.0000001191
location_phoenix	0.0000000364

Based upon the PCA analysis, the top 5 most critical variables are listed below in decreasing order of importance:

1. velocity: velocity of the vehicle
2. obj_density_video: total number of objects captured in the video camera
3. obj_density_lidar: total number of objects captured in the lidar point cloud
4. mean_proximity: mean distance of all the objects from the vehicle
5. objects_within_COV: total number of objects captured within the COV

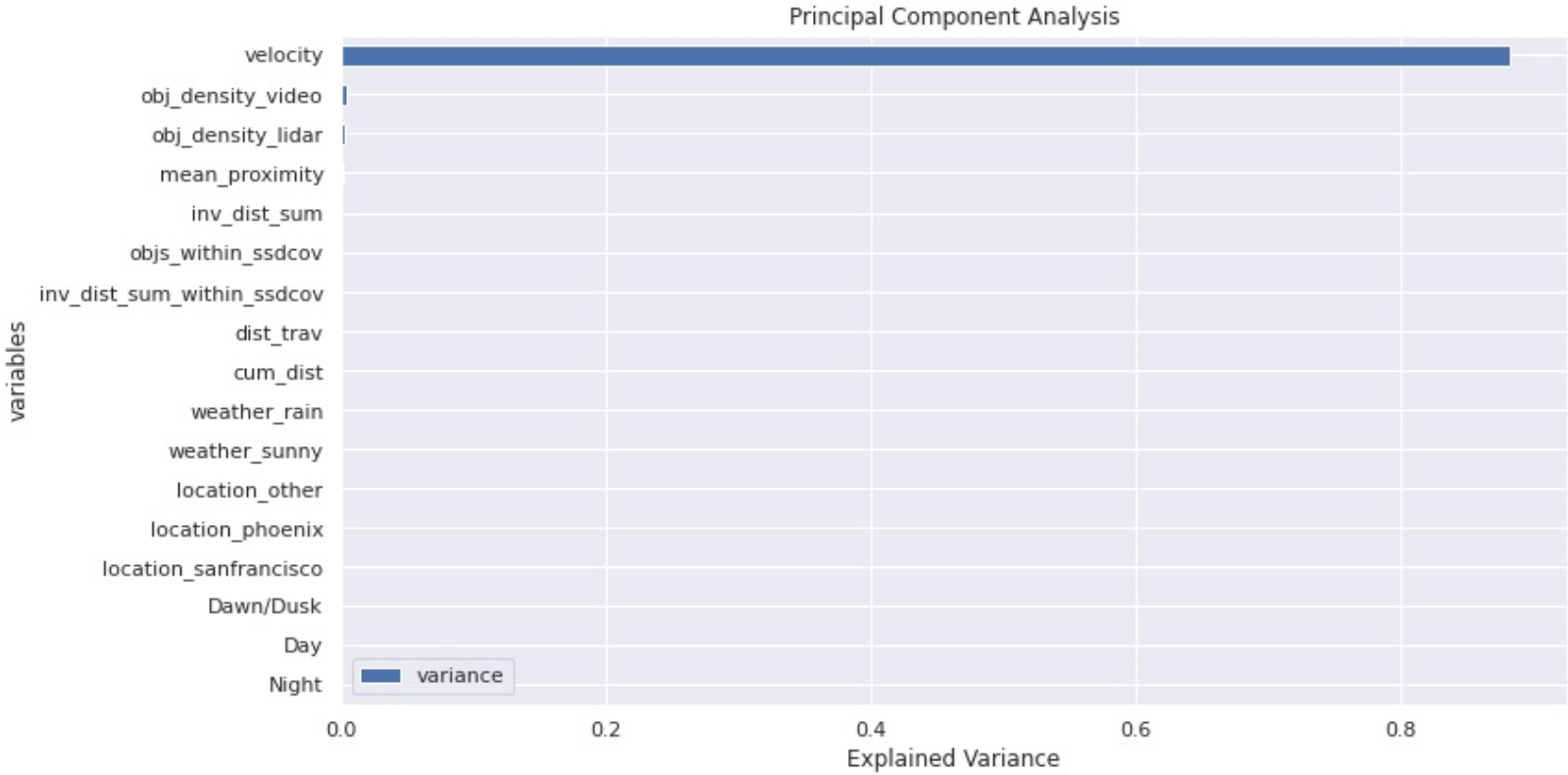

Figure 4.10. Principal Component Analysis Results

While PCA analysis identified the most important variables, it is also essential to identify the interaction between the variables. Table 4.5. shows the Pearson correlation coefficients between the variables. Green cells indicate a high positive correlation, and red cells indicate a high negative correlation. The variable "velocity" is highly correlated with variables "obj_density_lidar" and "obj_density_video." Velocity and total objects in LiDAR are negatively correlated, indicating that the total number of objects decreases as the velocity increases. On the other hand, "velocity" is positively correlated with "mean_proximity," indicating an increase in vehicle speed also increases the proximity of the surrounding vehicles. The proximity and density of the objects are weakly correlated.

Table 4.5. Correlation coefficients of variables

Pearson_Correlation_Coeff	**velocity**	**obj_density_video**	**obj_density_lidar**	**mean_proximity**	**objects_within_COV**
velocity	1	-0.2687	-0.4119	0.4139	0.5682
obj_density_video	-0.2687	1	0.8036	0.0053	0.0689
obj_density_lidar	-0.4119	0.8036	1	-0.1196	0.0927
mean_proximity	0.4139	0.0053	-0.1196	1	0.2134

From PCA and correlation results following variables are selected for clustering analysis:

1. velocity: This is the single most important variable with the highest variance that can be quantified and explained. Velocity also shows excellent interaction between other important variables (i.e., object density and proximity)
2. obj_density_lidar: Although PCA analysis ranked this variable below "obj_density_video," it shows superior correlation with velocity (Table 4.5).

Adopting the above variable will produce better model results because of its enhanced interaction.

3. mean_proximity: proximity to the nearest object is ranked fourth in the priority list captured from PCA analysis. It also demonstrates a significant correlation with the key variable “velocity.

Based on the inferences mentioned above, the author considered “velocity”, “object_density_lidar,” and “mean_proximity” to build the clustering model.

4.1.2.2. Clustering Analysis

Identifying an optimal number of clusters is essential for building a clustering model. However, for the intended audience of this research, i.e., DRSs, the author wanted to know how the clustering model would segregate the trips at different cluster values. The author used the elbow method to identify an ideal number of clusters through the distortion plots. The distortion is the sum of squares of points from cluster centers. It decreases with increasing clusters and becomes zero when the number of clusters equals the number of points.

Figure 4.11 shows the elbow line plot between cluster centers (x-axis) and the distortion (y-axis). The cluster centers range from a minimum of two to a maximum of 14 clusters.

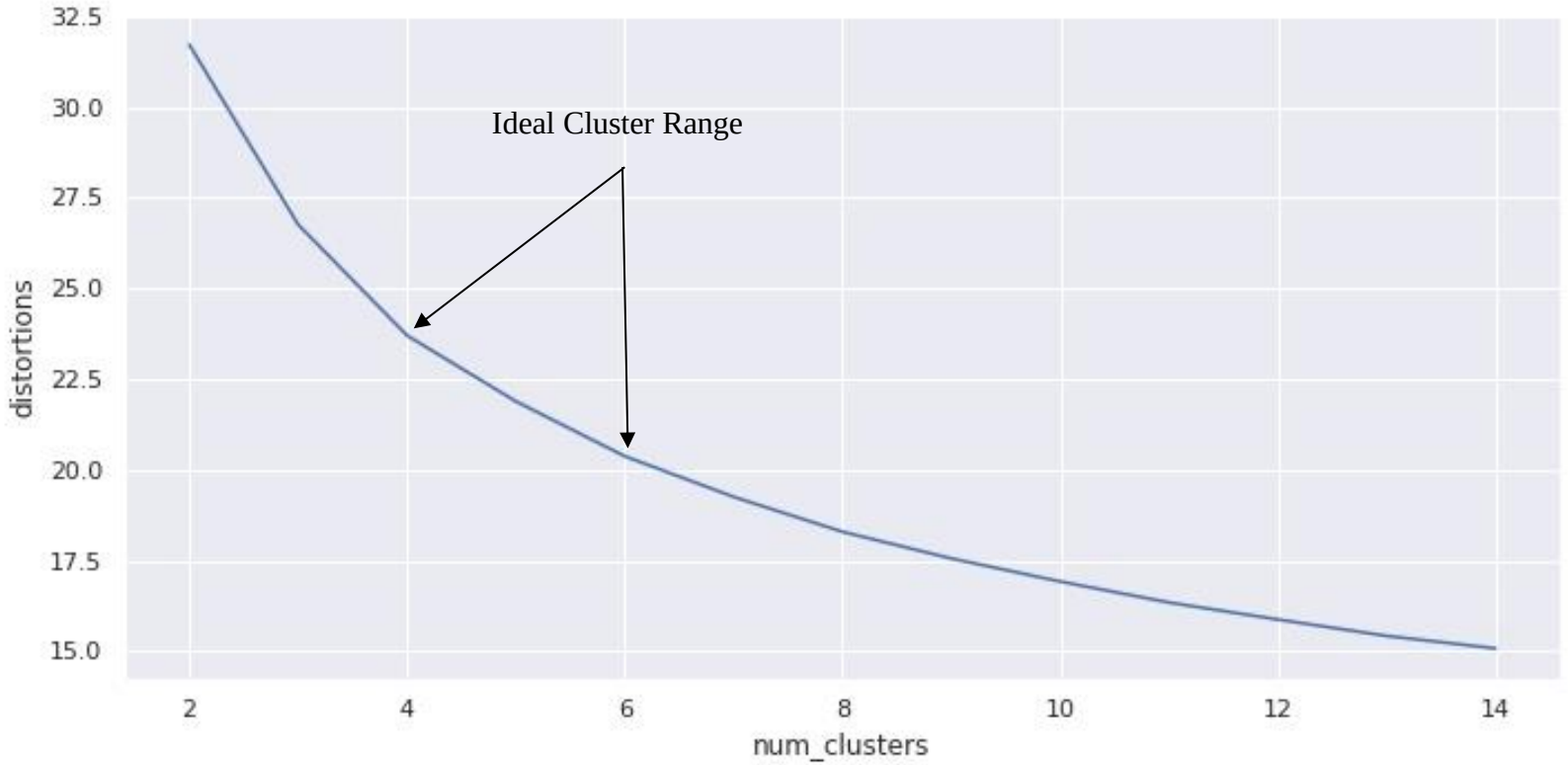

Figure 4.11. Distortion Plots from Clustering Analysis

The Elbow method indicates an optimal number of clusters for the model. It is generally identified at locations with an abrupt change in the slope of the line. The first abrupt change is observed at cluster 3; however, the distortion is still very high, indicating more separation possibility. Next, the difference is observed at clusters four, five, and six, after which the slope changes are barely noticeable. Anything less than four does not capture all the distinct grouping due to high distortion. Everything above six leads to too many groups and does not produce a notable reduction in distortion. Thus, the author considers an ideal cluster modeling spectrum ranges between four and five. Appendix A lists all 3D mesh plots for different cluster centers.

As emphasized earlier, the intended application of this research is to build a suitable and sufficient method for the DRS community to categorize contextual complexity. Despite the ideal cluster spectrum range of four to six, the author considered adopting results with three clusters. A value of three is also simple to categorize as High, Medium, and Low complexity categories.

Figure 4.12 below shows clustering results for k-means and hierarchical clustering methods for three cluster centers. The cluster groups are labeled zero, one, and two. Velocity is on the x-axis, object density is on the y-axis, and mean proximity is on the z-axis. Figure 4.13 compares cluster distribution between k-means and hierarchical clustering.

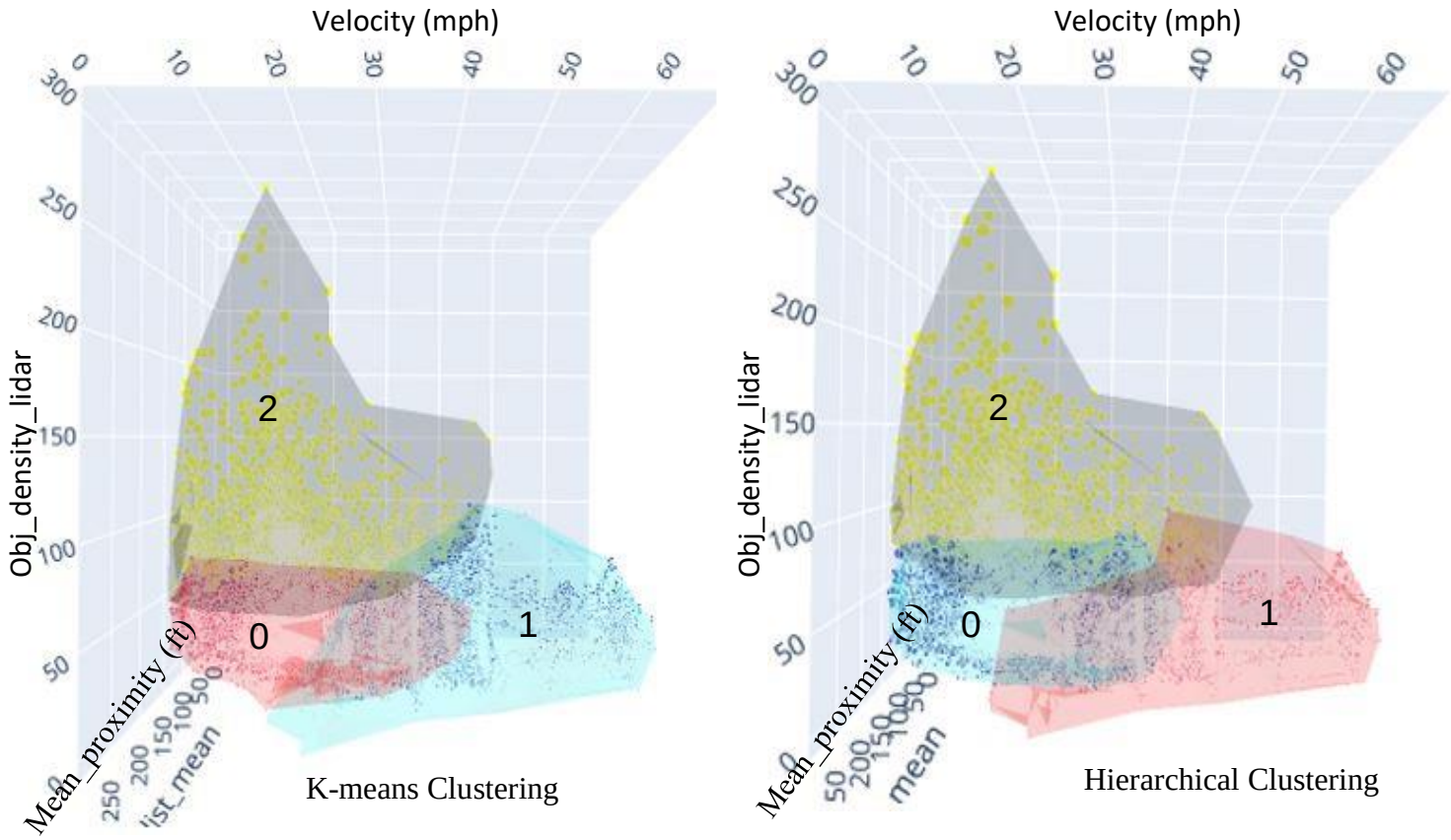

Figure 4.12. K-means Vs. Hierarchical Clustering

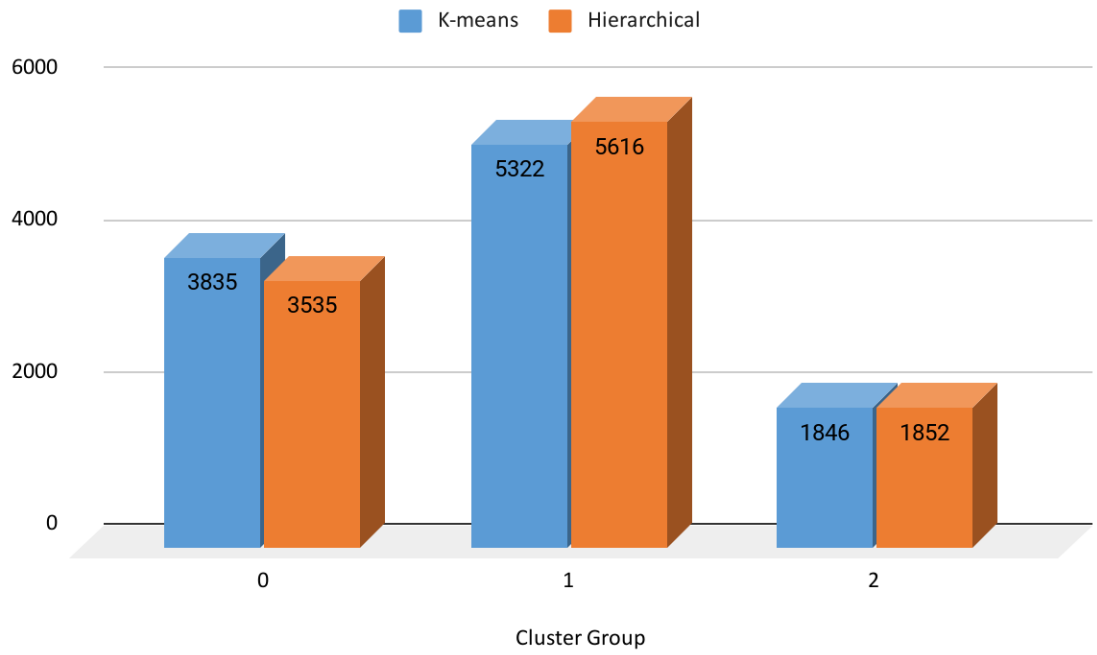

Figure 4.13. K-means vs. Hierarchical clustering - distribution of points

The Rand index was estimated to measure the similarity between k-means and hierarchical clustering models. Rand Index is a ratio of the number of pairs in agreement to the total number of pairs between two clusters and is represented by equation 4.1. Table 4.6 shows the Rand index comparison.

$$RI = \frac{Count\ of\ Pairs\ in\ Agreement}{Total\ Number\ of\ Pairs} \qquad \text{Equation 4.1}$$

Table 4.6. Rand Index for k-means and hierarchical clustering.

Rand Index	K-Means	Hierarchical
K-Means	1	0.7486
Hierarchical	0.7486	1

From Figures 4.12 and 4.13, it is evident that k-means and hierarchical clustering results look identical. The k-means clustering boundaries look continuous and fluid compared to the hierarchical clustering boundaries. The edges are sharp and wrinkled in the case of hierarchical clustering (Figure 4.12). From Figure 4.13, the number of points in each cluster grouping is indistinguishable, with marginal differences for clusters zero and one. The Rand index for k-means and hierarchical is 0.7486, which shows considerable resemblance. Since the models are identical, choosing either one of them would be acceptable. The author looked into the literature to identify any methodological nuances that would assist in selecting a model. Hierarchical clustering does not work as well as k-means clustering when the shape of the clusters is hyperspherical, i.e., circle in 2-dimension or a sphere in 3-dimension. The data we are using for modeling is not spherical in the structure; thus, the k-means clustering model has a superficial edge over the hierarchical clustering model, even though technically both are similar. Therefore the author chooses to consider the k-means clustering model to determine ranges for dynamic complexity determination.

4.1.2.3. Cluster Centers and Corresponding Dynamic Complexity

Understanding the parameters of the cluster grouping is essential for assigning a contextual complexity. The author chose three cluster center models because it will be easier to categorize into three distinct categories: high, medium, and low complexity. The k-means clustering model in Figure 4.12 displays three groups with labels zero, one, and two. Velocity is represented on the x-axis, object density on the y-axis, and proximity on the z-axis. Table 4.7. shows the cluster characteristics and their corresponding complexity rank. Cluster groups and the interpretation behind the assignment of complexity rank are elucidated below:

- Cluster zero: cluster group zero includes locations with low velocity and low density of objects compared to the other two groups. Cluster zero is also relatively safe due to the low density of objects and low speeds. In other words, these are areas with less traffic and speed. Due to these characteristics, cluster zero represents a low complexity environment.
- Cluster one: cluster group one includes locations with relatively high velocity, low-medium object density, and low-to-high proximity of objects. The areas classified in this group are more complex compared to cluster group zero. Hence, cluster one represents a “medium-complexity” environment.
- Cluster two: cluster group two includes areas with high object density and proximity. Broadly these locations have increased traffic which is tightly packed. They might represent locations in central business districts with increased activity.

Compared to the other two groupings, these locations present a relatively complicated driving context. Thus, cluster two represents areas with a "high-complexity" environment.

Table 4.7. Cluster group characteristics and their complexity rank

Cluster Group	Characteristics			Complexity Rank
	Velocity	Object Density	Object Proximity	
0	low-to-medium	low-to-medium	low-to-medium	Low
1	medium-to-high	low-to-medium	medium-to-high	Medium
2	low-to-medium	medium-to-high	medium-to-high	High

4.1.2.4. Dynamic ranges of attributes for complexity categorization

Adopting the results from the clustering analysis, the author further built the complexity ranges for the attributes (i.e., velocity, object density, and object proximity). Table 4.8 shows the computation of complexity ranges for each variable to categorize into low, medium, and high. Table 4.9 shows only the complexity ranges without other statics used for calculation.

Table 4.8. Attributes and their dynamic complexity ranges

Attributes		Dynamic Complexity		
		Low	Medium	High
Velocity (mph)	mean	6.1	18.98	16.55
	std	11.07	9.02	8.76
	mean-2*std	0	1	0
	mean+2*std	28	37	34
Object count	mean	27.09	34.78	114.12
	std	19.41	18	37.32
	mean-2*std	0	0	39
	mean+2*std	66	71	189
Object Proximity (feet)	mean	168.72	136.63	148.16
	std	20.27	17.5	16.81
	mean-2*std	128.18	101.63	114.54
	mean+2*std	209.26	171.63	181.78

Table 4.9. Dynamic complexity ranges for attributes.

Dynamic Complexity	Velocity (mph)	Object count	Object Proximity (feet)
Low	0-28	0-37	0-34
Medium	0-66	0-71	39-189
High	128-209	101-172	115-182

Velocity and object count are comparably easy to collect by DRSs; however, object proximity is virtually impossible to measure manually. Velocity can be obtained from the

vehicle's dashboard, which will be the vehicle's true speed. The DRSs can also obtain the object count relatively easily by counting the number of objects on their testing route.

4.2. Static Risk Model

The author analyzed all the critical variables listed in the Highway Safety Manual for urban and suburban highways. Tables 4.10 to 4.15 list all the variables for the roadway segments. Tables 4.16 to 4.23 shows groups of variables for intersections and their risk classification. Within each table, there are five columns. The first column catalogs the variable and its assortments. The “Max” and “Min” columns consist of estimated annual crash rates. The “Difference” column represents the range in the annual crash rate. Higher the value, the greater the sensitivity and risk. The last column, “Risk,” exhibits the risk designations for the different variations of the attribute type.

The author chose high, medium, and low category levels to represent the risk. The statistical quartiles obtained from the “Difference” column define the risk boundaries. Static variables below the 25th percentile are “low” risk, above 75th percentile are “high” risk, and everything in the inter-quartile range are classified as “medium” risk.

The DRSs can refer to these tables and the risk boundaries to categorize the static variables of their routes.

Table 4.10. Static risk of a road type.

Roadway Type	Max (crashes/yr)	Min (crashes/yr)	Difference (crashes/yr)	Risk
2 lane Undivided	7.86	0.20	7.66	LOW
3 lane with Center Turn Lane	8.31	0.38	7.93	LOW
4 lane undivided	10.24	0.55	9.69	MEDIUM
4 lane divided	13.59	0.69	12.90	MEDIUM
5 lane with Center Turn Lane	20.85	1.42	19.43	HIGH

Table 4.11. Static risk of an on-street parking type.

On-Street Parking	Max (crashes/yr)	Min (crashes/yr)	Difference (crashes/yr)	Risk
None	0.00	0.00	0.00	LOW
Parallel (Residential)	5.16	4.69	0.47	LOW
Parallel (Commercial)	8.01	4.69	3.32	MEDIUM
Angle (Residential)	12.07	4.69	7.38	MEDIUM
Angle (Commercial)	18.79	4.69	14.10	HIGH

Table 4.12. Static risk of roadway lighting.

Lighting	Max (crashes/yr)	Min (crashes/yr)	Difference (crashes/yr)	Risk
Not Present	4.69	4.69	0.00	High
Present	4.30	4.69	0.39	LOW

Table 4.13. Static risk of fixed object distance from the roadway.

Fixed Object Offset (feet)	Max (crashes/yr)	Min (crashes/yr)	Difference (crashes/yr)	Risk
30	4.69	4.69	0.00	LOW
25	4.69	4.69	0.00	LOW
20	4.71	4.69	0.02	MEDIUM
15	4.75	4.69	0.06	MEDIUM
10	4.82	4.69	0.13	HIGH
5	4.98	4.69	0.29	HIGH

Table 4.14. Static risk of median width

Median Width (Feet)	Max (crashes/yr)	Min (crashes/yr)	Difference (crashes/yr)	Risk
0	3.60	3.60	0.00	HIGH
10	3.63	3.60	0.04	HIGH
15	3.60	3.60	0.00	HIGH
20	3.56	3.60	-0.04	MEDIUM
30	3.52	3.60	-0.07	MEDIUM
40	3.49	3.60	-0.11	MEDIUM
50	3.45	3.60	-0.14	MEDIUM
60	3.42	3.60	-0.18	MEDIUM
70	3.38	3.60	-0.22	MEDIUM
80	3.34	3.60	-0.25	LOW
90	3.34	3.60	-0.25	LOW
100	3.31	3.60	-0.29	LOW

Table 4.15. Static risk of auto speed enforcement.

Auto Speed Enforcement	Max (crashes/yr)	Min (crashes/yr)	Difference (crashes/yr)	Risk
Not Present	4.67	4.67	0	HIGH
Present	4.45	4.67	0.215	LOW

Table 4.16. Static risk of intersection type.

Intersection Type	Max (crashes/yr)	Min (crashes/yr)	Difference (crashes/yr)	Risk
3 approach Signalized	11.31	0.56	10.75	MEDIUM
3 approach Stop Control	8.47	0.30	8.17	MEDIUM
4 approach Stop Control	7.21	0.69	6.53	LOW
4 approach Signalized	23.58	1.36	22.22	HIGH

Table 4.17. Static risk of intersection lighting.

Intersection Lighting	Max (crashes/yr)	Min (crashes/yr)	Difference (crashes/yr)	Risk
Not Present	9.99	9.99	0.00	HIGH
Present	10.98	9.99	0.99	LOW

Table 4.18. Left turn lanes and their static risk.

Approaches with Left Turn Lanes	Max (crashes/yr)	Min (crashes/yr)	Difference (crashes/yr)	Risk
0	10.98	7.25	3.73	HIGH
1	9.88	7.25	2.64	MEDIUM
2	8.89	7.25	1.65	MEDIUM
3	8.02	7.25	0.77	LOW
4	7.25	7.25	0.00	LOW

Table 4.19. Right turn lanes and their static risk.

Approaches with Right Turn Lanes	Max (crashes/yr)	Min (crashes/yr)	Difference (crashes/yr)	Risk
0	10.98	9.33	1.65	HIGH
1	10.54	9.33	1.22	MEDIUM
2	10.12	9.33	0.79	MEDIUM
3	9.71	9.33	0.39	LOW
4	9.33	9.33	0.00	LOW

Table 4.20. Left turn signal phasing and their static risk.

Approaches with Left Turn Signal Phasing	Max (crashes/yr)	Min (crashes/yr)	Difference (crashes/yr)	Risk
0	10.98	10.76	0.22	HIGH
1	10.98	10.76	0.22	HIGH
2	10.87	10.76	0.11	HIGH
3	10.76	10.76	0.00	LOW
4	10.76	10.76	0.00	LOW

Table 4.21. Signal phasing type and their static risk.

TYPE OF SIGNAL PHASING	Max (crashes/yr)	Min (crashes/yr)	Difference (crashes/yr)	Risk
Permissive	11.09	10.43	0.67	HIGH
Protected	10.43	10.43	0.00	LOW
Protected/Permissive	10.98	10.43	0.56	MEDIUM
Permissive/Protected	10.98	10.43	0.56	MEDIUM

Table 4.22. Approaches with right-turn-on-red (RTOR) restrictions and their risk.

Approaches with RTOR Prohibited	Max (crashes/yr)	Min (crashes/yr)	Difference (crashes/yr)	Risk
0	10.98	10.13	0.85	HIGH
1	10.76	10.13	0.63	MEDIUM
2	10.55	10.13	0.42	MEDIUM
3	10.33	10.13	0.21	LOW
4	10.13	10.13	0.00	LOW

Table 4.23. Risk of intersections with/without red-light running cameras

Intersection Redlight Running Cameras	Max (crashes/yr)	Min (crashes/yr)	Difference (crashes/yr)	Risk
Not Present	10.98	10.98	0	HIGH
Present	11.11	10.98	0.13	LOW

Table 4.24 and 4.25 below display the results of sensitivity analysis of all the significant variables listed in the Highway Safety Manual for urban and suburban roadways. The variables are ranked based upon the sensitivity weights. The roadway segment type, on-street parking, and lighting are the top three most important variables for urban and suburban roadways (Table 4.24). Intersection type, presence of lighting, and the number of approaches with left-turn lanes are the three most important variables that define the risk of urban/suburban intersections (Table 4.25).

Table 4.24.Sensitivity of roadway segment variables and their importance rank

Segment Attributes	Max Sensitivity	Weights	Rank
Road Type	19.4320	0.5598	1
Type of on-Street Parking	14.1000	0.4062	2
Lighting	0.3880	0.0112	3
Fixed object density	0.2870	0.0083	4
Median	0.2880	0.0083	6
Auto Speed Enforcement	0.2150	0.0062	5

Table 4.25. Sensitivity of intersection variables and their importance rank.

Intersection Attributes	Max Sensitivity	Weights	Rank
Intersection Type	22.2200	0.7801	1
Lighting	-0.9900	-0.0348	4
# Approachs with LT Lane	3.7330	0.1311	2
# Approaches with Right Turn Lane	1.6540	0.0581	3
# Approaches with Left Turn Phasing	0.2190	0.0077	6
Types of Signal Phasing	0.6660	0.0234	6
Approaches with RTOR Prohibited	0.8530	0.0299	5
Intersection Redlight Cameras	0.1270	0.0045	8

The priority list in Table 4.24 and 4.25 will serve as a tie-breaker when the frequency of risk for a segment/intersection is similar. For example, when the risk of a given intersection/segment is a stalemate with an equal number of variables in high and low categories, the risk classification of the most important variables will be used to determine. .

4.3. Absolute complexity Analysis

Absolute complexity is the composite of both static risk and dynamic complexity. About nine trips were chosen to determine the absolute complexity. The absolute contextual complexity of each trip that includes static risk and dynamic complexity combined is further discussed. A video link of an actual Waymo trip along with object bounding boxes and total counts is included in the description of each trip. Appendix B includes tables for each trip's sstatic risk analysis. This section provides concluding plots and tables derived from this detailed analysis.

4.3.1. Market St (Between 3rd and O' Farrel)

Market street is one of the busiest locations in the central business districts of San Francisco city. Figure 4.14 shows the location of the trip on Market Street that extends from 3rd street to O'Farrel street. The corresponding link to the video footage of the actual Waymo trip is provided in the hyperlink here.

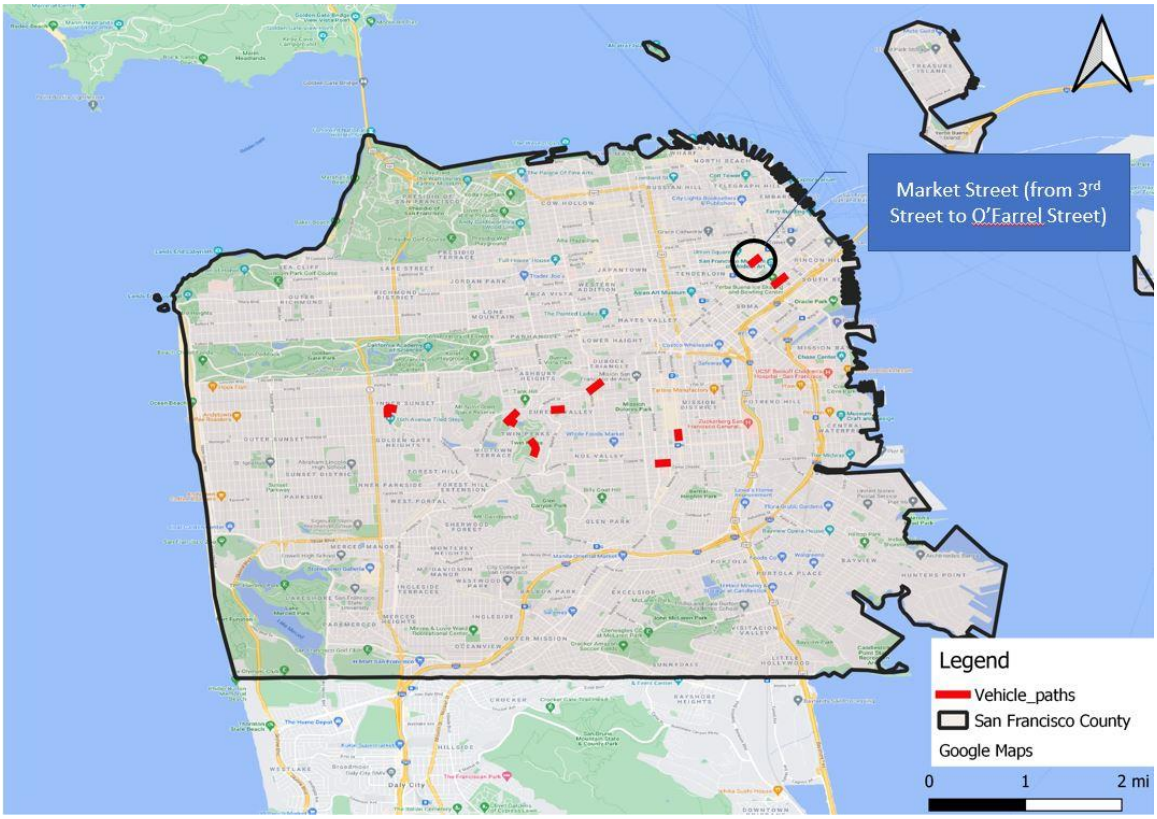

Figure 4.14. Trip location of Market St (Between 3rd and O' Farrel), San Francisco, CA.

This trip is carried out on an urban multilane undivided highway with a shared bus lane and a light rail track. It is evident/ from the video that there are plenty of pedestrians and bicycles in the vehicle's vicinity. Figure 4.15 shows the dynamic complexity plot for this

trip in addition to the graphs on the variation of density, proximity and velocity. The section was consistently rated “high” at every tenth of a second, indicating a busy driving context. additional graphs on the variation of density, proximity, and velocity for this trip.

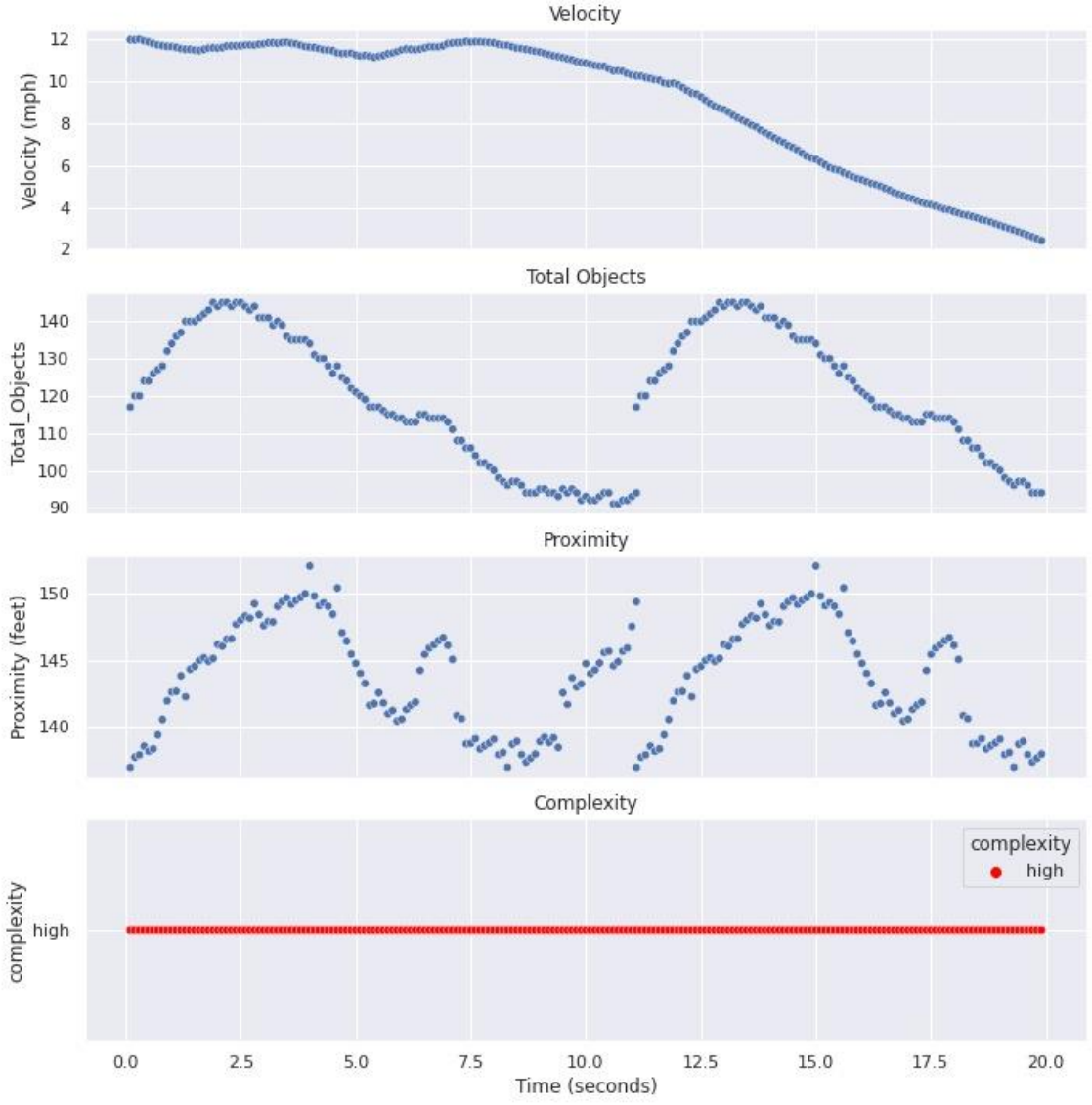

Figure 4.15. The dynamic complexity of trip on Market St (Between 3rd and O’ Farrel), San Francisco, CA.

This trip passes through two intersections on each end of the trip and a segment in-between. Table 4.26 presents the static risk results of the trip. Both the intersections and the segment were categorized as "high." Table B.1 to B.3 in Appendix B presents a detailed analysis of this trip's components (i.e., segments and intersections).

Table 4.26. Static risk of trip on Market St (Between 3rd and O' Farrel), San Francisco, CA.

TRIP 1: Market Street (Between 3rd & O'Farrel Street)				
Segment/Intersection Name	**High**	**Medium**	**Low**	**Static Risk**
Market Street	3	2	1	High
Market Street @ 3rd Street	7	0	1	High
Market Street @ O'Farrel Street	5	2	1	High
Absolute Static risk	**15**	**4**	**3**	**High**

Since the dynamic complexity and static risk were both categorized as "high" the absolute complexity of this trip is "high".

4.3.2. Market St (Between 16th and 17th Street)

This trip is on another section of the busy Market street between 16th and 17th Streets in the central business districts of San Francisco city. Figure 4.16 shows the location of the trip. The corresponding link to the video footage of the Waymo trip is included in the hyperlink here. The trip starts at Market Street and 16th Street intersection, traverses on an urban multilane-divided highway, and ends at Market Street and 17th Street.

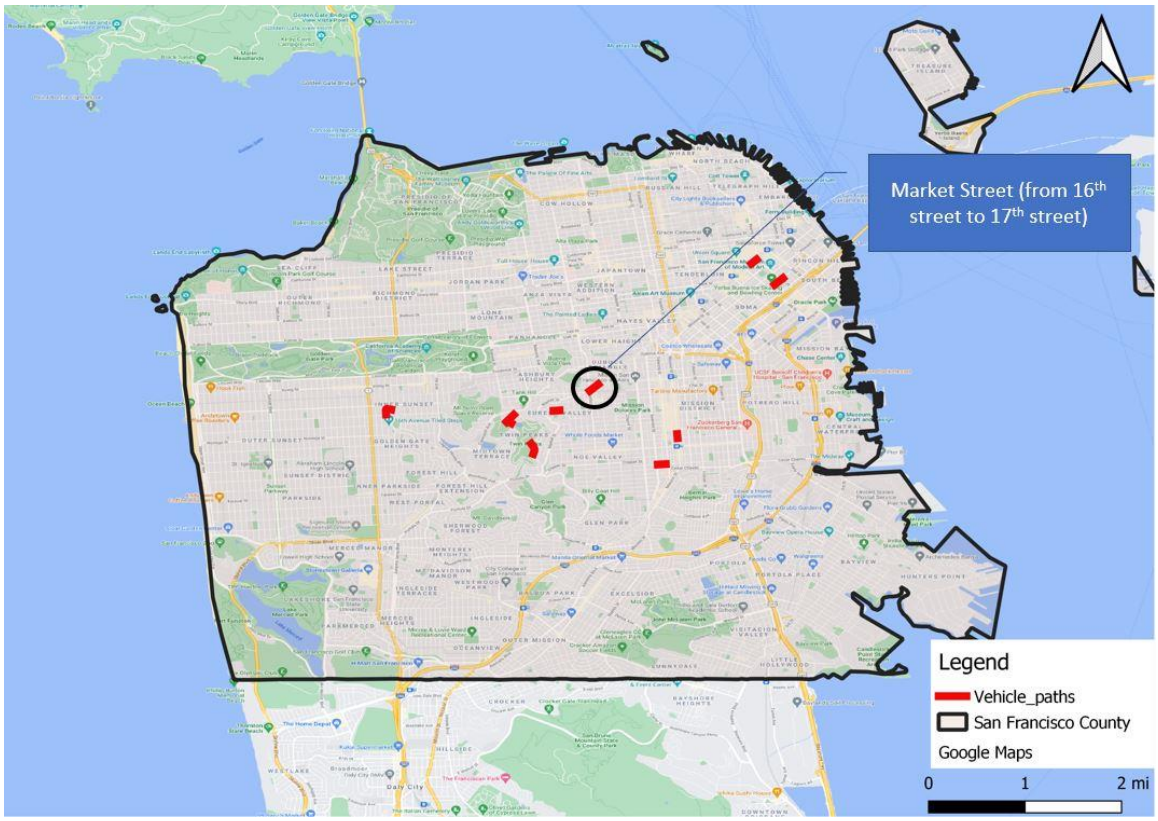

Figure 4.16. Trip location of Market St (Between 16th and 17th), San Francisco, CA.

Figure 4.17 presents the dynamic complexity plot. The entire trip is designated as a low dynamic complexity trip as it remains in that class for the entire length.

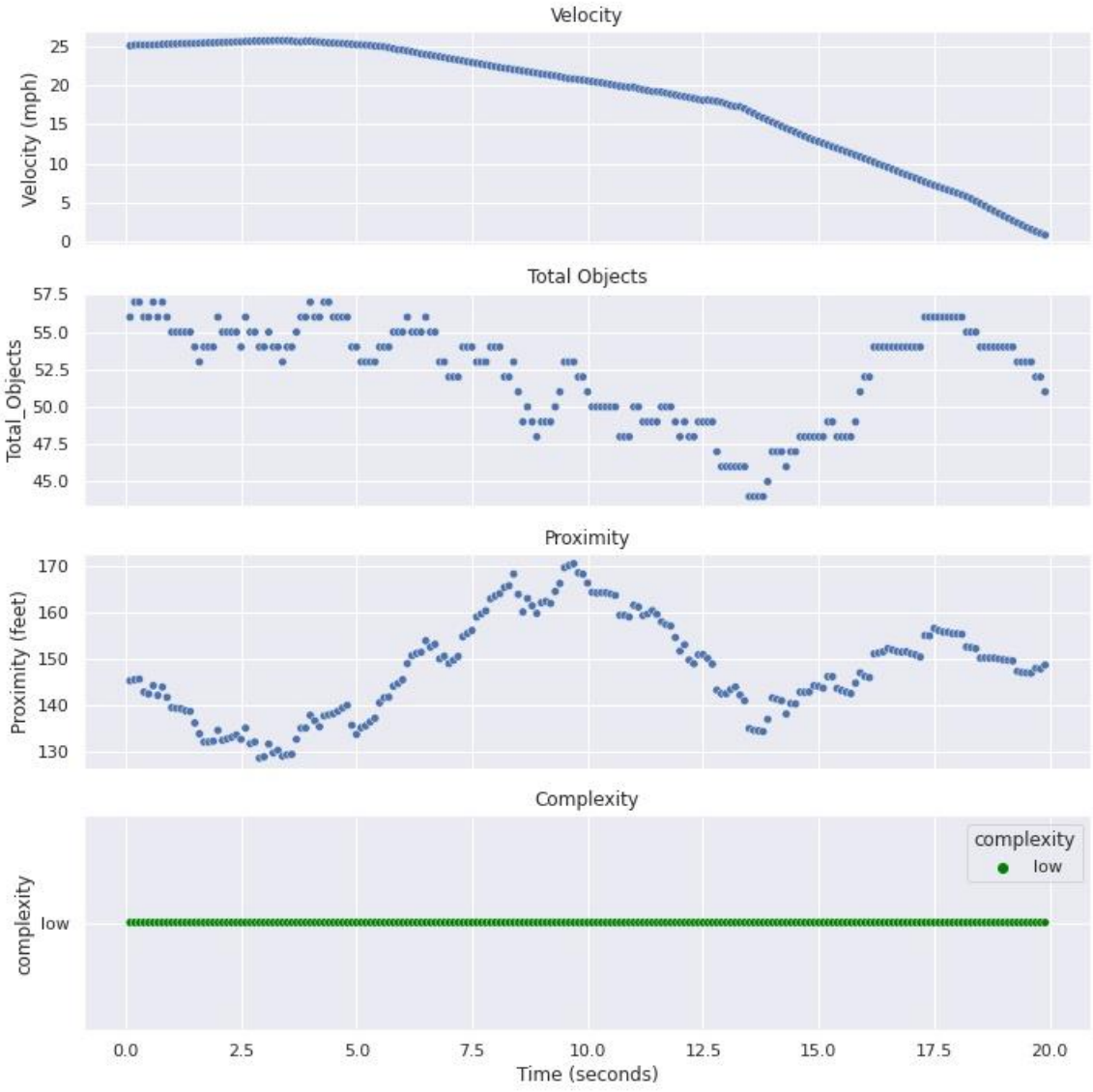

Figure 4.17. The dynamic complexity of the trip on Market St (Between 16th and 17th Street), San Francisco, CA.

On the other hand, the absolute static risk of the trip is classified as “high.” The trip traverses through two intersections (Market Street @ 16th Street and Market Street @ 17th

Street) and a segment in-between (Market Street). Table 4.27 lists the static risk results of the trip. Both the intersections and the segment are classified as “high” risk.

Table 4.27. Static risk of trip on Market St (Between 16th and 17th Street), San Francisco, CA.

TRIP 2: Market Street (Between 16th & 17th)				
Segment/Intersection Name	**High**	**Medium**	**Low**	**Static Risk**
Market Street	4	1	1	High
Market Street @ 16th Street	6	1	1	High
Market Street @ 17th Street	4	1	3	High
Absolute Static Risk	**14**	**3**	**5**	**High**

The dynamic complexity of this trip is “low”. The static risk is “high”. Thus, the absolute complexity of this trip is earmarked as “medium.”

4.3.3. Mission Street (between 22nd and 23rd Street)

This trip is on Mission Street between 22nd and 23rd Streets in the central business districts of San Francisco city. Figure 4.17 shows the location of the trip. The corresponding link to the video footage of the Waymo trip is included in the hyperlink here. The trip starts in the middle of Mission Street and ends at the 23rd Street intersection. Mission street is an urban two-lane undivided road with a dedicated bus lane.

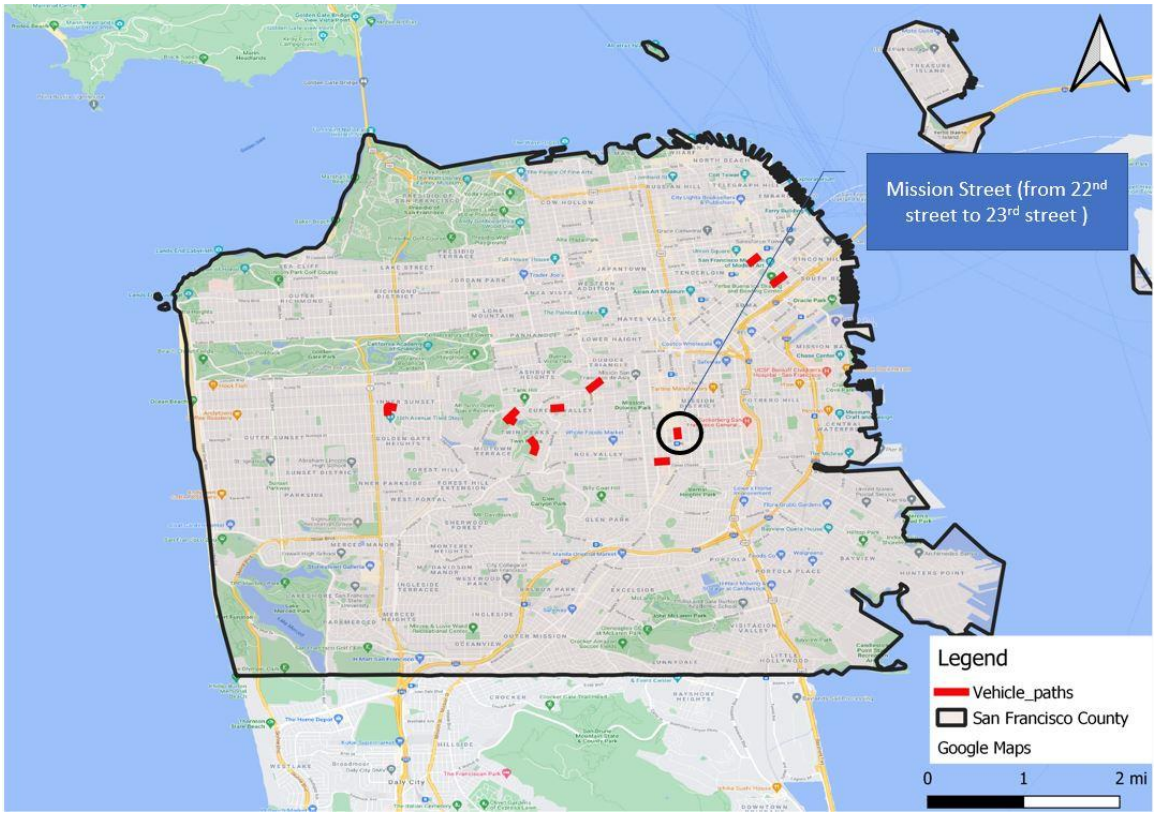

Figure 4.18. Trip location of Mission Street (between 22nd and 23rd Street), San Francisco, CA.

Figure 4.19 presents the dynamic complexity plot. The entire trip is designated as a high dynamic complexity as it remains in that class for the entire length.

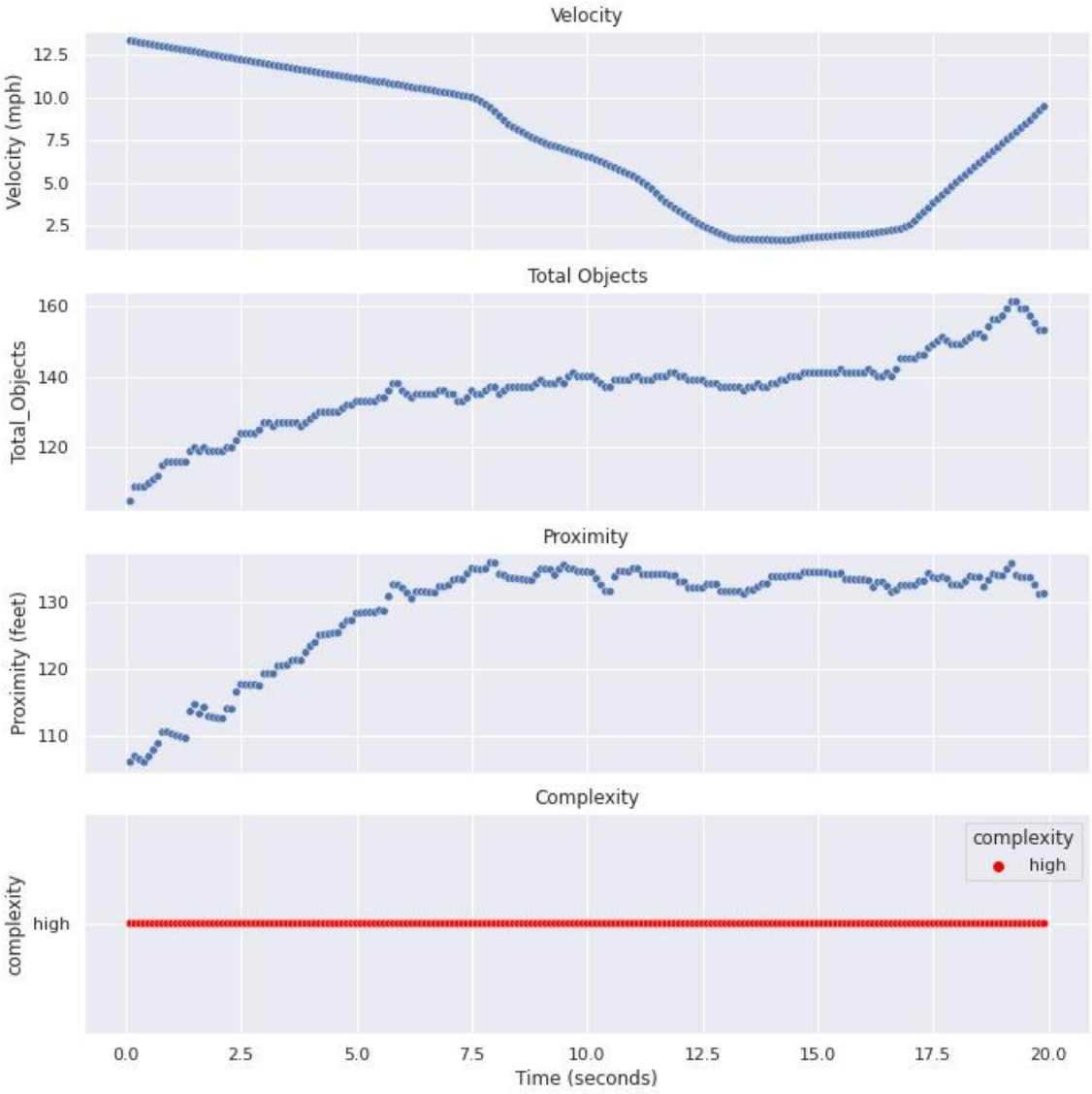

Figure 4.19. The dynamic complexity of trip on Mission Street (between 22nd and 23rd Street), San Francisco, CA.

This trip consists of one intersection and a segment. Table 4.28 presents the static risk results of the trip. The intersection and the segment were categorized as a ‘high” risk.

Table B.7 and B.8 in Appendix B presents a detailed analysis of this trip's components (i.e., segments and intersections).

Table 4.28. Static risk of trip on Market St (Between 16th and 17th Street), San Francisco, CA.

TRIP 3: Mission St (Between 22nd & 23rd)				
Segment/Intersection Name	**High**	**Medium**	**Low**	**Static Risk**
Mission Street	3	1	2	High
Mission St @ 23rd St	5	1	2	High
Absolute Static Risk	**8**	**2**	**4**	**High**

The dynamic complexity and static risk were both categorized a "high." Thus, the absolute complexity of this trip is also designated as a "high."

4.3.4. Folsom Street (between 3rd & Mabini Street)

This trip is on Folsom Street between 3rd and Mabini Streets in the central business districts of San Francisco city. Figure 4.20 shows the location of the trip. The corresponding link to the video footage of the Waymo trip is included in the hyperlink here. The trip starts at Mabini Street and Folsom Street intersection, traverses on an urban multilane highway, and ends at Folsom Street and 3rd Street intersection.

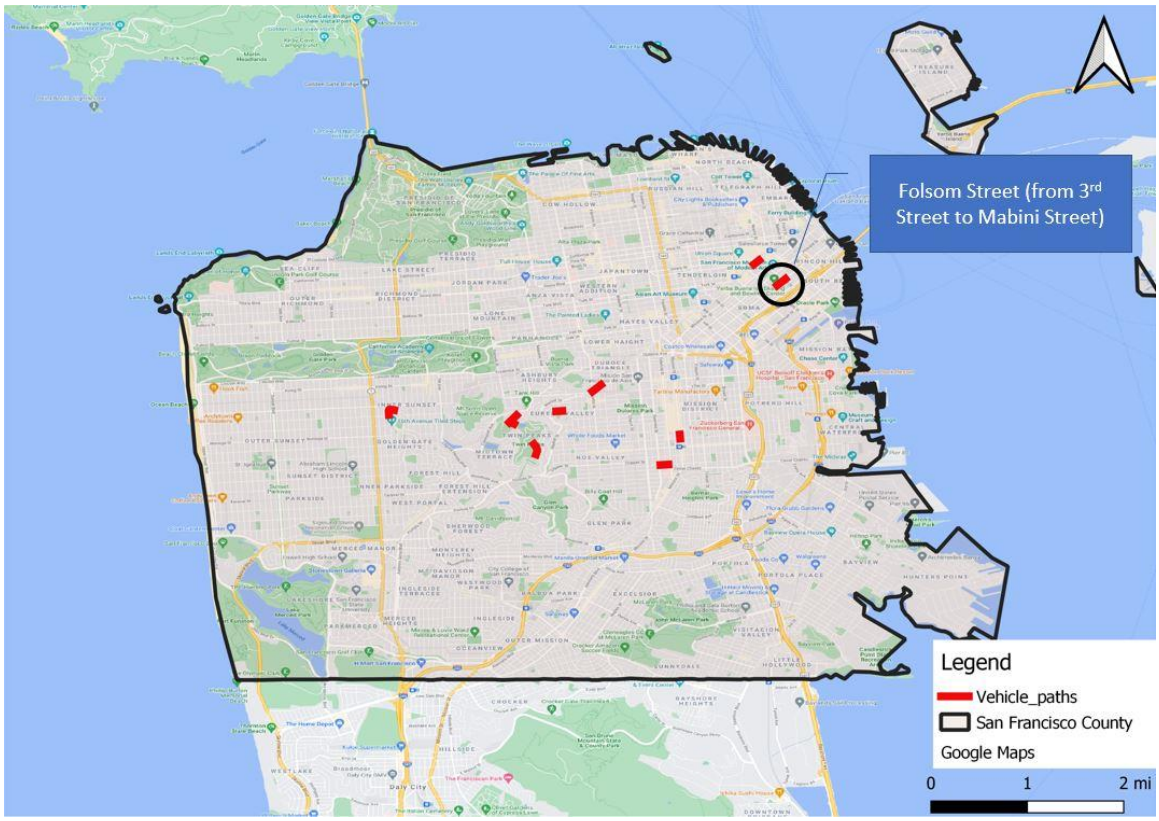

Figure 4.20. Trip location of Folsom Street (between 3rd & Mabini Street), San Francisco,

Figure 4.21 presents the dynamic complexity plot. The trip starts with a low complexity environment for the first second, then shifts into a high complexity environment.

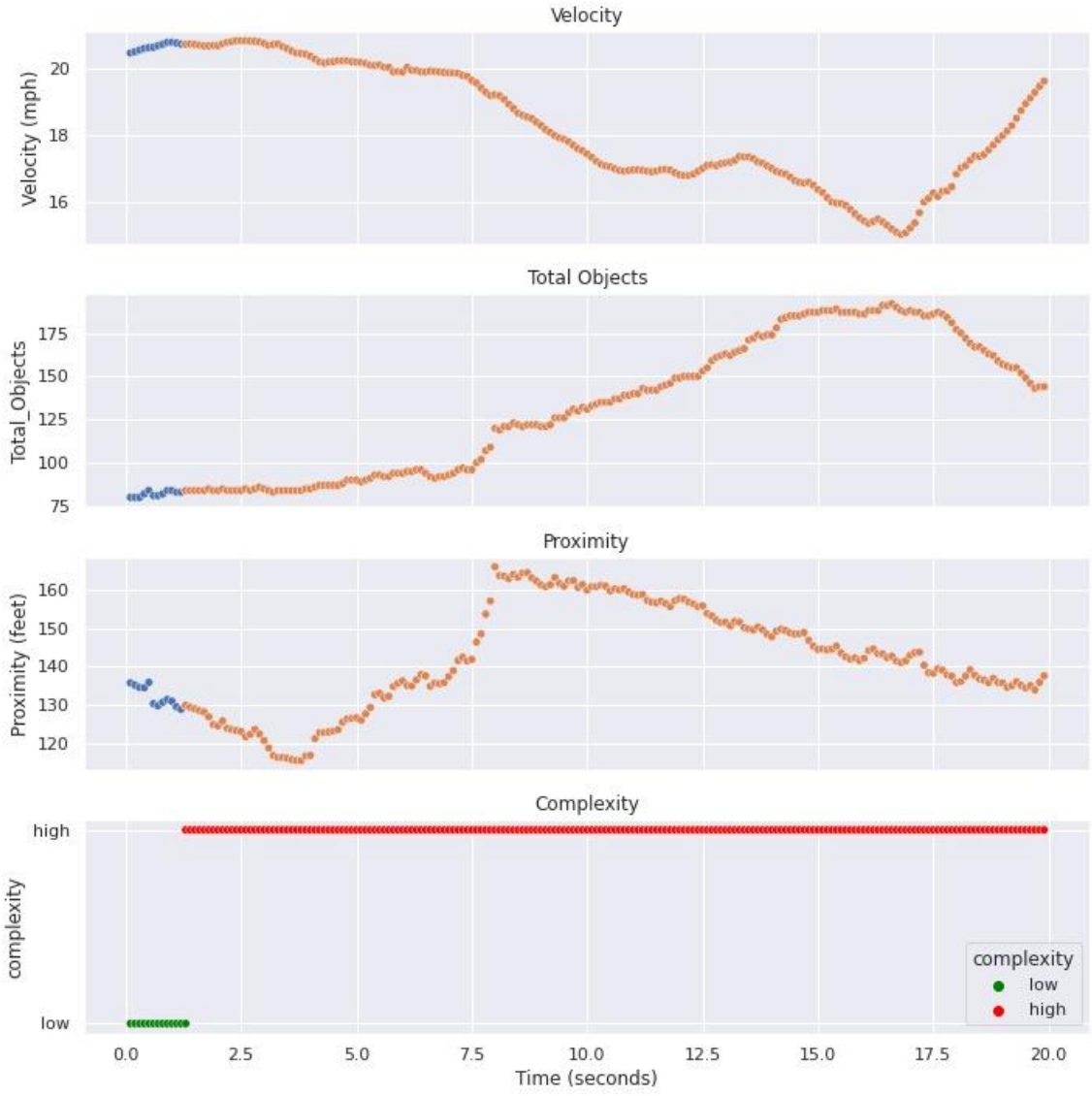

Figure 4.21. The dynamic complexity of the trip on Folsom Street (between 3rd & Mabini Street), San Francisco, CA.

This trip consists of two intersections (Folsom Street @ 3rd Street and Folsom Street @ Mabini Street) and a segment. Table 4.29 presents the static risk results of the trip. The Folsom Street segment was classified to be a “high-risk.” Folsom Street and 3rd Street

intersection was categorized as a “high-risk” intersection. However, the other intersection of Folsom and Mabini Street was designated to be “low-risk.” Table B.9 to B.11 in Appendix B presents a detailed analysis of this trip’s components (i.e., segments and intersections).

Table 4.29. Static risk of trip on Folsom Street (between 3rd & Mabini Street), San Francisco, CA.

TRIP 4: Folsom St (Between 3rd st & Mabini St)				
Segment/Intersection Name	**High**	**Medium**	**Low**	**Static Risk**
Folsom Street	3	1	2	HIGH
Folsom Street @ 3rd Street	5	0	3	HIGH
Folsom Street @ Mabini Street	2	1	5	LOW
Absolute Static Risk	**10**	**2**	**10**	**HIGH**

4.3.5. 26th street (between Guerrero St & Valencia Street)

This trip is on 26th Street between Guerrero Street and Valencia Street in San Francisco city. Figure 4.22 shows the location of the trip. The corresponding link to the video footage of the Waymo trip is included in the hyperlink here. The trip starts at the intersection of 26th and Valencia Stree and ends at 26th and Guerrero Street. The 26th Street segment is a multilane-divided highway facility.

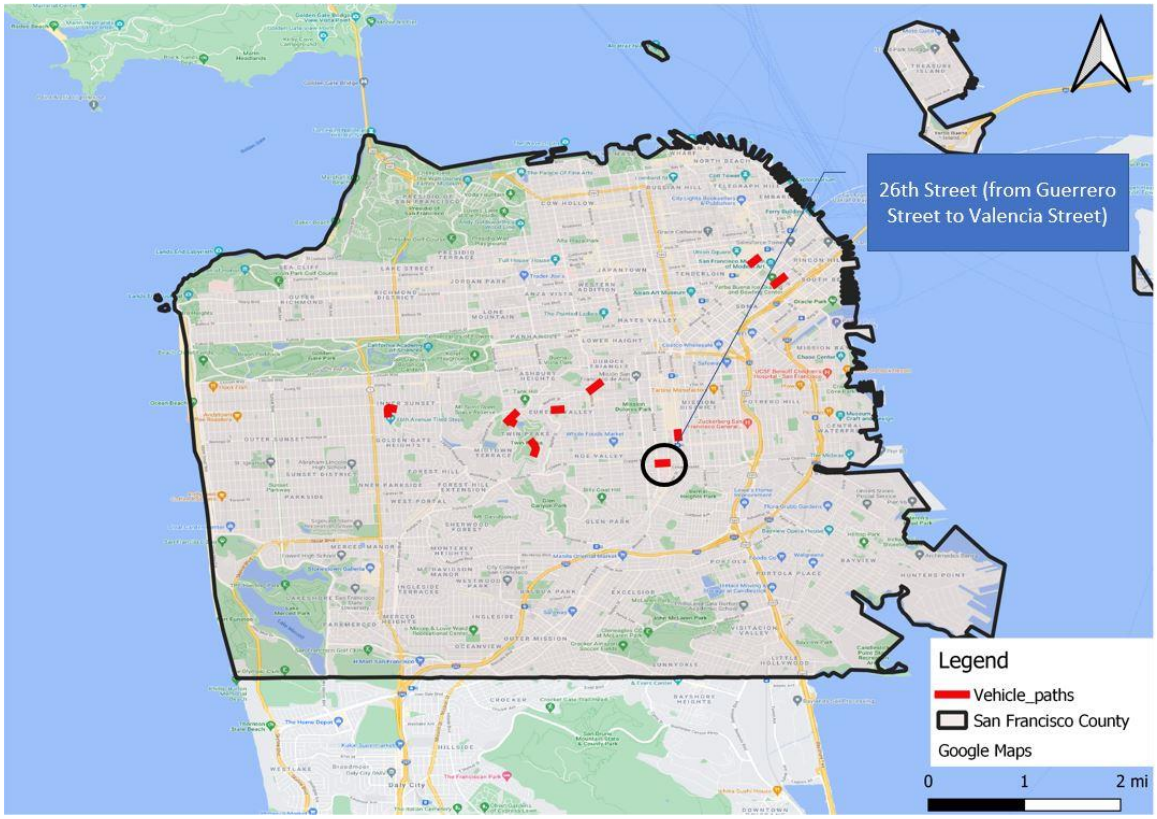

Figure 4.22. Trip location of 26th street (between Guerrero St & Valencia Street) , San Francisco, CA.

Figure 4.23 presents the dynamic complexity plot. Approximately half of the trip at the beginning till the 11-second point is classified as a low-complexity and rest of the trip switches into a “high” complexity environment. Since the trip splits between the low and high categories, the dynamic complexity is designated to be the average, i.e., “medium” complexity.

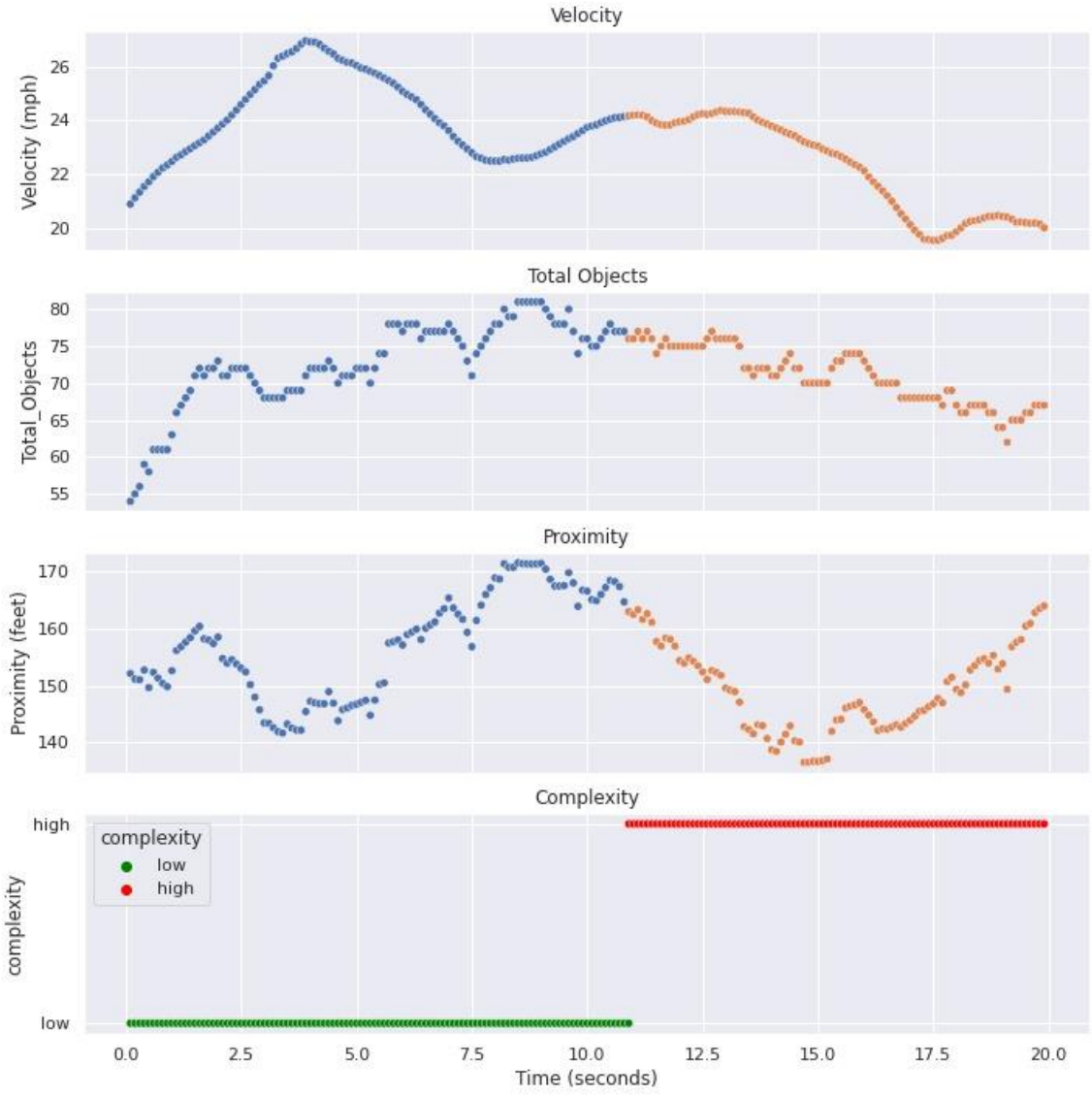

Figure 4.23. The dynamic complexity of the trip on 26th street (between Guerrero St & Valencia Street), San Francisco, CA.

This trip consists of two intersections and a segment. Table 4.30 presents the static risk results of the trip. The segment (26th Street)and an intersection (26th Street and San Jose Avenue) were categorized as “medium” risk. The intersection of 26th Street and Guerrero

Street intersection was classified into a "high" risk category. Table B.11 to B.13 in Appendix B presents a detailed analysis of this trip's components (i.e., segments and intersections). The absolute static risk of this trip was categorized as "medium-risk" as two out of three static components were recognized in that category.

Table 4.30. Static risk of trip on 26th street (between Guerrero St & Valencia Street), San Francisco, CA.

TRIP 5: 26th St (Between Guerrero St & Valencia St)				
Segment/Intersection Name	**High**	**Medium**	**Low**	**Static Risk**
26th Street	2	3	1	MEDIUM
26th st @ Guerrero St	6	1	1	HIGH
26th St @ San Jose Ave	2	2	0	MEDIUM
Absolute Static Risk	**10**	**6**	**2**	**MEDIUM**

The absolute complexity of this trip is "medium" as both dynamic complexity and static risk belong to that category.

4.3.6. 19th Street (Between Yukon and Seward Street)

This trip is on 19th Street between Yukon Street and Seward Street in a residential neighborhood in San Francisco city. Figure 4.24 shows the location of the trip. The corresponding link to the video footage of the Waymo trip is included in the hyperlink

here.

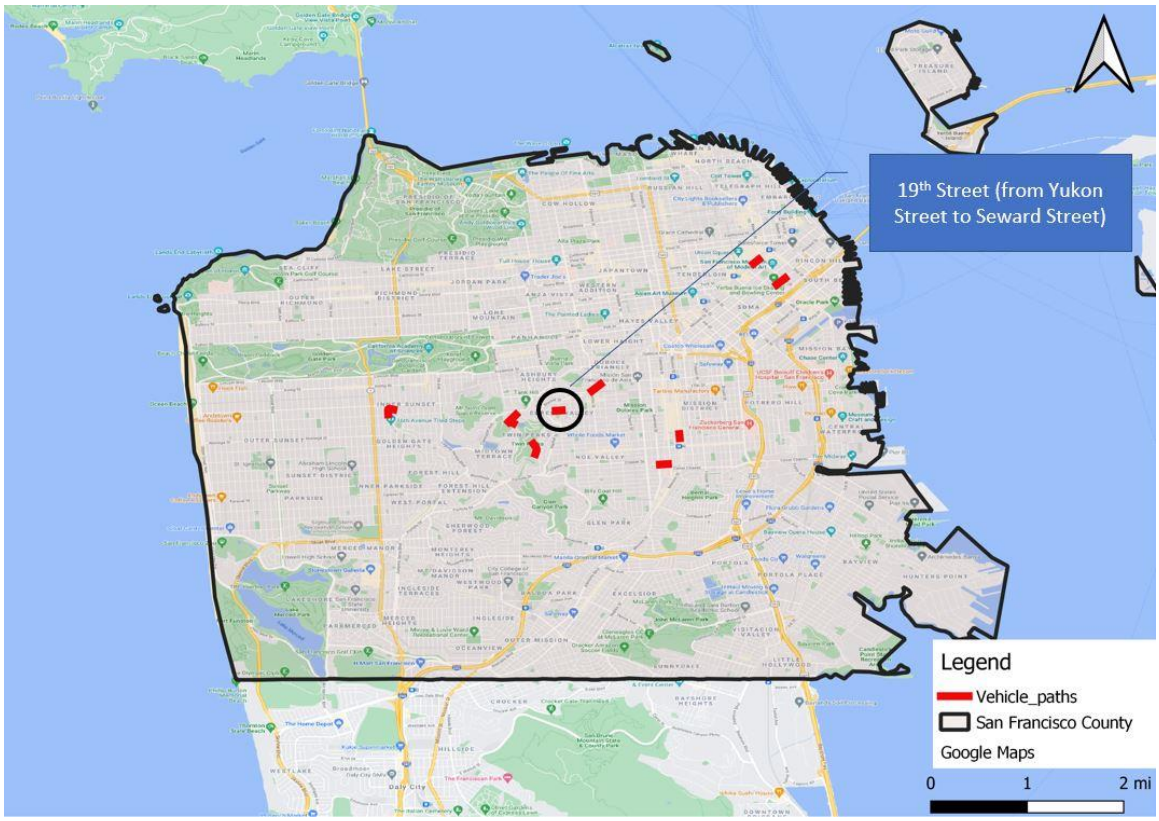

Figure 4.24. Trip location of 19th Street (Between Yukon and Seward Street), San Francisco, CA.

Figure 4.25 presents the dynamic complexity plot. The entire trip is designated as low dynamic complexity as it remains in that class for the entire length.

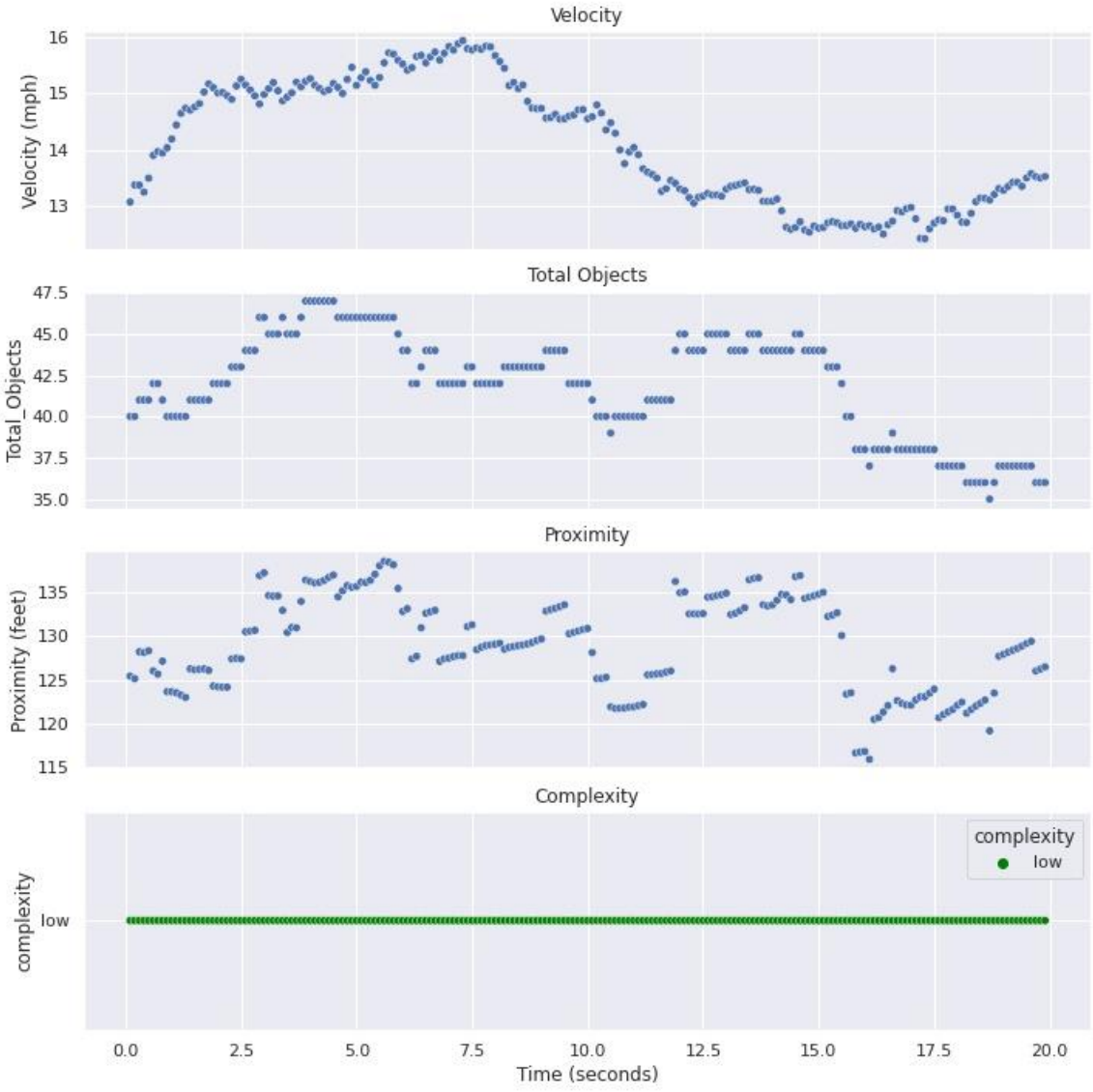

Figure 4.25. The dynamic complexity of trip on 19th Street (Between Yukon and Seward Street), San Francisco, CA.

This trip consists of one intersection and a segment. Table 4.31 presents the static risk results of the trip. The intersections were categorized as “low-risk,” while the segment was

designated as “medium-risk.” Table B.14 to B.16 in Appendix B presents a detailed analysis of this trip’s components (i.e., segments and intersections).

Table 4.31. Static risk of trip on19th Street (Between Yukon and Seward Street), San Francisco, CA.

TRIP 6: 19th St (Between Yukon St & Seward St)				
Segment/Intersection Name	**High**	**Medium**	**Low**	**Static Risk**
19th Street	2	2	2	MEDIUM
19th Street @ Yukon Street	2	0	2	LOW
19th Street @ Seward Street	2	0	2	LOW
Absolute Static Risk	**6**	**2**	**6**	**LOW/MEDIUM**

The absolute complexity of this trip is “Low” as both dynamic and static were categorized into that category.

4.3.7. Glenbrook Avenue (between Palo Alto Avenue and Mountain Spring Road)

Glenbrook Avenue is a two-lane local neighborhood road. This trip stretches between Palo Alto Avenue and Mountain Spring Road in San Francisco city. Figure 4.26 shows the location of the trip. The corresponding link to the video footage of the Waymo trip is included in the hyperlink here.

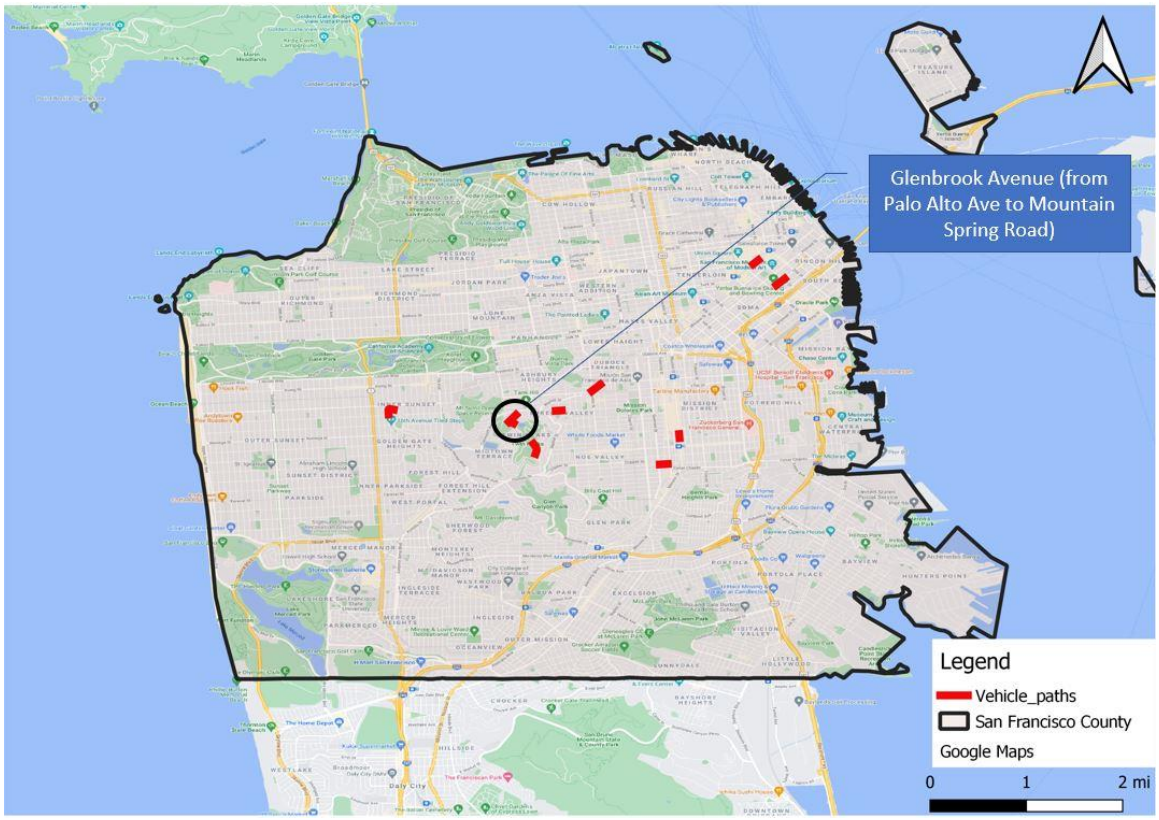

Figure 4.26. Trip location of Glenbrook Avenue (between Palo Alto Avenue and Mountain Spring Road), San Francisco, CA.

Figure 4.27 presents the dynamic complexity plot. The trip traverses in a relatively low-complexity environment and switches to a medium-complexity at 16 seconds into the trip. The dynamic complexity of this trip is “low” as the majority of the trip time is used in that category.

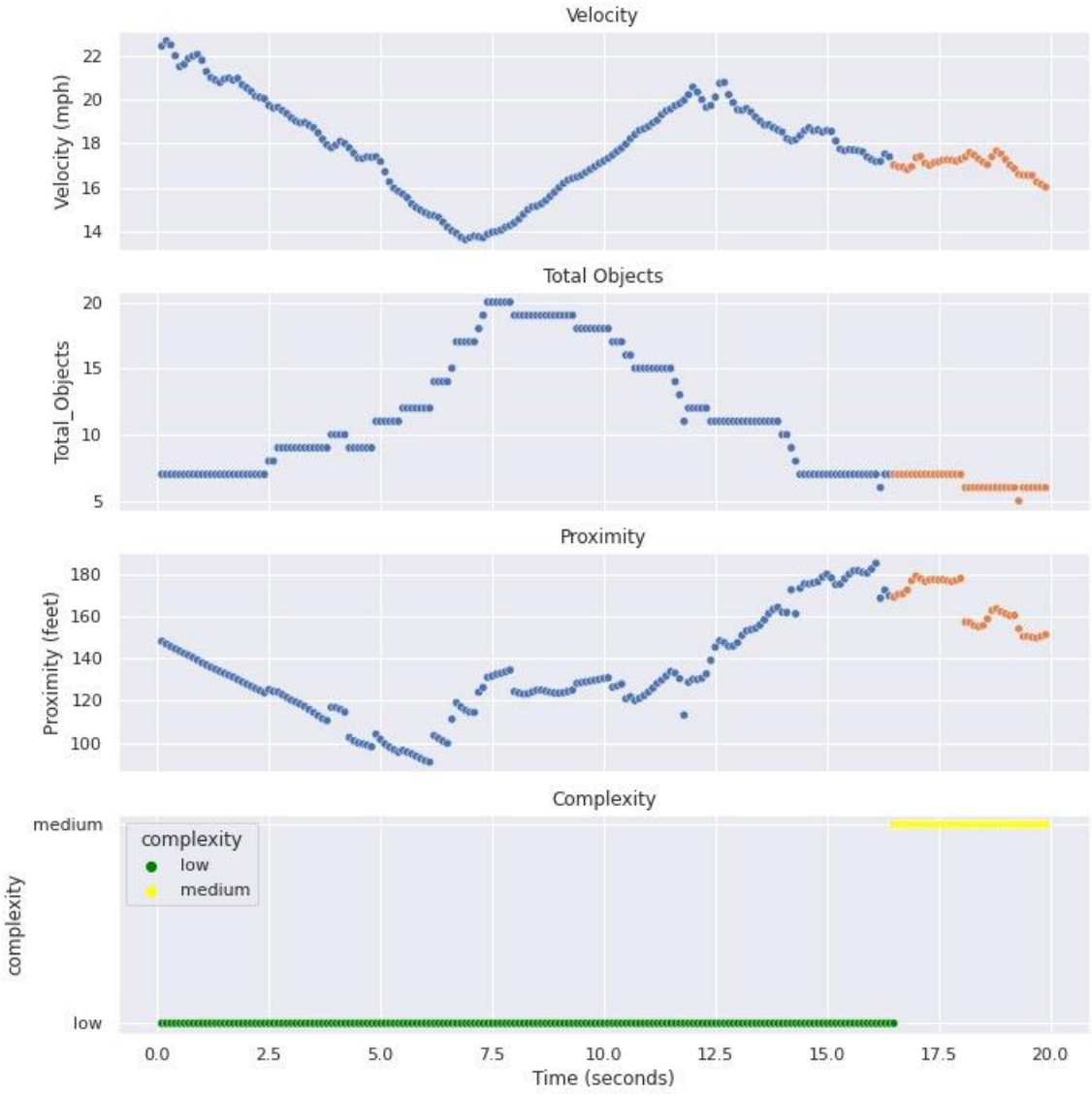

Figure 4.27. The dynamic complexity of trip on Glenbrook Avenue (between Palo Alto Avenue and Mountain Spring Road), San Francisco, CA.

This trip consists of two intersections and a segment. Table 4.32 presents the static risk results of the trip. Both intersection and the segment are classified as a “low-risk”. Table

B.17 and B.18 in Appendix B presents a detailed analysis of this trip's components (i.e., segments and intersections). The absolute static risk of this trip is "low-risk".

Table 4.32. Static risk of trip on Glenbrook Avenue (between Palo Alto Avenue and Mountain Spring Road), San Francisco, CA.

TRIP 7: Glenbrook Avenue (Palo Alto Avenue & Mountain Spring Road)				
Segment/Intersection Name	**High**	**Medium**	**Low**	**Static Risk**
Glenbrook Avenue	2	1	2	Low
Glenbrook Ave @ Mountain Spring Road	2	0	2	Low
Glenbrook Ave @ Palo Alto Ave	2	0	3	Low
Absolute Static Risk	**6**	**1**	**7**	**Low**

The absolute complexity of this trip is "low" as dynamic complexity and static risk fall into that category.

4.3.8. Parkridge Drive (between Crestline Drive and Burnett Avenue)

This trip is on Parkridge Drive between Crestline Drive and Burnett Avenue in San Francisco city. Parkridge Drive is a two-lane undivided local neighborhood road. Figure 4.28 shows the location of the trip. The corresponding link to the video footage of the Waymo trip is included in the hyperlink here.

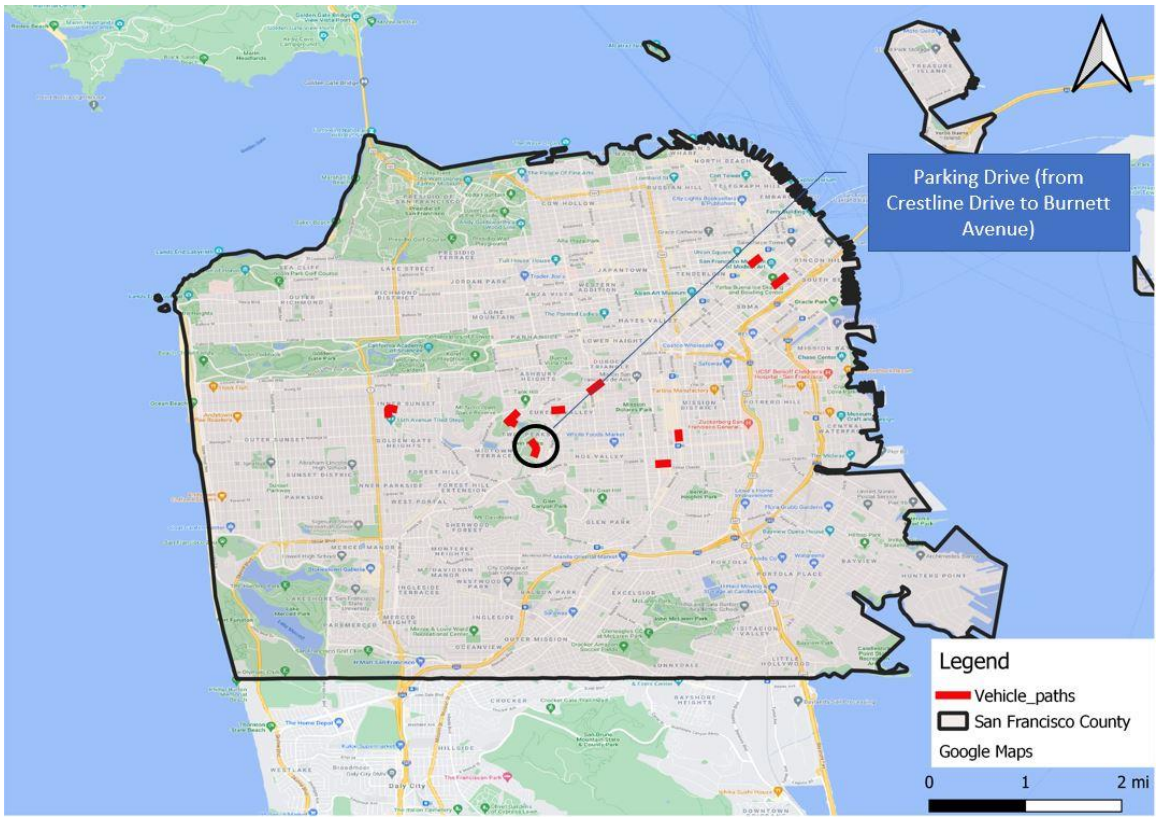

Figure 4.28. Trip location of Parkridge drive (between Crestline Drive and Burnett Avenue), San Francisco, CA.

Figure 4.29 presents the dynamic complexity plot. The entire trip is designated as low dynamic complexity as it remains in that class for the entire length.

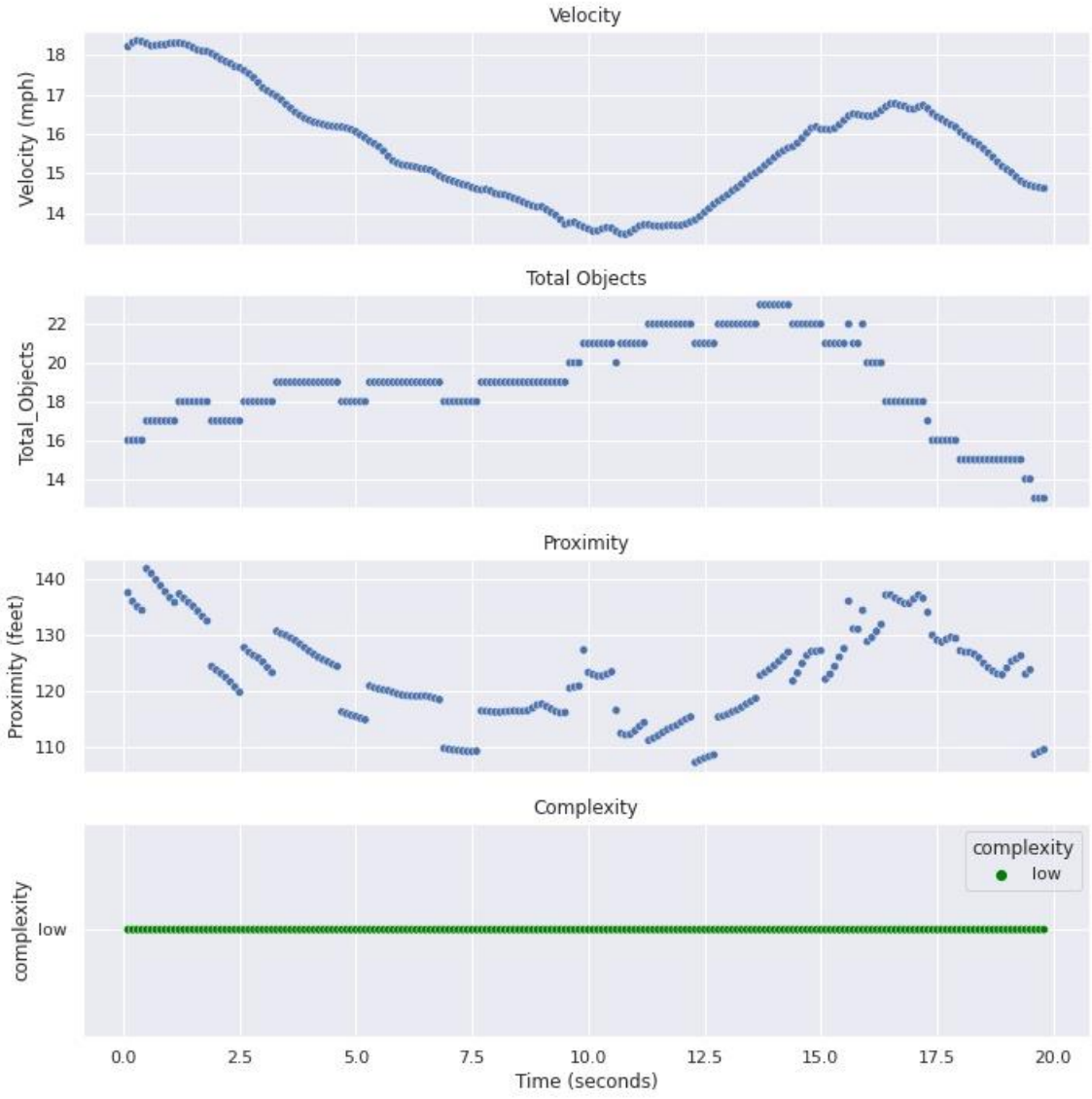

Figure 4.29. The dynamic complexity of the trip on Parkridge drive (between Crestline Drive and Burnett Avenue), San Francisco, CA.

This trip consists of two intersections and a segment. Table 4.33 presents the static risk results of the trip. The intersections, as well as the segment, were categorized as “low-risk.”

Table B.19 to B.21 in Appendix B presents a detailed analysis of this trip's components (i.e., segments and intersections).

Table 4.33. Static risk of trip on Parkridge drive (between Crestline Drive and Burnett Avenue), San Francisco, CA.

TRIP 8: Parkridege Dr (Crestline Dr & Burnett Ave)				
Segment/Intersection Name	**High**	**Medium**	**Low**	**Static Risk**
Parkridege Dr	1	0	3	Low
Parkridge Dr & Crestline Dr	2	0	2	Low
Parkridge Dr & Burnett Ave	2	0	2	Low
Absolute Static risk	**5**	**0**	**7**	**Low**

The absolute complexity of this trip is "low" as dynamic complexity and static risk fall into that category.

4.3.9. 16th Avenue (between Lomita Avenue and Lawton Street)

This trip is on 16th Avenue between Lomita Avenue and Lawton Street in San Francisco city. 16th Avenue is a two-lane undivided local neighborhood road. Figure 4.30 shows the location of the trip. The corresponding link to the video footage of the Waymo trip is included in the hyperlink here.

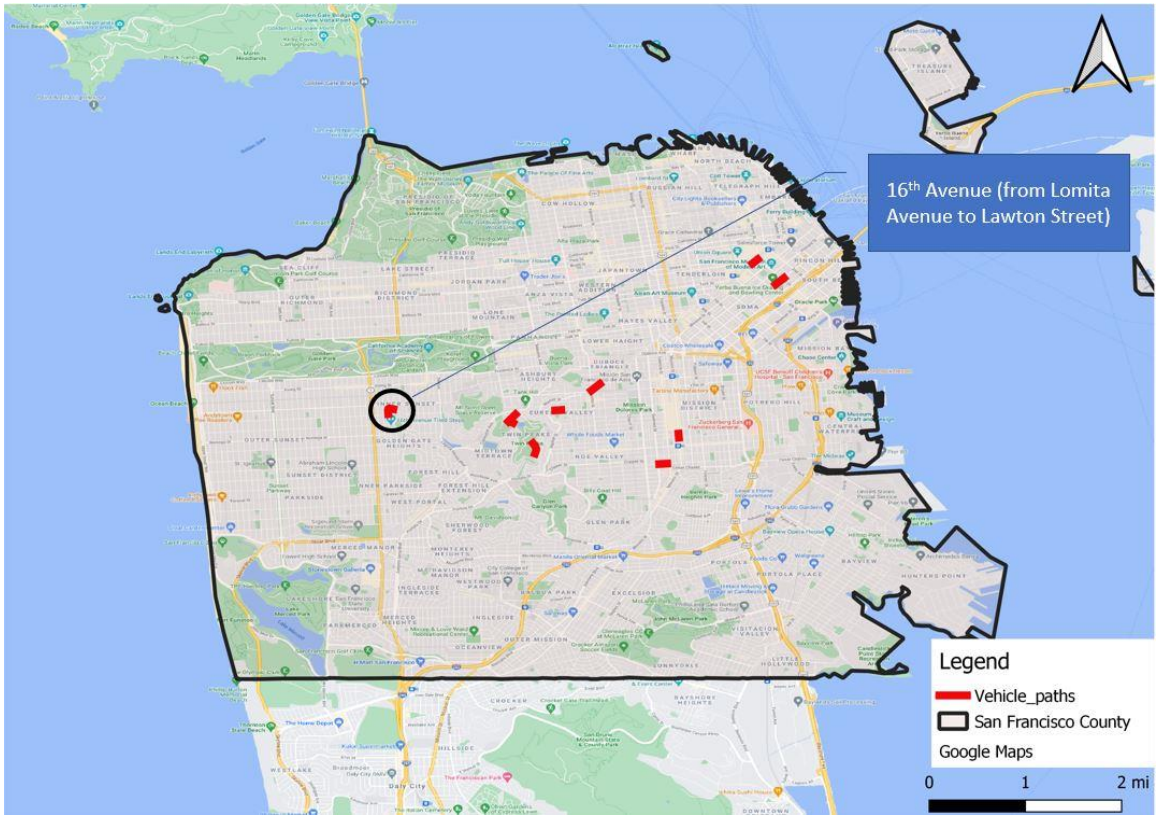

Figure 4.30. Trip location of 16th Avenue (between Lomita Avenue and Lawton Street), San Francisco, CA.

Figure 4.31 presents the dynamic complexity plot. The entire trip is designated as low dynamic complexity as it remains in that class for the entire length.

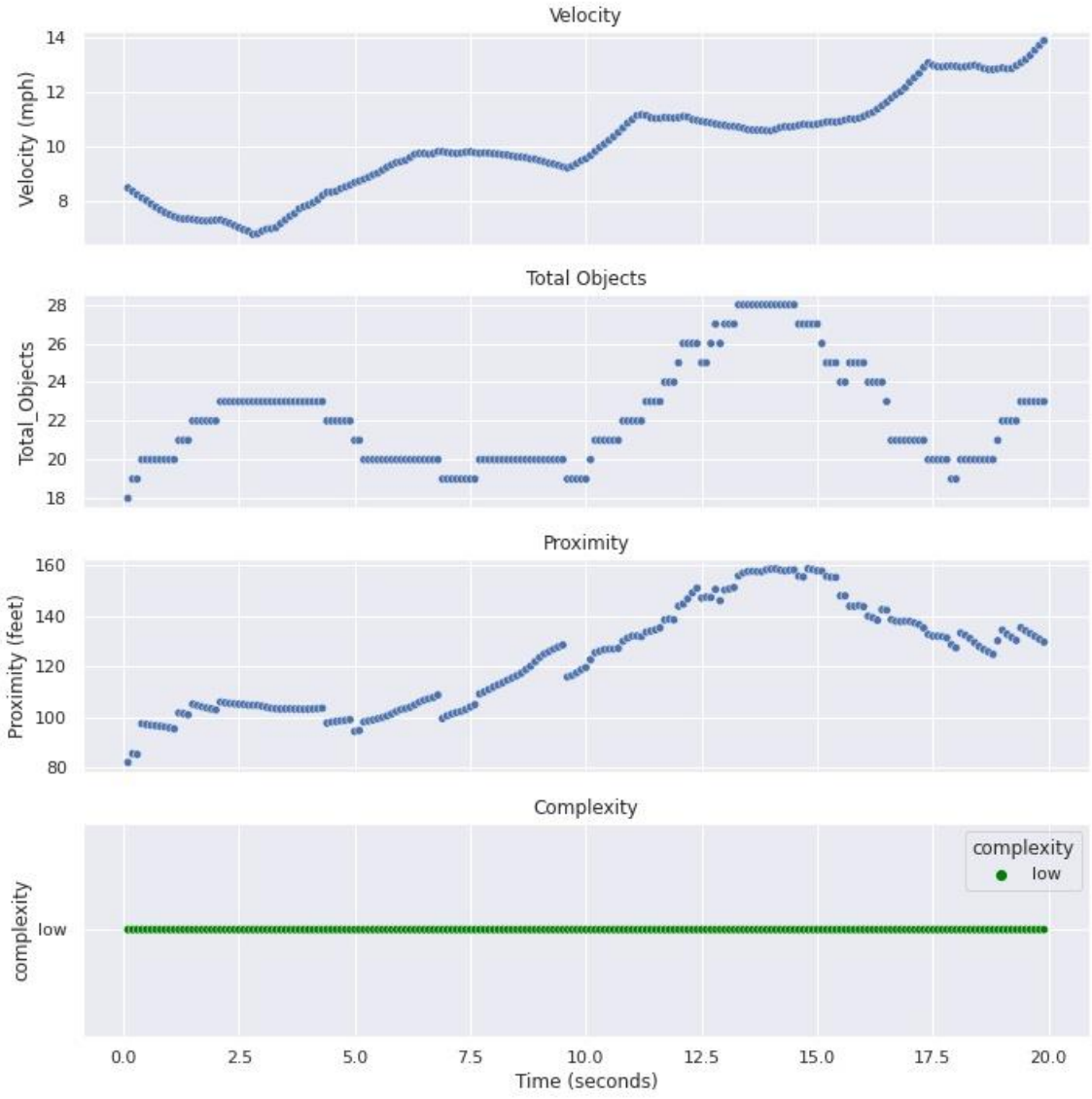

Figure 4.31. The dynamic complexity of the trip on 16th Avenue (between Lomita Avenue and Lawton Street), San Francisco, CA.

This trip consists of two intersections and a segment. Table 4.34 presents the static risk results of the trip. The intersections, as well as the segment, were categorized as “low-risk.”

Table B.19 to B.21 in Appendix B presents a detailed analysis of this trip's components (i.e., segments and intersections).

Table 4.34. Static risk of trip on16th Avenue (between Lomita Avenue and Lawton Street), San Francisco, CA.

TRIP 9: 16th Ave (Lomita Ave & Lawton ST)				
Segment/Intersection Name	**High**	**Medium**	**Low**	**Static** Risk
16th Avenue	1	0	3	Low
16th & Lomita Avenue	2	0	2	Low
16th & Lawton Street	2	0	2	Low
Absolute Static Risk	**5**	**0**	**7**	**Low**

The absolute complexity of this trip is "low" as dynamic complexity and static risk fall into that category.

CHAPTER FIVE

CONCLUSION

The goal of this research study was to develop a methodology to aid DRSs to measure and classify the contextual complexity of the routes used for on-road driving evaluations for medically-at-risk drivers considering both static and dynamic variables. The static variables (roadway type, median, lighting, etc.) were chosen from the Highway Safety Manual chapter on urban and suburban highways, which transportation engineers predominantly use to assess the safety of the roadway environment. Open source Waymo autonomous vehicle data was used to measure dynamic characteristics (object density, proximity, velocity, etc.) and develop a model. The on-road driving evaluation is considered to be the gold standard for testing and rehabilitation of medically-at-risk drivers. The product of this research was intended to build foundational work to build tools and methodology to measure the roadway context in order to enhance the consistency and validity of the on-road assessment procedures.

The first objective of this research was to develop a dynamic contextual complexity model to measure and categorize the roadway environment appropriately from high to low risk.

The dynamic complexity model was developed using two approaches i.e. statistical approach and the machine learning approach. The Contextual Complexity Factor Model developed using the statistical approach captures the density and proximity of the objects from the vehicle, which are the key parameters influencing the trip's complexity. The

machine learning model included similar key parameters (i.e. object density, proximity, and velocity) and was equally proficient in predicting the dynamic complexity with justifiable truthfulness. This was evident as the dynamic complexity results from both the models closely correlated with the historical crash data. Trips where the dynamic contextual complexity was categorized as "high" were also the ones with higher crash totals that included severe injuries. Predominantly, locations with a high volume of pedestrians and bicyclists appeared to have a tendency to be in the high-risk. This is logical as pedestrians and bicyclists take less space and are placed closely, increasing the object density and proximity and consecutively increasing the complexity. However, this interpretation should be substantiated in a further scientific study with location data to extract historical crash experience information.

The second objective of this dissertation was to build a static risk model to measure and categorize roadway environments into appropriate risk categories. The static contextual risk metrics were distilled from the Highway Safety Manual chapter on urban/suburban highways. The sensitivity analysis helped determine the most critical variables that affect the roadway's static risk. Furthermore, the results were utilized to define appropriate risk ranges to categorize the variables (i.e., high, medium, low). Each static variable is furnished with a table that includes fields/parameters to classify the variable into different risk levels. Static complexity is transferable compared to dynamic complexity.

The third objective of this research was to build an absolute contextual complexity model to measure and classify both dynamic and static characteristics of the driving environment. Static and dynamic complexity models were combined to construct absolute complexity, which illustrates the driving environment's complexity. The static and dynamic complexities may not necessarily correlate with each other, but, together, they provide a comprehensive understanding of the driving environment's complexity.

The static and dynamic risk ranges were used to develop the numerical rating system that categories a given variable into high, medium, or low complexity. The risk levels for each variable and its ranges are presented in a tabular format for easy adoption by DRSs.

The contributions of this research go much broader than the field of driving rehabilitation. Identifying and predicting the risk of the driving environment can significantly benefit safety research, driver education, auto-insurance risk assessment, autonomous vehicle route planning, and many more. For example, this research could assist in the route planning of autonomous vehicles. Current autonomous vehicle route planning strategies do not consider scene complexity, making it more challenging for drivers to take control of the autonomous vehicle when needed. All the highway safety manual models are built on the historical data and do not have context associated with them. However, with the advent of autonomous vehicles and the technology to process complex sensor fusion data generated from them can assists in building safety models that consider contextual complexity. Addition of context would inform how many cars were there, their

proximity, and arrangement prior to the crash. Such information is currently missing from safety models.

REFERENCES

AASHTO. (2018). *A Policy on Geometric Design of Highways and Streets, 2011*. AASHTO.

Abdel-Aty, M. A., & Radwan, A. E. (2000). Modeling traffic accident occurrence and involvement. *Accident Analysis & Prevention*, *32*(5), 633–642. https://doi.org/10.1016/S0001-4575(99)00094-9

Association for Driver Rehabilitation Specialists. (2019). *Association for Driver Rehabilitation Specialists (ADED) Candidate Handbook*. http://c.ymcdn.com/sites/www.aded.net/resource/resmgr/Docs/ADED-handbook-072014.pdf?hhSearchTerms=%22candidate+and+handbook%22 .

Center for Disease Control and Prevention. (2020, December 10). *Older Adult Drivers | Motor Vehicle Safety | CDC Injury Center*. https://www.cdc.gov/transportationsafety/older_adult_drivers/index.html

Center for Ergonomics, & LaTrobe University Human Factors. (1996). An Evaluation of Occupational Theraphy (OT) Driver Assessment Protocols and Recommendations for a Reliable and Valid Standard Test. *LaTrobe University, School of Human Bio-Sciences, Center for Ergonomics and Human Factors*.

Chauhan, N. (2019). What is Hierarchical Clustering? *KDnuggets*. https://www.kdnuggets.com/what-is-hierarchical-clustering.html/

Chen, M. (2022). *Kmeans Clustering*. MATLAB Central File Exchange. https://www.mathworks.com/matlabcentral/fileexchange/24616-kmeans-clustering

Christopher Frey, H., & Patil, S. R. (2002). Identification and Review of Sensitivity Analysis Methods. *Risk Analysis*, *22*(3), 553–578. https://doi.org/10.1111/0272-4332.00039

Cushman, L. A. (1996). COGNITIVE CAPACITY AND CONCURRENT DRIVING PERFORMANCE IN OLDER DRIVERS. *IATSS Research*. https://trid.trb.org/view/481452

Dewar, R. E., & Olson, P. L. (2002). HUMAN FACTORS IN TRAFFIC ACCIDENT LITIGATION. IN: HUMAN FACTORS IN TRAFFIC SAFETY. *Publication of: Lawyers & Judges Publishing Company, Incorporated*. https://trid.trb.org/view/712350

Di Stefano, M., & Lovell, R. K. (2006). Using a participatory research method to develop a handbook for driving instructors to assist with teaching older drivers. *Australian Occupational Therapy Journal*, *53*(2), 132–135. https://doi.org/10.1111/j.1440-1630.2006.00560.x

Di Stefano, M., & Macdonald, W. (2010). Australian Occupational Therapy Driver Assessors' Opinions on Improving On-Road Driver Assessment Procedures. *American Journal of Occupational Therapy*, *64*(2), 325–335. https://doi.org/10.5014/ajot.64.2.325

Di Stefano, M., & Macdonald, W. (2012). Design of occupational therapy on-road test routes and related validity issues: DESIGN OF OTDA ON-ROAD TEST ROUTES. *Australian Occupational Therapy Journal*, *59*(1), 37–46. https://doi.org/10.1111/j.1440-1630.2011.00990.x

Dickerson, A. E. (2013). Driving Assessment Tools Used by Driver Rehabilitation Specialists: Survey of Use and Implications for Practice. *American Journal of Occupational Therapy*, *67*(5), 564–573. https://doi.org/10.5014/ajot.2013.007823

Dobbs, A. R., Heller, R. B., & Schopflocher, D. (1998). A comparative approach to identify unsafe older drivers. *Accident Analysis & Prevention*, *30*(3), 363–370. https://doi.org/10.1016/S0001-4575(97)00110-3

Galski, T., Ehle, H. T., & Bruno, R. L. (1990). An Assessment of Measures to Predict the Outcome of Driving Evaluations in Patients With Cerebral Damage. *The American Journal of Occupational Therapy*, *44*(8), 709–713. https://doi.org/10.5014/ajot.44.8.709

Govender, P., & Sivakumar, V. (2020). Application of k-means and hierarchical clustering techniques for analysis of air pollution: A review (1980–2019). *Atmospheric Pollution Research*, *11*(1), 40–56. https://doi.org/10.1016/j.apr.2019.09.009

Hunt, L. A., Murphy, C. F., Carr, D., Duchek, J. M., Buckles, V., & Morris, J. C. (1997). Reliability of the Washington University Road Test: A Performance-Based Assessment for Drivers With Dementia of the Alzheimer Type. *Archives of Neurology*, *54*(6), 707–712. https://doi.org/10.1001/archneur.1997.00550180029008

Janke, M. K., & Eberhard, J. W. (1998). Assessing medically impaired older drivers in a licensing agency setting. *Accident Analysis & Prevention*, *30*(3), 347–361. https://doi.org/10.1016/S0001-4575(97)00112-7

Justiss, M. D., Mann, W. C., Stav, W., & Velozo, C. (2006). Development of a Behind-the-Wheel Driving Performance Assessment for Older Adults: *Topics in Geriatric Rehabilitation*, *22*(2), 121–128. https://doi.org/10.1097/00013614-200604000-00004

Kanungo, T., Mount, D. M., Netanyahu, N. S., Piatko, C. D., Silverman, R., & Wu, A. Y. (2002). An efficient k-means clustering algorithm: Analysis and implementation. *IEEE Transactions on Pattern Analysis and Machine Intelligence*, *24*(7), 881–892. https://doi.org/10.1109/TPAMI.2002.1017616

Kay, L., Bundy, A., Clemson, L., & Jolly, N. (2008). Validity and reliability of the on-road driving assessment with senior drivers. *Accident Analysis & Prevention*, *40*(2), 751–759. https://doi.org/10.1016/j.aap.2007.09.012

Korner-Bitensky, N., Bitensky, J., Sofer, S., Man-Son-Hing, M., & Gelinas, I. (2006). Driving Evaluation Practices of Clinicians Working in the United States and Canada. *American Journal of Occupational Therapy*, *60*(4), 428–434. https://doi.org/10.5014/ajot.60.4.428

Krawczyk, B. (2016). Learning from imbalanced data: Open challenges and future directions. *Progress in Artificial Intelligence*, *5*(4), 221–232. https://doi.org/10.1007/s13748-016-0094-0

Messinger-Rapport, B. J. (2002). How to assess and counsel the older driver. *Cleveland Clinic Journal of Medicine*, *69*(3), 184–185, 189–190, 192. https://doi.org/10.3949/ccjm.69.3.184

Montazeri-Gh, M., & Fotouhi, A. (2011). Traffic condition recognition using the k-means

clustering method. *Scientia Iranica*, *18*(4), 930–937. https://doi.org/10.1016/j.scient.2011.07.004

Monty, R. A., & Senders, J. W. (Eds.). (1976). Stimulus Density Limits the Useful Field of View. In *Eye Movements and Psychological Processes*. Routledge.

Murtagh, F., & Contreras, P. (2017). *Algorithms for hierarchical clustering: An overview—Murtagh—2012—WIREs Data Mining and Knowledge Discovery—Wiley Online Library* (Vol. 7). https://wires.onlinelibrary.wiley.com/doi/abs/10.1002/widm.53

National Research Council, Transportation Research Board, Task force on Development of the Highway Safety Manual and Transportation officials, & Joint Task Force on the Highway Safety Manual. (2010). *Highway Safety Manual* (Vol. 1). AASHTO.

Olson, P. L. (1996). *FORENSIC ASPECTS OF DRIVER PERCEPTION AND RESPONSE*. https://trid.trb.org/view/453958

Paas, F., Tuovinen, J. E., Tabbers, H., & Van Gerven, P. W. M. (2003). Cognitive Load Measurement as a Means to Advance Cognitive Load Theory. *Educational Psychologist*, *38*(1), 63–71. https://doi.org/10.1207/S15326985EP3801_8

Pellerito, J. M. (2006). *Driver rehabilitation and community mobility: Principles and practice - Southern Cross University*. https://scu.esploro.exlibrisgroup.com/discovery/fulldisplay/alma99001708752040 2368/61SCU_INST:ResearchRepository

Radloff, J. C. (2014). Driving And Community Mobility: Occupational Therapy

Strategies Across The Lifespan. *Occupational Therapy In Health Care*, *28*(2), 229–230. https://doi.org/10.3109/07380577.2014.899416

Roess, R. P., Prassas, E. S., & Mcshane, W. R. (2004). *TRAFFIC ENGINEERING*. https://trid.trb.org/view/310674

Rogé, J., Pébayle, T., Lambilliotte, E., Spitzenstetter, F., Giselbrecht, D., & Muzet, A. (2004). Influence of age, speed and duration of monotonous driving task in traffic on the driver's useful visual field. *Vision Research*, *44*(23), 2737–2744. https://doi.org/10.1016/j.visres.2004.05.026

Route Planning Checklist. (2016). Center for Biomedical Engineering Rehabilitation Science at Louisiana Tech University.

Schultheis, M. T., Garay, E., & DeLuca, J. (2001). The influence of cognitive impairment on driving performance in multiple sclerosis. *Neurology*, *56*(8), 1089–1094. https://doi.org/10.1212/WNL.56.8.1089

Shechtman, O, Awadzi, K. D., Classen, S., Lanford, D. N., & Joo, Y. (2010). Validity and Critical Driving Errors of On-Road Assessment for Older Drivers. *American Journal of Occupational Therapy*, *64*(2), 242–251. https://doi.org/10.5014/ajot.64.2.242

Shinar, D., Mcdowell, E., & Rockwell, T. (1977). *Eye Movements in Curve Negotiation*. https://journals.sagepub.com/doi/abs/10.1177/001872087701900107?journalCode=hfsa

Siegrist, S. (1999). *Driver Training, Testing and Licensing—Towards theory-based management of young drivers' injury risk in road traffic Results of EU-Project*

GADGET, Work Package 3. 12.

Stav, W. (2004). Driver rehabilitation: A guide for assessment and intervention. *Occupational Therapy Faculty Books and Book Chapters*, 1–80.

Stefano, D., & Macdonald, W. (2006). On-the-road evaluation of driving performance. *Driver Rehabilitation and Community Mobility*, 255–275.

Sun, P., Kretzschmar, H., Dotiwalla, X., Chouard, A., Patnaik, V., Tsui, P., Guo, J., Zhou, Y., Chai, Y., Caine, B., Vasudevan, V., Han, W., Ngiam, J., Zhao, H., Timofeev, A., Ettinger, S., Krivokon, M., Gao, A., Joshi, A., … Anguelov, D. (2020). Scalability in Perception for Autonomous Driving: Waymo Open Dataset. *ArXiv:1912.04838 [Cs, Stat]*. http://arxiv.org/abs/1912.04838

Warren, J., & Smalley, B. (2014). *Rural Public Health: Best Practices and Preventive Models*. Springer Publishing Company.

APPENDICES

Appendix A

K-means and Hierarchical Clustering Plots

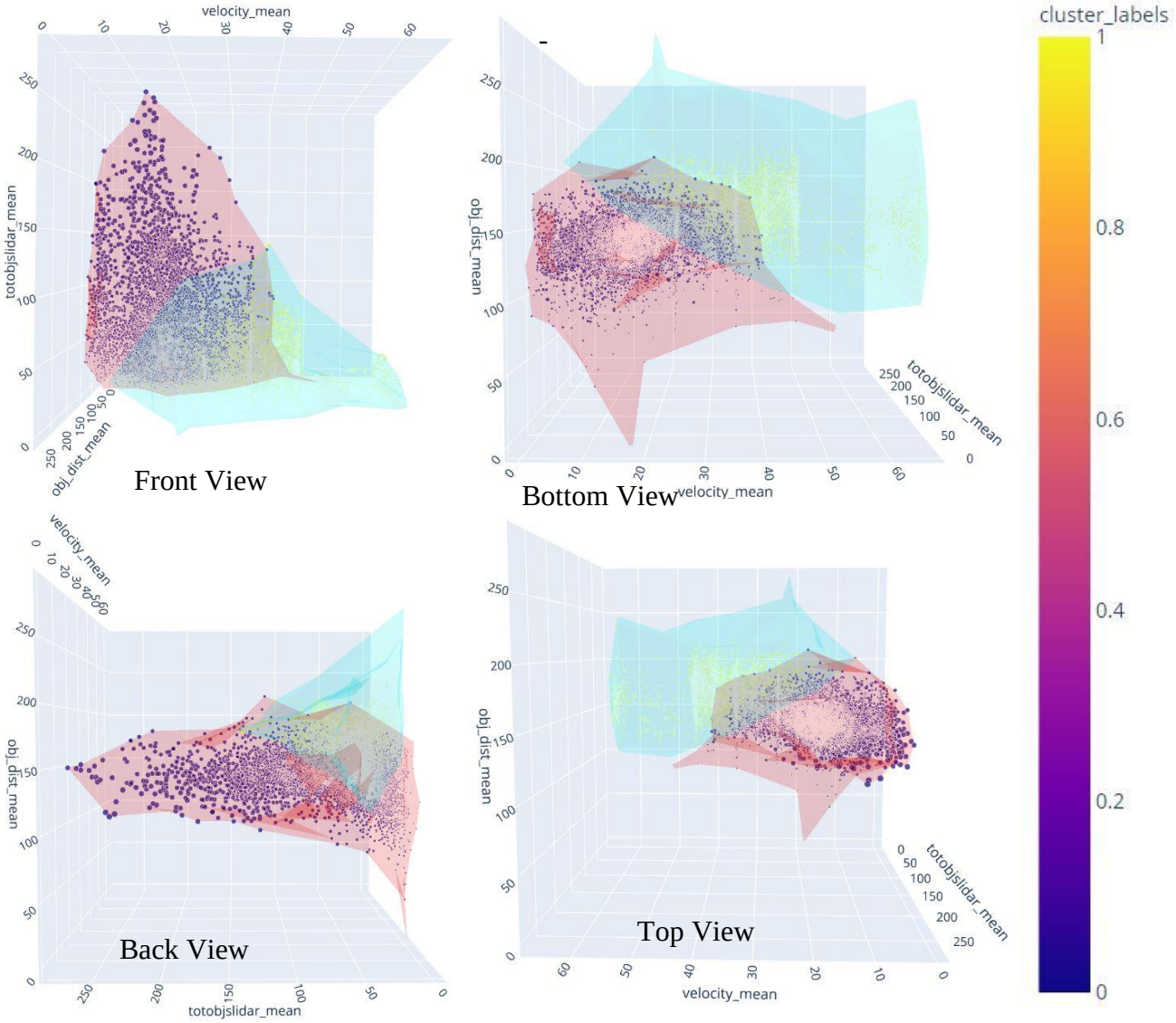

Figure A.1. K-means clustering (K=2)

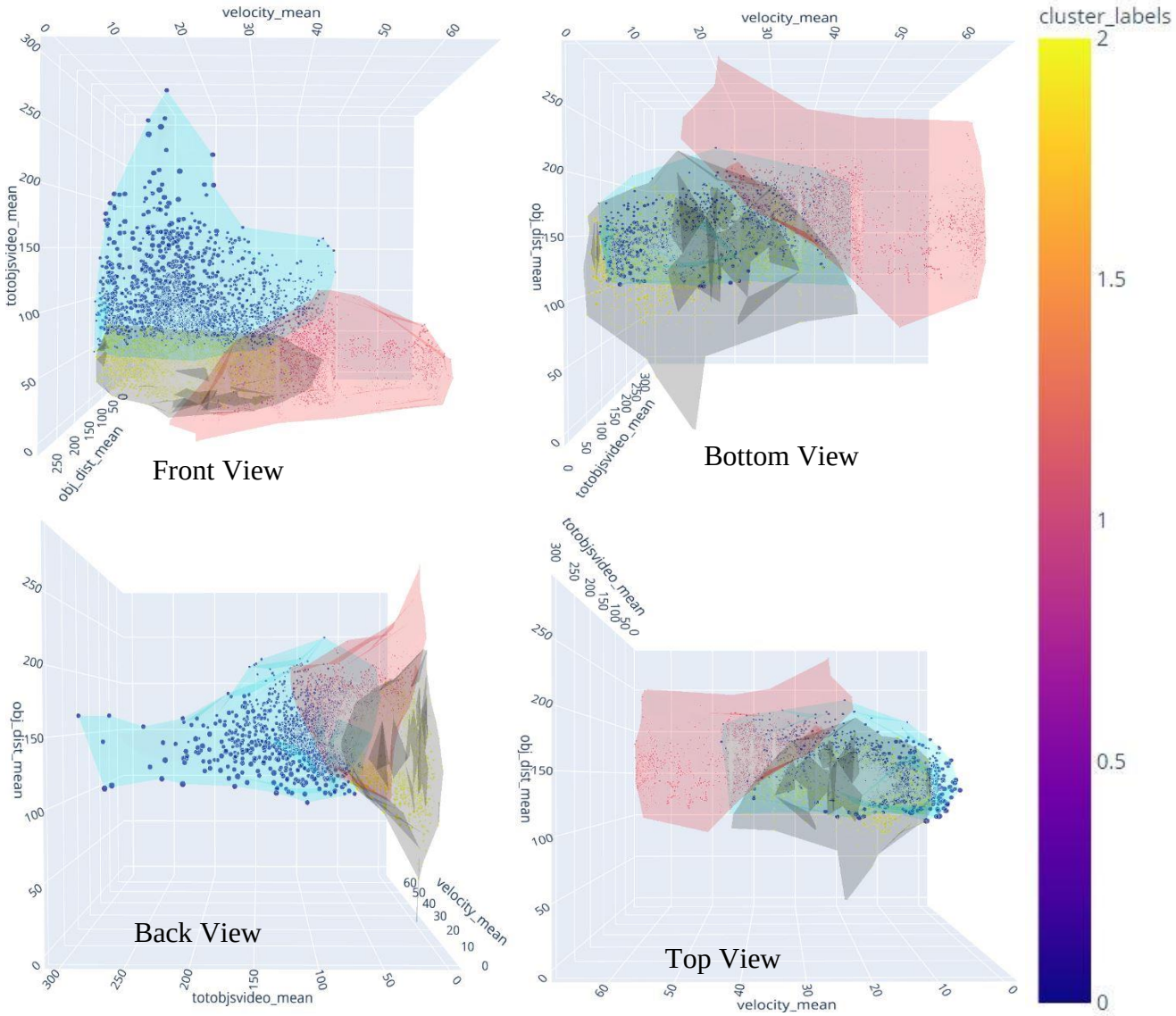

Figure A.2. K-means clustering (K=3)

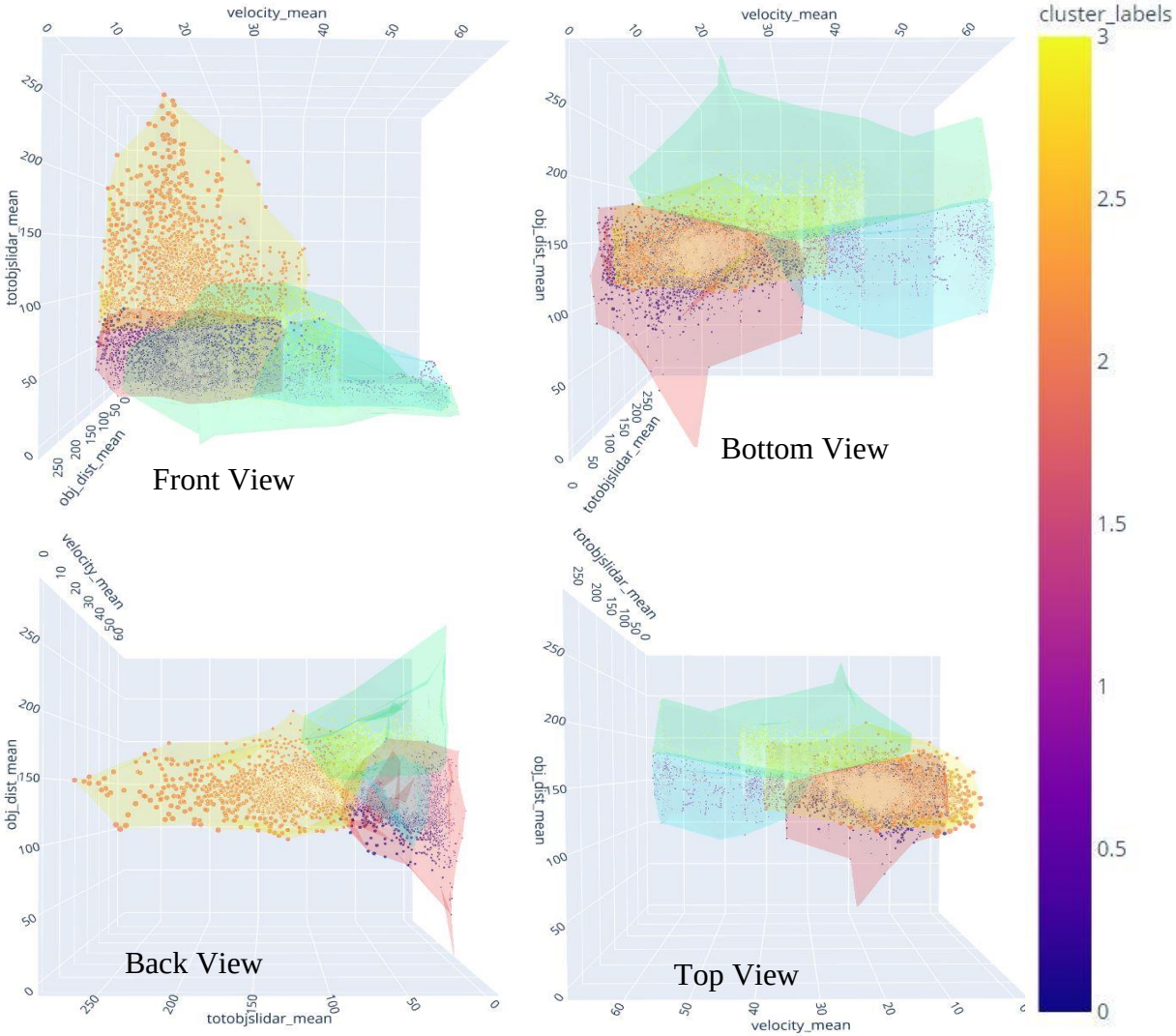

Figure A.3. K-means clustering (K=4)

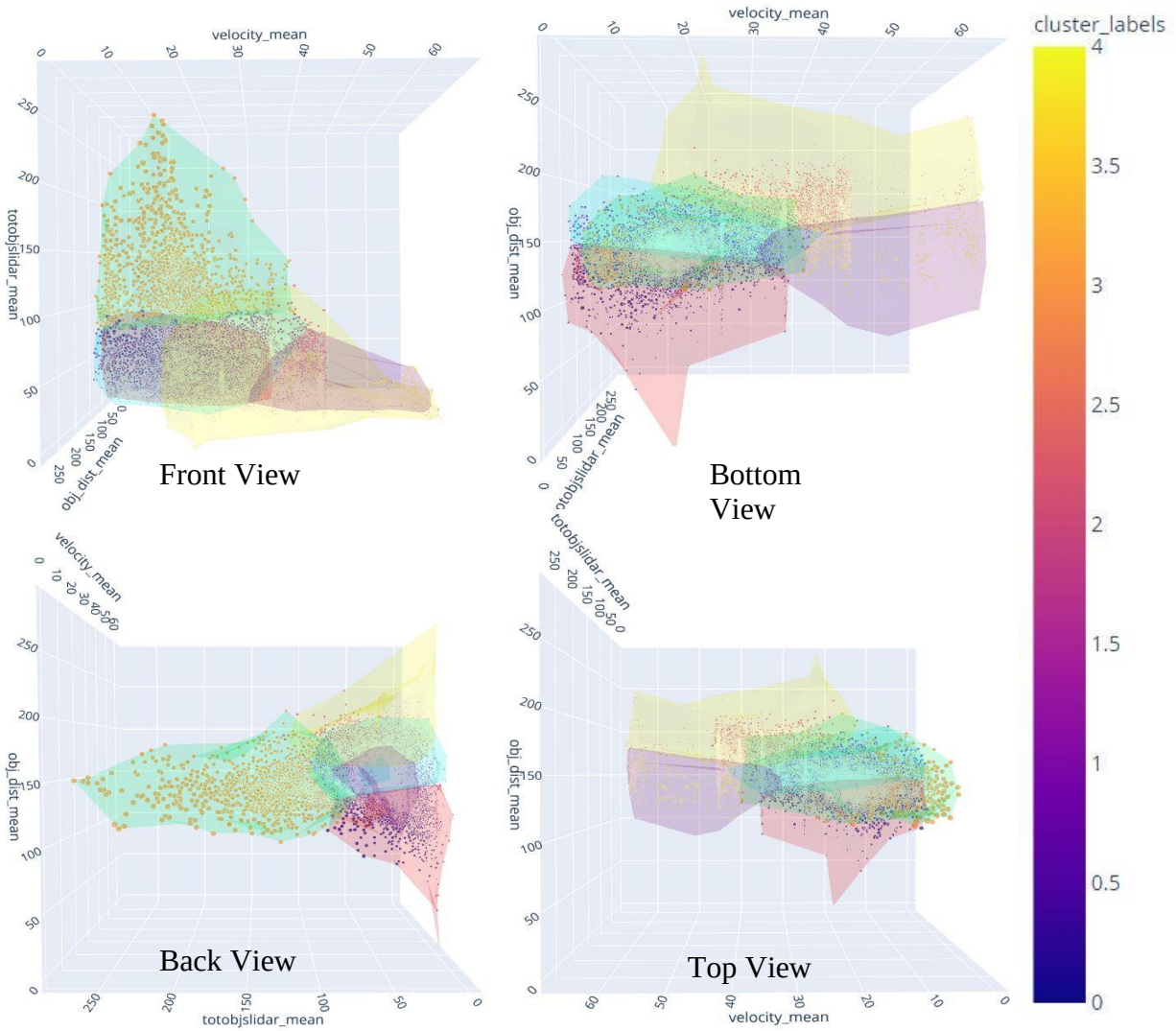

Figure A.4. K-means clustering (K=5)

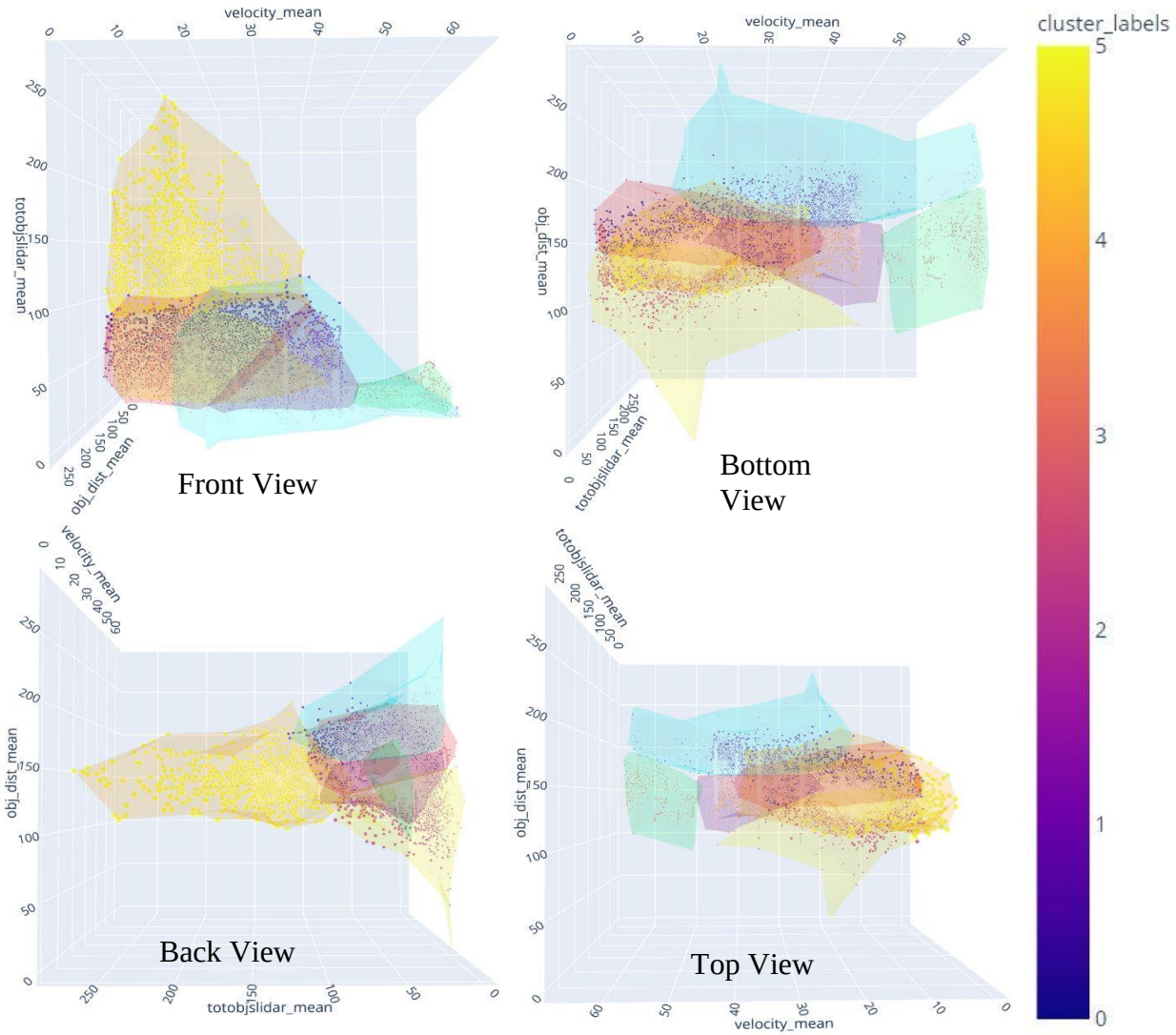

Figure A.5. K-means clustering (K=6)

APPENDIX B

Absolute Contextual Complexity Plots

B.1. Market Street (Between 3rd St and O'Farrel St)

Table B.1. Static complexity analysis results of Market Street Segment.

SEGMENTID	**segment-4641822195449131669_380_000_400_000_with_camera_labels**	
Market Street (Between 3rd St and O'Farrel St)		**Complexity**
Roadway Type	4U	Medium
On Street Parking	Parallel Commercial	Medium
Median width (ft)	10	High
Lighting	Present	Low
Fixed Object Offset	5	High
Auto Speed Enforcement	Not Present	High
SEGMENT RISK		**High**

Table B.2. Static complexity analysis results of intersection at Market Street and 3rd Street.

Intersection: Market St @ 3rd St		
Intersection Type	4 Approach Signalized	High
Intersection Lighting	Present	Low
Approaches with Left Turn Lanes	0	High
Approaches with Right Turn Lanes	0	High
Approaches with Left Turn Signal Phasing	0	High
Type of Signal Phasing	Permissive	High
Approaches RTOR Prohibited	0	High
Intersection Red Light Running	Not Present	High
INTERSECTION RISK		**HIGH**

Table B.3. Static complexity analysis results of intersection at Market Street & O'Farrel Street.

Intersection: Market St @ O'Farrel St		
Intersection Type	3 Approach Signalized	Medium
Intersection Lighting	Present	Low
Approaches with Left Turn Lanes	1	Medium
Approaches with Right Turn Lanes	0	High
Approaches with Left Turn Signal Phasing	0	High
Type of Signal Phasing	Permissive	High
Approaches RTOR Prohibited	0	High
Intersection Red Light Running	Not Present	High
INTERSECTION RISK		**HIGH**

B.2. Market Street (Between 16th & 17th St)

Table B.4. Static complexity analysis results of Market Street (Between 16th & 17th Street) segment.

SEGMENTID	**segment-10876852935525353526_1640_000_1660_000_with_camera_labels**	
Market Street (Between 16th & 17th St)		**Complexity**
Roadway Type	4 Lane Divided	Medium
On Street Parking	Parallel Commercial	High
Median width (ft)	10	High
Lighting	Present	Low
Fixed Object Offset	5	High
Auto Speed Enforcement	Not Present	High
SEGMENT RISK		**HIGH**

Table B.5. Static complexity analysis results of intersection on Market Street & 16th Street.

Intersection: Market St @ 16rd St		**Complexity**
Intersection Type	6 Approach Signalized	High
Intersection Lighting	Present	Low
Approaches with Left Turn Lanes	2	Medium
Approaches with Right Turn Lanes	1	High
Approaches with Left Turn Signal Phasing	0	High
Type of Signal Phasing	Permissive	High
Approaches RTOR Prohibited	0	High

Intersection Red Light Running	Not Present	High
INTERSECTION RISK		**HIGH**

Table. B.6. Static complexity analysis results of intersection on Market Street & 17th Street.

Intersection: Market St @ 17th St		**Complexity**
Intersection Type	6 Approach Signalized	High
Intersection Lighting	Present	Low
Approaches with Left Turn Lanes	2	Medium
Approaches with Right Turn Lanes	4	Low
Approaches with Left Turn Signal Phasing	0	High
Type of Signal Phasing	Permissive	High
Approaches RTOR Prohibited	3	Low
Intersection Red Light Running	Not Present	High
INTERSECTION RISK		**HIGH**

B.3. Mission Street (Between 22nd Street & 23rd Street)

Table B. 7. Static complexity analysis of segment on Mission Street (between 22nd street and 23rd street).

SEGMENTID	**segment-1192522414802314551 0_1040_000_1060_000_with_camera_labels**	
Mission St (Between 22nd & 23rd)		**Complexity**
Roadway Type	2 Lane Undivided	Low
On Street Parking	Parallel - Commercial	Medium
Median width (ft)	None	High
Lighting	yes	Low
Fixed Object Offset	5	High
Auto Speed Enforcement	None	High
SEGMENT RISK		**High**

Table B.8. Static complexity analysis of intersection on Mission Street and 23rd Street.

Intersection: Mission St @ 23rd St		**Complexity**
Fixed Object Offset	4 Leg Signalized	High
Intersection Lighting	Present	Low
Approaches with Left Turn Lanes	0	High
Approaches with Right Turn Lanes	2	Medium
Approaches with Left Turn Signal Phasing	0	High
Type of Signal Phasing	Permissive	High
Approaches RTOR Prohibited	0	High
Intersection Red Light Running	0	Low
INTERSECTION RISK		**High**

B.4. Folsom Street (Between 3rd Street & Mabini Street)

Table B.9. Static complexity analysis of segment on Folsom Street (between 3rd street and Mabini Street)

SEGMENTID	**segment-11928449532664718059_1200_000_1220_000_with_camera_labels**	
Folsom St (Between 3rd st & Mabini St)		**Complexity**
Roadway Type	4D	Medium
On Street Parking	Parallel-Commercial	Medium
Median width (ft)	None (One Way)	Low
Lighting	Yes	Low
Fixed Object Offset	10	High
Auto Speed Enforcement	No	High
SEGMENT RISK		**MEDIUM**

Table B.10. Static complexity analysis of intersection on Folsom Street and 3rd Street.

Intersection: Folsom St @ 3rd Street		**Complexity**
Intersection Type	4 leg Signalized	High
Intersection Lighting	Present	Low
Approaches with Left Turn Lanes	4	Low
Approaches with Right Turn Lanes	4	Low
Approaches with Left Turn Signal Phasing	4	Low
Type of Signal Phasing	Protected	Low
Approaches RTOR Prohibited	0	High
Intersection Red Light Running	Not Present	High
INTERSECTION RISK		**LOW**

Table B. 11. Static Complexity analysis of intersection on Folsom Street and Mabini Street, San Francisco, CA.

Intersection: Folsom St @ Mabini St.		**Complexity**
Intersection Type	3 Approach Signalized	Medium
Intersection Lighting	Present	Low
Approaches with Left Turn Lanes	3	Low
Approaches with Right Turn Lanes	3	Low
Approaches with Left Turn Signal Phasing	3	Low
Type of Signal Phasing	Protected	Low
Approaches RTOR Prohibited	0	High
Intersection Red Light Running	Not Present	High
INTERSECTION RISK		**LOW**

B. 5. 26th Street (Between Guerrero Street & Valencia Street)

Table B.11. Static complexity analysis of segment on 26th street (between Guerrero Street and Valencia Street)

SEGMENTID	**segment-13619063687271391084_1519_680_1539_680_with_camera_labels**	
26th St (Between Guerrero St & Valencia St)		**Complexity**
Roadway Type	4 lane Divided	Medium
On Street Parking	Parallel-Residential	Medium
Median width (ft)	0	High
Lighting	Present	Low
Fixed Object Offset	15	Medium
Auto Speed Enforcement	None	High
SEGMENT RISK		**Medium**

Table B.12. Static complexity analysis of intersection on 26th Street and Guerrero Street.

Intersection: 26th st @ Guerrero St		**Complexity**
Intersection Type	4 Approach Signalized	Medium
Intersection Lighting	Present	Low
Approaches with Left Turn Lanes	0	High
Approaches with Right Turn Lanes	0	High
Approaches with Left Turn Signal Phasing	0	High
Type of Signal Phasing	Permissive	High
Approaches RTOR Prohibited	0	High
Intersection Red Light Running	Not Present	High
INTERSECTION RISK		**HIGH**

Table B.13. Static complexity analysis of intersection on 26th street and San Jose Avenue.

Intersection: 26th St @ San Jose Ave		**Complexity**
Intersection Type	3 Approach stop	Medium
Intersection Lighting	Not Present	High
Approaches with Left Turn Lanes	0	High
Approaches with Right Turn Lanes	0	High
Approaches with Left Turn Signal Phasing	0	NA
Type of Signal Phasing	NA	NA
Approaches RTOR Prohibited	NA	NA
Intersection Red Light Running	0	NA
INTERSECTION RISK		**HIGH**

B.6. 19th Street (Between Yukon Street and Seward Street)

Table. B.14. Static complexity analysis of segment on 19th Street (between Yukon Street and Seward Street).

SEGMENTID	**segment-1486973297290314865 7_2420_000_2440_000_with_camera_labels**	
19th St (Between Yukon St & Seward St)		**Complexity**
Segment Type	2 lane undivided	Low
On Street Parking	Parallel-Residential	Low
Median width (ft)	0	Medium
Lighting	Present	Low
Fixed Object Offset	5	High
Auto Speed Enforcement	None	Low
SEGMENT RISK		**Low**

Table B.15. Static complexity analysis of intersection on 19th Street and Yukon Street.

Intersection: 19th St @ Yukon St		**Complexity**
Intersection Control Type	4 leg stop	Low
Intersection Lighting	Present	Low
Approaches with Left Turn Lanes	0	High
Approaches with Right Turn Lanes	0	High
Approaches with Left Turn Signal Phasing	NA	NA
Type of Signal Phasing	NA	NA
Approaches RTOR Prohibited	NA	NA
Intersection Red Light Running	0	NA
INTERSECTION RISK		**Low**

Table B.16. Static complexity analysis of intersection on 19th Street and Seward Street.

Intersection: 19th St @ Seward St		**Complexity**
Intersection Control Type	Yield	Low
Intersection Lighting	Present	Low
Approaches with Left Turn Lanes	0	High
Approaches with Right Turn Lanes	0	High
Approaches with Left Turn Signal Phasing	0	NA
Type of Signal Phasing	NA	NA
Approaches RTOR Prohibited	NA	NA
Intersection Red Light Running	0	NA
INTERSECTION RISK		**Low**

B.7. Glenbrook Avenue (Between Palo Alto Avenue and Mountain Spring Road)

Table B.17. Static complexity analysis of segment on Glenbrook Avenue (between Palo Alto Avenue and Mountain Spring Road).

SEGMENTID	**segment-3363533094480067586_1580_000_1600_000_with_camera_labels**	
Glenbrook Ave (Palo Alto Ave & Mountain Spring Rd)		**Complexity**
Roadway Type	2 lane undivided	Low
On Street Parking	Parallel-Residential	Low
Median width (ft)	10	Medium
Lighting	Not Present	High
Fixed Object Offset	5	High
Auto Speed Enforcement	None	NA
SEGMENT RISK		**Low**

Table B.18. Static complexity analysis of

Intersection: Glenbrook Ave @ Mountain Spring Rd		**Complexity**
Intersection Type	Minor Road Yield	Low
Intersection Lighting	Present	Low
Approaches with Left Turn Lanes	0	High
Approaches with Right Turn Lanes	0	High
Approaches with Left Turn Signal Phasing	NA	NA
Type of Signal Phasing	NA	NA
Approaches RTOR Prohibited	NA	NA
Intersection Red Light Running	0	NA
INTERSECTION RISK		**Low**

B.8. Parkridge Drive (Between Crestine Drive and Burnett Avenue)

Table B.19. Static complexity analysis results for segment on Parkridge Drive (between Crestline Drive and Burnett Avenue).

SEGMENTID	**segment-5328596138024684667_2180_000_2200_000_with_camera_labels**	
Parkridege Dr (Crestline Dr & Burnett Ave)		**Complexity**
Roadway Type	2 lane undivided	Low
Parking Type	Parallel-Residential	Low
Median width (ft)	0	NA
Lighting Present	Present	Low
Fixed Object Offset	5	High
Auto Speed Enforcement	None	NA
SEGMENT RISK		**Low**

Table B.20. Static complexity analysis results for intersection on Parkridge Drive and Crestline Drive.

Intersection: Parkridge Dr & Crestline Dr		**Complexity**
Intersection Type	Minor Road Yield	Low
Intersection Lighting	Present	Low
Approaches with Left Turn Lanes	0	High
Approaches with Right Turn Lanes	0	High
Approaches with Left Turn Signal Phasing	NA	NA
Type of Signal Phasing	NA	NA
Approaches RTOR Prohibited	NA	NA
Intersection Red Light Running	0	NA
INTERSECTION RISK		**Low**

Table B.21. Static complexity analysis results for intersection on Parkridge Drive and Burnette Avenue.

Intersection: Parkridge Dr & Burnett Ave		**Complexity**
Intersection Type	Minor Road Yield	Low
Intersection Lighting	Present	Low
Approaches with Left Turn Lanes	0	High
Approaches with Right Turn Lanes	0	High
Approaches with Left Turn Signal Phasing	NA	NA
Type of Signal Phasing	NA	NA
Approaches RTOR Prohibited	NA	NA
Intersection Red Light Running	0	NA
INTERSECTION RISK		**Low**

B.9. 16th Avenue (Between Lomita Avenue and Lawton Street)

Table B.22. Static complexity analysis of segment on 16th Avenue (between Lomita Avenue and Lawton Street).

SEGMENTID	**segment-3919438171935923501_280_000_300_000_with_camera_labels**	
16th Ave (Lomita Ave & Lawton St)		**Complexity**
Roadway type	2 Lane Undivided	Low
Parking Type	Parallel-Residential	Low
Median width (ft)	0	NA
Lighting Present	Present	Low
Fixed Object Offset	5	High
Auto Speed Enforcement	None	NA
SEGMENT RISK		**Low**

Table B.23. Static complexity analysis of intersection on 16th Avenue and Lomita Avenue.

Intersection: 16th & Lomita Ave		**Complexity**
Intersection Type	Minor Road Yield	Low
Intersection Lighting	Present	Low
Approaches with Left Turn Lanes	0	High
Approaches with Right Turn Lanes	0	High
Approaches with Left Turn Signal Phasing	NA	NA
Type of Signal Phasing	NA	NA
Approaches RTOR Prohibited	NA	NA
Intersection Red Light Running	0	NA
INTERSECTION RISK		**Low**

Table B.24. Static complexity analysis results of intersection on 16th avenue and Lawton Street.

Intersection: 16th & Lawton ST		**Complexity**
Intersection Type	Minor Road Yield	Low
Intersection Lighting	Present	Low
Approaches with Left Turn Lanes	0	High
Approaches with Right Turn Lanes	0	High
Approaches with Left Turn Signal Phasing	NA	NA
Type of Signal Phasing	NA	NA
Approaches RTOR Prohibited	NA	NA
Intersection Red Light Running	0	NA
INTERSECTION RISK		**Low**